

Erstgutachter: Prof. Dr. Uwe Ulbrich

Freie Universität Berlin, Institut für Meteorologie

Zweitgutachter: apl. Prof. Dr. Jürgen P. Kropp

Universität Potsdam, Institut für Erd- und Umweltwissenschaften
Potsdam-Institut für Klimafolgenforschung (PIK)

Tag der Disputation: 20. Januar 2017

Sometimes fate is like a small sandstorm that keeps changing directions. You change direction but the sandstorm chases you. You turn again, but the storm adjusts. { . . . } But one thing is certain. When you come out of the storm you won't be the same person who walked in. That's what this storm's all about.

— Haruki Murakami, *Kafka on the Shore*

Abstract

Globally the number of climate-related disasters and the associated loss figures are on the rise. The changing climate as well as the increasing exposure in terms of people and assets could induce unprecedented damage levels. Damage functions constitute the crucial link between hazard, exposure and the resulting damage. As such, they provide vulnerability and damage-cost information, which are essential for disaster risk reduction and for the evaluation of climate-change adaptation options. With this purpose in mind, the overarching goal of the work at hand is to contribute to the fundamental understanding of damage functions and to provide systematic and versatile damage assessment.

Only few damage functions are available for a regional damage assessment. Data scarcity, for example, is a major obstacle for the development of storm damage functions. For the work at hand, newly available data on German storm loss permit a fresh look at the wind–loss relation. Based on these data, a novel storm damage function is developed and compared against existing approaches. The results show that the wind–loss relation is well described by power-law curves with exponents that are considerably higher than previously expected. While the steepness of the curves at extreme wind speeds is comparable to other damage functions, the novel damage function is capable of predicting damages over a wider range of wind speeds. It is found that the uncertainty of the damage estimates is mainly driven by uncertainty from the wind measurement and approximates to a log-normal uncertainty distribution. Exploring further damage functions beyond the domain of storm damage, analogous approaches are identified for coastal flooding and, schematically, for heat-related mortality. Together, these are formulated as a unified damage function. With its wide applicability the unified approach forms the basis for undertaking a fundamental analysis of uncertainty. Here, in contrast to prior studies, the work at hand puts emphasis on the propagation of uncertainty from the microscale to the macroscale level. The results show that the relevance of intrinsic uncertainties on the microscale level is carried over to the aggregate macroscale level. However, extrinsic sources of uncertainty, such as the aforementioned measurement error of wind speed, dominate overall.

In summary, this work delivers multiple contributions to the understanding of damage functions. The novel storm damage function provides improved loss estimates and will help to assess the significance of changes in storm climate. The comparison brings together the rather fragmented research on storm damage functions and sheds light on their performance. Furthermore, the findings suggest a rebuttal of the cubic power-law assumption for macroscale storm loss. Finally, the unified approach for damage estimation facilitates knowledge transfer between various climate-related hazards. As one example, the findings on the relevance of uncertainty sources have broad applicability and may guide future research to reduce the uncertainty of damage estimation. With its inter-

disciplinary approach, this work has strong relevance to practitioners in the various domains of natural hazards research and in the atmospheric sciences.

Zusammenfassung

Im globalen Maßstab sind sowohl die Anzahl als auch die Schäden klimabedingter Naturkatastrophen im Anstieg begriffen. Durch das Zusammenspiel von Klimawandel und zunehmender Exposition von Menschen und Vermögen ist von einem weiterhin zunehmenden Schadensniveau auszugehen. Schadensfunktionen beschreiben die Schnittstelle zwischen den verursachten Schäden, der Exposition, sowie der zugrunde liegenden Naturgefahr. Sie ermöglichen die Abschätzung der Gefährdung sowie des potentiellen Schadenaufwands und liefern somit essentielle Informationen für den Umgang mit künftigen Katastrophenschäden und die Evaluierung von möglichen Anpassungsmaßnahmen. Es ist daher das vorrangige Ziel dieser Arbeit, das grundlegende Verständnis von Schadensfunktionen zu stärken, um eine systematische und übergreifende Schadensabschätzung zu ermöglichen.

Schadensfunktionen zur Abschätzung regionaler Schäden sind oft nur eingeschränkt verfügbar, da mangelnde Datenverfügbarkeit ein wesentliches Hindernis für deren Entwicklung und Kalibrierung darstellt. In der vorliegenden Arbeit erlauben neu verfügbare und hoch aufgelöste Sturmschadensdaten einen frischen Blick auf die Relation zwischen Windstärke und Sturmschaden. Auf Grundlage dieser Daten, wird eine neuartige Sturmschadensfunktion entwickelt und mit bestehenden Schadensfunktionen verglichen. Es zeigt sich, dass die Relation des Schadens zum verursachenden Wind einem einfachen Potenzgesetz folgt, dessen Exponent jedoch einen signifikant höheren Wert annimmt als eingangs erwartet. Während der Verlauf der Kurve bei extremen Windgeschwindigkeiten bestehenden Schadensfunktionen ähnelt, lässt die neu entwickelte Schadenfunktion die Abschätzung potentieller Schäden über einen deutlich breiteren Windbereich zu. Bezüglich beobachteter Schäden zeigt sich, dass die Schwankungen der Schadenswerte im Wesentlichen durch Unsicherheit in der Windermittlung begründet sind. Diese Schwankungen lassen sich in guter Näherung durch eine Lognormalverteilung beschreiben.

Über das Spektrum von Windschäden hinaus werden analoge Ansätze zur Abschätzung von Schäden durch Küstenfluten sowie, auf schematischer Ebene, zur Modellierung von hitzebedingten Todesfällen identifiziert. Diese Ansätze lassen sich in eine einheitliche mathematische Form bringen und dienen als Basis für die Analyse des Einflusses verschiedener Unsicherheitsfaktoren auf die Schadenshöhe. Hierbei liegt der Schwerpunkt der Unsicherheitsanalyse, im Gegensatz zu vorhergehenden Studien, auf der Transformation von Unsicherheit zwischen der Mikro- und der Makroskala. Die Ergebnisse zeigen, dass die Relevanz mikroskaliger Unsicherheiten auf der Makroebene erhalten bleibt. Schlussendlich dominieren jedoch extrinsische Unsicherheitsquellen, wie die bereits erwähnte Unsicherheit aus der Windermittlung.

Insgesamt liefert die vorliegende Arbeit eine Vielfalt von Erkenntnissen für das Verständnis von Schadensfunktionen. So bietet die neuartige Sturmscha-

densfunktion eine Verbesserung der Schadensprognose und ermöglicht eine genauere Beurteilung der negativen Auswirkungen des Klimawandels. In einem umfassenden Vergleich werden zudem erstmals die bestehenden Ansätze zusammengebracht und quantitativ verglichen. Darüber hinaus sprechen die Ergebnisse für die Widerlegung der Hypothese einer kubischen Wind-Schaden-Relation. Es ist im Weiteren davon auszugehen, dass die Vereinheitlichung klimarelevanter Schadensfunktionen den Wissenstransfer zwischen den verschiedenen Feldern der Naturgefahrenforschung erleichtert. So bildet z.B. die Unsicherheitsanalyse eine Grundlage um künftige Arbeiten zur Reduzierung von Unsicherheiten auf wesentliche Unsicherheitsquellen zu fokussieren. Mit ihrem interdisziplinären Ansatz ist die vorliegende Arbeit von hoher Relevanz für die Naturgefahrenforschung sowie die Atmosphärenwissenschaften.

Publications

The work at hand is presented as a thesis by publication and comprises the following research articles that were published in ISI-indexed journals:

- Chapter II: Prah, B. F., Rybski, D., Kropp, J. P., Burghoff, O., and Held, H. (2012). Applying stochastic small-scale damage functions to German winter storms. *Geophys. Res. Lett.*, 39(6):L06806, doi: 10.1029/2012GL050961.
- Chapter III: Prah, B. F., Rybski, D., Burghoff, O., and Kropp, J. P. (2015). Comparison of storm damage functions and their performance. *Nat. Hazards Earth Syst. Sci.*, 15(4):769–788, doi: 10.5194/nhess-15-769-2015.
- Chapter IV: Prah, B. F., Rybski, D., Boettle, M., and Kropp, J. P. (2016). Damage functions for climate-related hazards: Unification and uncertainty analysis. *Nat. Hazards Earth Syst. Sci.*, 16(5):1189–1203, doi: 10.5194/nhess-16-1189-2016.

In order to provide a consistent appearance of the research articles, minor spelling and technical changes have been made to the corresponding chapters. A few additional comments on the published text were added as footnotes.

Acknowledgments

I would like to thank Jürgen Kropp, Hermann Held, Jörg Pietsch, and Hans Joachim Schellnhuber for the opportunity of writing my doctoral thesis at the Potsdam Institute for Climate Impact Research (PIK). In particular, I want to thank Jürgen for his valuable advice and his support to work freely on such an interesting topic.

I am also very grateful to Uwe Ulbrich for the regular meetings and fruitful discussions as well as the possibility to do a doctorate under his supervision.

I am indebted to Diego Rybksi for his constructive mentoring and for his timely insistence to proceed on my chosen path.

I would like to thank the German Insurance Association and in particular Olaf Burghoff for providing the data on which much of my work relies.

I very much enjoyed the vibrant and joyful company of my fellow researchers in the CCD group at PIK, many of whom I gladly count among my friends. Special regards go to Markus Böttle, Ramana Gudipudi, Linda Krummenauer, and Carsten Walter for all the happy moments we shared together.

I am much obliged to Kerrin Franke for sharing the emotional weight during the early stages of my research.

Also noteworthy are the numerous foosball aficionados with whom I spent many an hour relieving the stress of my work. I have been literally indebted to Christian Pape, to whom I lost no less than twelve beers one late afternoon.

Last but not least, I am deeply grateful to my parents for their unconditional love and support.

Contents

I	Introduction and Research Agenda	1
1.1	Motivation	1
1.2	Introduction to Damage Functions	2
1.2.1	Translating Hazard Intensity to Loss	2
1.2.2	Storm Damage Functions	5
1.2.3	Coastal Flood Damage Functions	7
1.3	The Challenge from Hazard–Loss Data	9
1.4	Research Questions	10
1.4.1	The Wind–Loss Relationship	10
1.4.2	The Role of Uncertainties in Damage Functions	11
1.4.3	The Unification of Damage Functions	12
1.5	Methods and Structure of the Thesis	13
II	Applying Stochastic Small-Scale Damage Functions to German Winter Storms	15
2.1	Introduction	16
2.2	Data	17
2.3	Motivation of the Damage Function	17
2.4	Parametric Simplification	21
2.5	Modelling Results	23
2.6	Discussion	25
III	Comparison of Storm Damage Functions and their Performance	29
3.1	Introduction	30
3.2	Data and Methods	32
3.2.1	Insurance Data	32
3.2.2	Wind Gust Data	34
3.2.3	Model Calibration	36
3.2.4	Model Estimation Procedure	36
3.2.5	Validation Metrics	37
3.3	Storm Damage Models	38
3.3.1	Generic Exponential Damage Function	38
3.3.2	Probabilistic Power-Law Damage Function	39
3.3.3	Cubic Excess-Over-Threshold Damage Function	40
3.3.4	Probabilistic Claim-Based Damage Function	42
3.4	Comparison Results	43
3.4.1	Daily Loss per District	44
3.4.2	Countrywide Daily Loss	46
3.4.3	Most Severe Storm Events	49
3.5	Towards a Synthesis of Storm Damage Functions	52
3.6	Discussion and Concluding Remarks	54

Appendices to Chapter III	
3.A	Mathematical Model Description and Calibration Setup 59
3.A1	Generic Exponential Damage Function 59
3.A2	Probabilistic Power-Law Damage Function 59
3.A3	Cubic Excess-Over-Threshold Damage Function 61
3.A4	Probabilistic Claim-Based Damage Function 62
3.B	Supplementary Material 66
3.B1	Binomial Test for Model Performance 66
3.B2	Results for Different Set-Ups of Models K and H 66
3.B3	Countrywide Test Results Based on ERA-I Data 68
3.B4	Winter Storm Results Obtained from ERA-I Data 70
IV Damage Functions for Climate-Related Hazards: Unification and Uncertainty Analysis 73	
4.1	Introduction 74
4.2	Unified Damage Functions 75
4.2.1	Coastal Floods – Explicit Threshold Representation 75
4.2.2	Wind Storms – Implicit Threshold Representation 78
4.2.3	Extension to Heat-Related Mortality 79
4.3	Uncertainty 80
4.3.1	Brief Taxonomy of Uncertainty Sources 80
4.3.2	Probabilistic Description of Uncertainty 82
4.4	Case Studies for the Sensitivity Analysis 83
4.5	Sensitivity Analysis 86
4.5.1	Method 86
4.5.2	Results from the Sensitivity Analysis 90
4.6	Conclusions 92
Appendices to Chapter IV	
4.A	Uncertainty Parameterization 97
4.A1	Lisbon Case Study for Coastal Flooding 97
4.A2	Storm Damages in a German Building Portfolio 98
4.B	Supplementary Material 99
4.B1	Additional Indices for the Sensitivity Analysis 99
4.B2	Additional Results for the Lisbon Case Study 100
4.B3	Additional Results for the Storm Case Study 102
V Conclusions and Outlook 105	
5.1	General Achievements 105
5.2	The Challenge from Hazard–Loss Data 107
5.3	The Wind–Loss Relationship (RQ1) 109
5.4	The Role of Uncertainties in Damage Functions (RQ2) 111
5.5	The Unification of Damage Functions (RQ3) 113
5.6	Outlook and Concluding Remarks 116
Bibliography 119	

List of Figures

Figure 1.1	The main contributions of the different chapters for answering the research questions	13
Figure 2.1	Example of the damage function and the occurrence probability for an arbitrary district	18
Figure 2.2	Spatial distribution of the exponent and the available DWD stations	20
Figure 2.3	Correlations among model parameters and external factors	22
Figure 2.4	Model estimates for the winter storms Lothar, Jeanett, and Kyrill	23
Figure 2.5	Model estimates for annual winter-storm loss	24
Figure 3.1	The distribution of losses during the winter half-year and the locations of DWD stations	33
Figure 3.2	Example of model predictions for a single district obtained from each of the four damage functions	41
Figure 3.3	A map of Germany showing the minimum coefficients of variation for DWD and ERA-I data	45
Figure 3.4	Comparison of national loss estimates from each model with observations	47
Figure 3.5	Loss estimates for the six most severe winter storms based on DWD data	51
Figure 3.6	Gust dependence of the loss and claim ratios	53
Figure 3.7	Results of the binomial test for varying loss ranges	67
Figure 3.8	Comparison of national loss estimates from additional model setups with observations	69
Figure 3.9	Loss estimates for the six most severe winter storms based on ERA-I data	71
Figure 4.1	Examples of three empirical damage functions	77
Figure 4.2	Schematic composition of the damage function	77
Figure 4.3	Classification of the sources of uncertainty into intrinsic and extrinsic	81
Figure 4.4	The Lisbon urban cluster	84
Figure 4.5	Damage functions derived for the two case studies	89
Figure 4.6	Sensitivity results for the Lisbon case study	91
Figure 4.7	Sensitivity results for the German storm damage case study	93
Figure 4.8	First- and second-order indices of intrinsic and extrinsic uncertainty for the Lisbon case study	100
Figure 4.9	First- and higher-order indices of intrinsic uncertainty sources for the Lisbon case study	101

Figure 4.10	First- and second-order indices of intrinsic and extrinsic uncertainty for the German storm damage case study . . .	102
Figure 4.11	First- and higher-order indices of intrinsic uncertainty sources for the German storm damage case study	103

List of Tables

Table 3.1	The three loss classes defined for the winter half-year . . .	34
Table 3.2	Spatial averages of the coefficient of variation for each model	44
Table 3.3	Results from a binomial test for the prediction accuracy of the different models based on daily loss estimates	48
Table 3.4	MAPE and MPE estimates for each of the competing models and loss classes	49
Table 3.5	Dates of the six most severe winter storms during the period 1997–2007	50
Table 3.6	Ranking of the four damage functions according to their prediction quality, variability, and applicability . . .	57
Table 3.7	Comparison of the parameter values obtained for the federal state of Baden-Württemberg with the figures published by Heneka and Ruck (2008)	64
Table 3.8	Results from the binomial test for the prediction accuracy of the different models based on ERA-I wind gust data	68
Table 3.9	MAPE and MPE estimates for each of the competing models and loss classes based on ERA-I data	70
Table 4.1	The number of inundated buildings within the Lisbon urban cluster at hypothetical flood levels	85
Table 4.2	The parameterization of the Lisbon case study	87
Table 4.3	The parameterization of the German storm damage case study	87

Acronyms

CLC	CORINE Land Cover
CR	Claim ratio
CV	Coefficient of variation
DEM	Digital elevation model
DWD	German Weather Service (Deutscher Wetterdienst)
ERA-I	ERA-Interim reanalysis
GDV	German Insurance Association (Gesamtverband der Deutschen Versicherungswirtschaft e.V.)
IPCC	Intergovernmental Panel on Climate Change
LR	Loss ratio
MAPE	Mean absolute percentage error
MLE	Maximum likelihood estimation
MPE	Mean percentage error
PDF	Probability density function
RMSE	Root-mean-squared error
SLR	Sea level rise
VBSA	Variance-based sensitivity analysis
WH	Winter half-year

I

Introduction and Research Agenda

1.1 Motivation

Globally there is an increase of the number of climate-related disasters and their associated loss figures (CRED, 2015; Munich Re, 2015). The trend is driven by growing exposure, i.e. the accumulation of people and assets in risk-prone areas, as well as regional changes in climate, e.g. causing increased flood levels or prolonged heat waves. In order to prevent unprecedented damage levels, the abatement of the adverse effects of anthropogenic climate change – by means of mitigation and adaptation – has become a challenge for decision makers around the globe (IPCC, 2014).

Damage functions are unique in their role of providing the link between hazard, exposure and the resulting damage. As a key component of cost assessment, damage functions support and guide decision makers in natural hazards management and climate change adaptation (Meyer et al., 2013). With the capacity to differentiate regional vulnerability, damage functions provide essential information for targeted action in disaster risk reduction.

However, data scarcity and the complexity of the damaging processes are the main reasons that scientific advances in damage cost assessment have been lagging behind hazard modelling (Merz et al., 2010). The fragmentation of the information on damage functions is mostly due to non-public, regionally limited, or inconsistent data. In particular, data availability is an issue for many developing countries, where detailed post-disaster information (e.g. from well-developed insurance markets) is not available (de Moel et al., 2015). These aspects hinder both the development and the validation of damage functions. Furthermore, as damage functions are typically developed on a case study basis, a fundamental theoretical understanding of damage functions is missing. Existing approaches are highly specific to the considered hazard, leaving potential for knowledge transfer (Merz et al., 2010).

It is the overarching goal of this thesis to contribute to the understanding of damage functions, both from a practical perspective on damage functions for windstorms and from a theoretical perspective on the unification of damage functions for climate-related hazards. Accordingly, this work provides insight

on the wind–loss relation and discusses the functional form of storm damage functions. In the more general context of climate-related hazards, this work addresses the applicability of a common damage function to different hazards. Finally, based on a unified approach the role and interrelation of uncertainty sources is investigated at different spatial scales.

1.2 Introduction to Damage Functions

1.2.1 Translating Hazard Intensity to Loss

Damage functions are widely employed to model the relation between a hazard and the inflicted damage. The general concept of a damage function represents an idealization of the complex damaging processes, which are both poorly understood and difficult to observe. Accordingly, damage functions relate one or more indicators for the hazard intensity to a specific damage type, e.g. gust speed to monetary storm damage. Moreover, they may relate to either a single structure or a portfolio of structures (Merz et al., 2010; Walker, 2011).

Across the different disciplines, damage functions are discussed under various names. With a focus on specific damage states, structural engineers have coined the phrase *fragility curves* (Unanwa et al., 2000), while from an economic perspective the term *loss function* (Watson and Johnson, 2004) is employed. Dependent on the research goal, the natural hazards community employs several terms: *damage function* (Merz et al., 2010), *susceptibility function* (Meyer et al., 2013), and *vulnerability function* (Fuchs et al., 2007).

The damage function is an integral component of risk assessment. Such risk is determined not only by the *hazard* (e.g. climate and weather events) but also by the *exposure* and the *vulnerability* to these hazards (Cardona et al., 2012). Since a variety of alternative notions for risk are employed in the different scientific communities (Costa and Kropp, 2013; Thywissen, 2006), this work defines the constituents of risk as follows.

The hazard component represents a probabilistic description of the occurrence of an event which may cause adverse effects. The exposure component refers to the inventory of elements (e.g. people or assets) in an area in which hazard events may occur (Cardona et al., 2012). The vulnerability component then relates the intensity of the hazard event to the severity of the adverse effects. When adverse effects take the form of damages, the vulnerability component can be represented by a damage function.

One key difference of the various connotations of damage functions is the differentiation of relative and absolute damage. The focus may be either on what fraction of a structure is damaged or on the estimation of potential monetary loss. The work at hand follows the first definition, with the intention to generalize the functional form of damage functions and transform the relative damage to loss at a later stage.

The definition of relative damage is inherently challenging as it requires to value the damaged fraction against the whole. When dealing with economic losses, the damage ratio can be defined as the ratio of repair cost to the replacement value of a structure. However, from an insurance perspective it may be more adequate to compare repair cost in the form of insurance payout against insured value. Hence, the relative damage is dependent on the choice of reference, either the initial or the current value¹.

Whatever the reference, the damage function is physically limited between no damage and complete destruction, i.e. zero and one in relative terms. Actual damages to individual structures are a consequence of cascading failures of its components (Unanwa et al., 2000) and hence increase incrementally (Vickery et al., 2006; Hamid et al., 2010). During a storm, for example, a breach of the building envelope due to a broken window severely compromises the resistance of the remaining structure and can cause a sudden leap in damage. Without intricate knowledge of the incident wind and the failure state of each component, a damage function can merely reflect the mean response of a class of structures to the hazard (Pita et al., 2013). Hence, throughout this work the term damage function refers to a mean damage function that represents a smooth and monotonous statistical average of the actual damages.

The shape of the damage function is determined by a set of properties that characterize the structures under consideration. These properties (e.g. building type, construction type, materials, etc.) could be chosen to differentiate between important hazard response types. In practice, the number of discernible response types is often limited by data availability such that only a basic subdivision is feasible, e.g. residential versus commercial use.

Evidently, the response of a structure is dependent on the specific hazard. Certain perils such as hurricanes may combine more than one hazard, e.g. storm surge, extreme wind gusts, and heavy precipitation. Accordingly, damage functions can be employed to model each sub-peril or, alternatively, their joint effect. In each case the response of the structure to the particular hazard determines the shape of the damage function.

Beyond physical considerations, risk tolerance and socio-economic conditions may influence (insured) losses and with them the shape of the inferred damage function. Stakeholders in one region may be more tolerant to minor damages, while in another region complete repair is considered good custom. Additionally, socio-economic conditions have an influence on maintenance and lead to variations in the vulnerability of otherwise similar structures. These soft aspects are difficult to quantify and detailed information is required to infer their effect in practice.

Of particular importance is the spatial scale at which the damage function operates. Even under seemingly similar settings, disparate scales can result in varied shapes of the respective damage functions (Merz et al., 2010). This aspect

¹ Note that there is a discussion whether to employ replacement values or depreciated values (Merz et al., 2010).

is often overlooked when comparing damage functions that relate to a structure, a sub-structure, or a system of multiple structural components. In line with Merz et al. (2010), this work relates *microscale* with single structures at risk, while the entire system is referred to as *macroscale*. Naturally, both scales are related since any macroscale damage is comprised of a number of microscale damages. So far, this relationship has been considered for some climate-related hazards, most notably for coastal flooding (e.g. Hinkel et al., 2014) and for winter-storm damage (e.g. Heneka and Ruck, 2008). However, in general little attention has been paid to the crossover of scales, in particular with regard to uncertainty.

When considering the impact of a natural hazard on a wider portfolio of structures, e.g. an urban agglomeration, the damage assessment may incorporate both *direct* and *indirect* damages (Merz et al., 2010). While the former are a direct consequence of the incidence of the peril (e.g. damage to infrastructure, crops, housing), the latter comprise secondary (e.g. induced production losses, unemployment) or higher order impacts (e.g. loss of tax revenue due to indirect production losses, market destabilization). Of particular importance for indirect damages is the identification of critical infrastructure, which typically form a part of a wider network of elements (Hammond et al., 2015).

Post disaster research has shown, that indirect socio-economic losses can potentially surmount direct losses from property damage (Hallegatte et al., 2007). For the landfall of hurricane *Kathrina*, Hallegatte (2008) has estimated indirect losses for the economy of Louisiana at about 40% of direct losses. Koks et al. (2015) show that expected annual loss is dominated by direct loss, while indirect losses drastically increase for very-low probability events.

Due to greater accessibility, a wide body of research has focussed on the assessment of direct damage to portfolios of specific structures (e.g. Meyer et al., 2013; Hammond et al., 2015). Direct damages are also the focus of the work at hand. In fact, the availability of established damage functions opens up the opportunity for a comparison of modelling approaches for various hazards and the identification of the common grounds of damage functions.

Damage functions are reliant on detailed loss data for calibration and validation. In general, these are subject to the rare occurrence of extreme events (e.g. coastal floods) and are only available within well-developed insurance markets. However, the proprietary nature of insured-loss data still limits the information available and impedes a fundamental understanding of the shape of damage functions (Merz et al., 2010; Walker, 2011). The lack of damage information also reduces the transferability of damage functions to developing countries.

If available, damage information typically takes the form of insurance-claim data. These data are characterized by a wide distribution of economic losses, comprising a large number of smaller losses and few extremely large losses. For the case of German storm damage, for example, average loss per residential building is of the order of €1000 while extreme losses can breach the million

Euro threshold (GDV, 2013). This fact is indicative of a very high dynamic range in conjunction with a heavily skewed probability distribution. In fact, actuarial research has shown that there is no simple parametric form for the damage probability distribution and modellers frequently resort to creating more complex approximations via mixing or splicing (Klugman et al., 2008).

The involved statistical averaging implies that damage functions are ill-suited for the prediction of actual damage of single structures (Merz et al., 2004; Walker, 2011). Typical storm damages, for example, involve a number of largely unharmed buildings, while comprising a few massive losses – neither of which are well captured by an expected value from a damage function. Instead, typical applications of damage functions include the prediction of expected losses in an insurance context, or the distinction of regional vulnerability patterns.

The low predictability of actual damages, including the potential absence of damage, must also be considered when assessing the predictive power of damage functions. Any validation that is based solely on cases of actual damage will be subject to selection bias, since the damage function represents the average damage related to both damaged and unharmed structures.

1.2.2 Storm Damage Functions

Global storm damages amount to 40 % of world-wide economic losses and 58 % of insured losses between 1980 and 2014 (Munich Re, 2015). For Europe, insured loss from the largest event so far, winter storm *Daria* in 1990, was estimated at \$ 8.6 billion in 2013 values (Swiss Re, 2014).

European storm loss is dominated by wind damage from extra-tropical cyclones that are common during the autumn and winter months, so called winter storms. Putting an emphasis on German storm loss, the work at hand hence focusses on windstorm damages. Accordingly, the term *storm damage function* is used to denote a damage function for windstorm damage, as opposed to other storm categories such as hailstorms, tornadoes, or rainstorms.

Climate change is envisaged to have an amplifying effect on the intensity and, arguably, on the frequency of winter storms in Central and Western Europe (Feser et al., 2015; Mölter et al., 2016). For the evaluation of the adverse effects of a changing storm climate, accurate storm damage functions are required. Sound storm damage estimates may reveal adaptation potential and can be employed to assess the effectiveness of adaptation measures. Furthermore, climate change could affect the insurability of storm risk (Held et al., 2013), and its assessment hinges on the choice and quality of the employed storm damage function.

A storm damage function relates meteorological indicators to storm loss. Suitable indicators provide a measure of the intensity of a storm, which defines the strength of the storm with respect to the severity of the damage caused. For windstorms the academic literature mainly focusses on simple univariate damage functions that employ some measure of peak wind speed, e.g. maximum

daily gust. Hence, typical quantities used are the maximum gust (3-seconds average) or the maximum sustained wind speed averaged over 10 minutes (Walker, 2011). In practice the choice of wind measure is also limited by the resolution of the spatio-temporal wind field data and the involved measurement (or modelling) uncertainty.

Further meteorological parameters, such as storm duration and precipitation, are likely to have an effect on the total damage. During a long-lasting storm local structures face a higher probability of experiencing the maximum gust speed indicated. Moreover, fatigue from continued material stress could increase the probability of structural failure. Indeed, Swiss Re (1993) has reported² a dependence of the number of insurance claims on the duration of winter storms. However, this could not be confirmed by Dorland et al. (1999), who did not find a statistically significant dependence between insured losses and storm duration. Addressing the potential impact of precipitation, Sparks and Bhinderwala (1994) have reported a strong damage increase if damaged roofs or windows allow rain to enter the interiors. In practice, the limited availability of data and the high level of uncertainty hinders the calibration of models that include such additional meteorological or physio-graphical (e.g. surface roughness) variables.

Storm damage functions are typically tailored to the exposed assets and calibrated to structural classes. For instance, a statistical damage function developed from residential insured loss is specific to the residential class of buildings. In engineering-based approaches building classes are defined by their substructure, and corresponding damage functions are based on detailed load modelling as well as wind-tunnel experiment (Walker, 2011). Hence, the engineering-based approach offers greater versatility, due to the capacity of composing building classes from sub-structures. Thus, once calibrated the approach benefits from being less reliant on observational data, and if the individual components of the structural class are known, engineering-based damage functions can in principle also be employed for data-scarce regions. However, actual losses are also influenced by socio-economic conditions and specific construction variants. Since their effect on loss cannot be evaluated without observational data, the transfer of damage functions requires both expert judgement and statistical validation.

While engineering-based approaches have become the standard for the modelling of hurricane wind damage in the USA³, equivalent approaches for European storm damage are lacking. With an emphasis on German storm loss, the work at hand hence considers a variety of statistical storm damage functions.

As previously stated, damage functions describe the mean response of a specific class of structures to a certain hazard intensity. It follows from this definition that one should expect differences between damage functions across different classes and even regions, but academic literature even reports considerable

² As reproduced in Table 3 of Heneka and Ruck (2004).

³ As applied, for example, in the HAZUS-MH model (Vickery et al., 2006) or the Florida Public Hurricane Loss Model (Pinelli et al., 2008).

differences for identical class and region. For the case of German residential buildings – a focus of this study – several different shapes of damage functions have been reported. For instance, the analysis of reinsurance data by Munich Re (1993, 2001) indicated a power-law relation between loss and wind gust, albeit exponents appeared to fluctuate for different storms. In contrast, Klawa and Ulbrich (2003) applied a cubic power law to the exceedance of wind speed above a local threshold. Assuming an individual threshold for each building, Heneka et al. (2006) proposed a damage function derived from the cumulative distribution of thresholds.

In summary, there is considerable ambiguity about the shape of storm damage functions and their theoretical support. Arguments that relate the kinetic energy of the wind to the caused losses are not well supported by empirical data. Comprehensive analysis is hampered by the availability of loss data that are of a proprietary nature and by uncertainties in the representation of the wind field. Furthermore, actual damages may be caused by both structural failure (overstressing) under peak wind loads and fatigue under fluctuating loads at lower wind levels (Holmes, 2015). Damages of the latter kind are often not reflected in the existing damage functions, which focus on direct damage caused by peak gusts.

1.2.3 Coastal Flood Damage Functions

Coastal regions are of high relevance for human habitation and economic activity (McGranahan et al., 2007; Blackburn et al., 2013). Under the constant threat of coastal flooding, protection measures are deployed to minimize adverse effects on livelihoods, commerce, and industry. However, in the wake of anthropogenic climate change, sea level rise (SLR) will severely compromise existing flood protection levels. By the year 2100, global annual loss from coastal flooding could amount to 0.3–9.3% of the global gross domestic product (Hinkel et al., 2014). The devastating magnitude of estimated losses becomes evident if compared against the mean annual economic loss from natural hazards between 2005 and 2014 – approximately 0.23% of global GDP (Munich Re, 2015; World Bank, 2015).

Nowadays, two out of three cities with a population of above 5 million are located at least partially within low-elevation coastal zones (McGranahan et al., 2007). Moreover, coastal zones tend to be the most urbanized ecosystems in all regions of the world (UN-Habitat, 2008). Due to the high population density and the associated accumulation of risk in built-up areas, the majority of economic loss caused by coastal flooding is in fact attributed to urban areas (Jongman et al., 2012). These losses are typically caused by property damage, displacement of residents, and disruption of transportation (UN-Habitat, 2011).

In practice, there is a complex relationship between the occurrence of coastal floods and the associated destruction and loss. On the one hand, it is difficult to characterize the flood level, which is subject to storm surge, astronomic tide,

and wave action. On the other hand, the damaging processes are poorly understood and very much reliant on local conditions. Clearly, damages are related to inundation depth, but they are also influenced by factors such as flood duration, flow velocity, debris, and contamination (Merz and Thieken, 2009; Merz et al., 2010). The number of potential impact factors and the de facto lack of corresponding data are the limiting factors for flood damage functions and lead to a concentration on the effect of inundation depth only (Cammerer et al., 2013).

Accordingly, depth–damage functions⁴ are the accepted standard for translating a given inundation level into monetary damage (Merz et al., 2010; Cammerer et al., 2013). These damage functions can be calibrated on data from actual flood events, either for single buildings (microscale) or entire cities or regions (macroscale).

If not measured directly, the inundation level can be estimated by offsetting the flood level with elevation data, which are typically obtained from LiDAR measurement or digital elevation models. Modellers also frequently resort to a steady state water depth called *stillwater*, instead of considering the actual flood level. Stillwater refers to the flood level not including the effects of waves or tsunamis, but including storm surge and astronomic tide (Divoky et al., 2005). This is also the approach followed in the work at hand.

The fact that flood damages do not directly correspond to the hazard intensity (flood level), but rather depend on a derived quantity (inundation), is in contrast to other hazards such as windstorms, where structures are directly exposed to the full intensity of the hazard. In practice, the modelling of inundation contributes additional uncertainty to the damage assessment.

Similar to other hazards, data availability poses a severe constraint for the derivation and validation of flood damage functions. In particular, information about macroscale damage is scarce and few studies discuss the shape of macroscale damage functions (Boettle et al., 2013). While there is more information on microscale damages, the data show a high level of dispersion (Merz et al., 2004). It is a consequence of certain hazard or building characteristics that are insufficiently represented either by the employed geographical data or within the modelling process.

Furthermore, since all data are specific to the location and time of observation, spatial and temporal transfer remains a challenge (Merz et al., 2010). Often, the only resort is the application of synthetic damage function, where flood damage curves are based on expert judgement. However, without the possibility of validating against empirical data, these damage functions yield little insight on the general characteristics of flood damage functions.

⁴ Often referred to as stage–damage curves. See Smith (1994) on the historical development of the concept.

1.3 The Challenge from Hazard–Loss Data

Empirical data on the intensity and corresponding loss of a hazard event are essential for the development, calibration, and validation of damage functions. From a general point of view, these data can be characterized by four distinct properties: i) high dynamic range, ii) a skewed distribution, iii) heteroscedasticity, and iv) ambiguity between affected and unaffected structures.

Dynamic range is defined as the ratio between the largest and smallest values of a changeable quantity. In the hazard context, it reflects the difference in magnitude of small events and severe catastrophes. For instance, the storm losses observed by the German Insurance Association (GDV) at the NUTS 3 level range over approximately 4 orders of magnitude.

The frequency distribution of loss events is typically very uneven and in fact strongly skewed towards frequent small events. Catastrophic high impact events are exceedingly rare, and extrapolation – typically via extreme value theory – is required to consider return periods around or beyond the observed time frame.

Heteroscedasticity is frequently encountered when relating indicators for the hazard intensity to empirical loss data. It refers to the variance of losses being conditional on the magnitude of the hazard. For instance, heteroscedastic relations are observed for storm damage, where variance increases with storm intensity (e.g. Heneka and Ruck, 2008).

When dealing with stochastic damage processes there is a general ambiguity whether a particular structure is affected by a given hazard or not. Such is the case for storm damages, where the occurrence of loss for a specific building cannot be predicted due to incomplete information on the incident wind and the failure state of its structural components. Consequently, similar structures may experience different degrees of damage – or no damage at all – even under comparable conditions. Thus, spatial loss patterns are often incoherent and difficult to predict on a local scale.

These four properties of natural hazard data pose a challenge for the development, the calibration, and the validation of damage functions. Despite its high relevance, the issue has not received much attention in the academic literature on damage functions. The challenge from hazard–loss data is addressed at multiple points throughout this work and solutions are found in order to support the three research questions described in the following.

1.4 Research Questions

1.4.1 The Wind–Loss Relationship

Strong wind constitutes the chief cause of storm damage. It is common practice to relate losses to a measure of maximum wind speed, such as maximum 3 s gust or maximum 10 min averaged wind (Walker, 2011). Detailed loss data are almost always of a proprietary nature and thus not widely available to the scientific community. Therefore, previous studies on German storm loss have been based either on aggregate data (Klawa and Ulbrich, 2003) or on data sets that are only regionally available (e.g. for the state of Baden-Württemberg see Heneka and Ruck, 2008). For the first time, the GDV has recently made available highly resolved data covering all German administrative districts (NUTS 3 level, Held et al., 2013). These data open up new pathways to the analysis of the wind–loss relationship.

The vulnerability of buildings to windstorms has been shown to vary regionally (e.g. Khanduri and Morrow, 2003; Donat et al., 2011b). In fact, there is a wide range of proposed models, comprising exponential, power-law, and threshold models⁵. The multitude of damage functions raises the question, whether there exists a genuine damage function that can be regionally parameterized or whether the regional damage characteristics differ more substantially.

On theoretical grounds, the occurrence of storm damage has been linked to the dissipation of wind kinetic energy, which is described by a cubic function of wind velocity (Emanuel, 2005; Kantha, 2008). Despite partially drawing on this idea, available damage functions for German storm loss (Klawa and Ulbrich, 2003; Heneka and Ruck, 2008) deviate from a purely cubic relation. Furthermore, there is evidence on damage functions with much higher exponents that drastically deviate from the cubic assumption (Nordhaus, 2010). Deviation of this sort have strong implications for damage assessment of extreme storm events and must be addressed especially in the light of a changing climate.

The GDV data at hand allow to investigate further into the optimal shape of a storm damage function and to evaluate existing approaches. This gives rise to the First Research Question (RQ1).

Research Question 1

What is the statistical wind–loss relationship for German residential buildings, and how does it compare to existing damage functions?

⁵ Threshold models consider the exceedance of hazard intensity above a certain threshold level. They may be of a similar functional form as the competing models, e.g. power law or exponential.

1.4.2 The Role of Uncertainties in Damage Functions

Damage functions approximate the average outcome of complex physical processes and are hence subject to uncertainty. In fact, research on flood and storm damage reveals daunting levels of uncertainty (Merz et al., 2004; Heneka and Ruck, 2008; Nordhaus, 2010; de Moel et al., 2012). This aspect highlights the importance of identifying relevant sources of uncertainty and scrutinising how uncertainty is propagated through the modelling chain.

The definition of uncertainty is intrinsically linked to the modern understanding of probability. In fact, probability theory defines two kinds of uncertainty: statistical uncertainty that arises from random processes, as well as epistemological uncertainty that reflects incomplete knowledge or degrees of belief about a system (Hacking, 1984).

These two facets of uncertainty are frequently taken up in natural hazards research, where the differentiation between *aleatory* (i.e. statistical) and *epistemic* uncertainty is made (Apel et al., 2004). Depending on the scientific aim, many alternative categorisation of uncertainty have been developed (Thunnissen, 2003), often putting particular emphasis on aspects, such as model and parametric uncertainty, that otherwise may have been classified as epistemic (e.g. Bedford and Cooke, 2001).

Aleatory uncertainty is regarded as a measurable uncertainty that can be grasped by statistical methods (Deck and Verdel, 2012). As such it is tractable and has been widely studied in the field of natural hazards (e.g. for the case of flood risk see Apel et al., 2004; Merz and Thielen, 2009). However, the focus of prior research has been on the attribution of overall uncertainty, irrespective of the hazard intensity and neglecting the scale of the analysis. In the case of a regional assessment of damages, local damages must be aggregated on a wider scale. However, it is generally unclear how the associated uncertainties propagate between the different scales. As a matter of fact, macroscale damage functions are intimately connected with their microscale counterparts (an aspect that is subject to the Third Research Question as defined in the following section). This connection opens up the opportunity for analysing the interaction of uncertainty sources across spatial scales and leads to the Second Research Question (RQ2).

Research Question 2

How are the sources of statistical uncertainty in damage functions interrelated, and what is their importance on different scales?

1.4.3 The Unification of Damage Functions for Climate-Related Hazards

Damage functions are an essential part of damage assessment in natural hazards research. However, there has been limited interchange between research conducted in the different hazard domains. The resulting difficulties when comparing damage assessment across hazards and sectors have implications for decision support and policy development (Meyer et al., 2013).

Even within a particular hazard domain, e.g. flood hazard, there is incomplete integration across scales. De Moel et al. (2015) have argued that better integration of scales would enable rapid assessments of flood risk for local policy makers in regions where few data are available. Similarly the Intergovernmental Panel on Climate Change (IPCC, 2012) concludes that “there is room for improved integration across scales from international to local”.

However, the comparability of the various approaches is hampered by different data sources, terminologies, and methodological approaches (World Bank and United Nations, 2010; Meyer et al., 2013). As a result, there is a need for the development of damage models on an intermediate level of complexity, bridging the gap between interregional and local impact assessment and providing transparent and transferable methodology.

It has further been acknowledged, for example, that advances in flood damage assessment could trigger methodological improvement in areas such as windstorms (Merz et al., 2010). However, in order to expedite such knowledge transfer a unification of damage functions for different hazards is required.

Consequently, the goal of the Third Research Question (RQ3) is the identification of the common grounds of damage functions for the main climate-related hazards, (coastal) flooding and storm damages. At intermediate complexity, the sought-after damage function should bridge scales by allowing for a rapid top-down appraisal of total damage as well as a detailed view on local damages. Furthermore, a unified damage function should provide a probabilistic view on damage estimates and incorporate uncertainty as addressed by the previous research question.

Research Question 3

What are the commonalities between damage functions for the different climate-related hazards windstorm and coastal flooding, and how could these damage functions be unified?

1.5 Methods and Structure of the Thesis

The mechanisms that determine damage functions are a central theme of the work at hand. The presented research explores these mechanisms with a view on three complementary research facets: *depth*, *breadth*, and *scope*. As illustrated by Fig. 1.1, each facet is represented by a separate chapter. Each of these chapters has been written and published as a stand-alone and peer-reviewed research article.

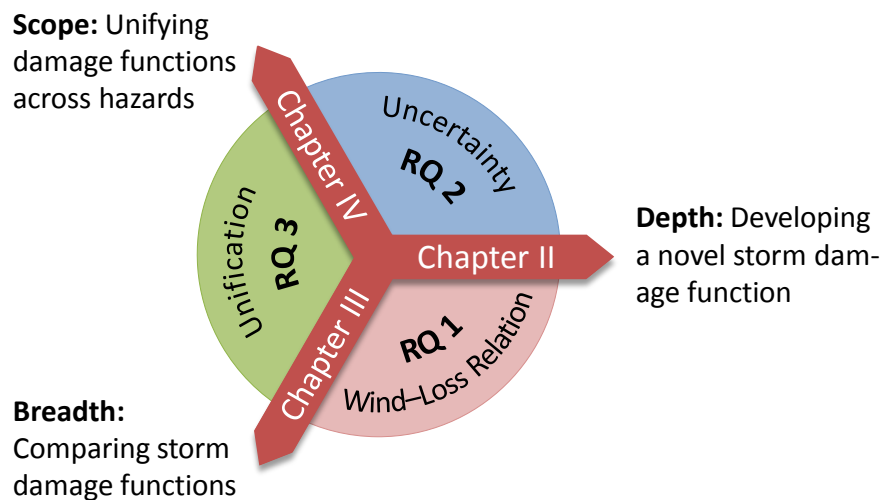


Figure 1.1: The main contributions of the different chapters for answering the research questions. Beginning with the storm hazard, a novel storm damage function is elaborated in *depth* (Chapter II) and its performance is compared against the *breadth* of existing storm damage functions (Chapter III). Finally, the *scope* of the considered damage functions is widened to further climate-related hazards (Chapter IV).

In Chapter II, a novel storm damage function is developed for residential buildings in Germany. German insurance losses are related to extreme wind gusts at the scale of single administrative districts (NUTS 3 level) based on the newly available data obtained from the GDV.

Using statistical estimation techniques, in particular maximum likelihood regression, a power-law model⁶ is calibrated on the available data. Addressing RQ1, the steepness of the damage function is analysed and compared against both theoretical and empirical expectations. Log-normal uncertainty bands are derived from the data and the potential sources of uncertainty are discussed, thus contributing to RQ2.

Chapter III is devoted to a comparison of existing storm damage functions for German residential losses. In order to establish a level playing field, four

⁶ If losses are small in comparison to the insured value, a power law is an approximation to the more general log-logistic curve.

distinct models including the novel damage function are set up on identical meteorological and loss data. Wind-gust data from observations by the German Weather Service (DWD) and the ERA-Interim reanalysis (ERA-I) are put into context with the high-resolution loss data provided by the GDV.

Addressing the key challenge of dealing with natural hazard data, the issue of skewed, heteroscedastic data with high dynamic range is explored and the practical consequences are elaborated. In an effort to establish more robust calibration and evaluation of damage functions, conventional metrics are employed together with a newly developed statistical test based on straight-forward binomial statistics.

Beyond a mere assessment of the performance of damage functions, the comparison provides insight into the commonalities between the different approaches, contributing to RQ3. Of particular concern is the evident disaccord between the theoretical proposition of a cubic wind-loss relationship and any of the available damage functions. Providing a possible solution to this problem, it is shown how a simple threshold could reconcile both theoretical and practical approaches. These considerations also further contribute to RQ1 dealing with the nature of the wind-loss relation.

The third research paper is presented in Chapter IV. Here, the scope broadens from storm damage functions to further climate-related hazards. By identifying the common grounds of damage functions for windstorm and coastal flooding, the skeletal structure of a unified damage function is established. Guided by RQ3, a unified damage function is derived from first principles. The example of heat-related mortality demonstrates the potential of the unified approach for providing an accessible solution to the modelling of damages from very diverse hazards at intermediate complexity.

Furthermore, RQ2 is addressed by a comprehensive characterization of uncertainties along the modelling chain. The relevance of the different sources of uncertainty for the estimation of loss is assessed by means of a variance-based sensitivity analysis. For the first time, this approach considers the effects of uncertainties on both the local and the regional scale.

II

Applying Stochastic Small-Scale Damage Functions to German Winter Storms

Abstract. Analysing insurance loss data we derive stochastic storm damage functions for residential buildings. On district level we fit power-law relations between daily loss and maximum wind speed, typically spanning more than four orders of magnitude. The estimated exponents for 439 German districts roughly range from 8 to 12. In addition, we find correlations among the parameters and socio-demographic data which we employ in a simplified parameterization of the damage function with just three independent parameters for each district. A Monte Carlo method is used to generate loss estimates and confidence bounds of daily and annual storm damages in Germany. Our approach reproduces the annual progression of winter-storm losses and enables to estimate daily losses over a wide range of magnitudes.

This chapter has been published as:

Prahl, B. F., Rybski, D., Kropp, J. P., Burghoff, O., and Held, H. (2012). Applying stochastic small-scale damage functions to German winter storms. *Geophys. Res. Lett.*, 39(6):L06806, doi: 10.1029/2012GL050961.

© American Geophysical Union 2012.

2.1 Introduction

A storm damage function describes losses as a function of observable meteorological parameters, typically maximum wind speed. For winter storms occurring in central Europe several storm damage functions for residential buildings are described in the literature. The reinsurance company Munich Re (1993, 2001) found a power-law damage function of maximum wind speed with varying exponents of roughly 3 as well as 4–5, depending on the storm event and country being analysed. Klawns and Ulbrich (2003) proposed a power-law damage function with exponent 3, refined in Donat et al. (2011b), using excess wind speed over threshold instead of absolute maximum wind speed. Similarly, Heneka and Ruck (2008) used a power-law damage propagation function of excess wind speed with exponent of either 2 or 3, assuming proportionality to the force or the kinetic energy of the wind, respectively. Both groups define threshold wind speed as the empirical 98th percentile of the wind distribution. For the Netherlands Dorland et al. (1999) derived a damage function for residential property that can be reformulated as a power law of maximum wind speed with exponent 0.5. When comparing these studies with literature on hurricane losses in the United States (see Watson and Johnson, 2004, for an overview), one must be aware of the many differences in building structure and the nature of the hazard. However, following a similar approach to this article Huang et al. (2001) describe an exponential damage model for residential property in the South-Eastern United States based on 10 min averaged wind speed.

Our work is based on daily insurance loss data (years 1997–2007) with a regional resolution of administrative districts. From theoretical considerations we propose a stochastic power-law damage function depending on maximum daily wind speed to describe empirical losses. We find exponents typically ranging from 8 to 12. Statistical deviations are modelled by a spatially correlated stochastic variable drawn from a log-normal distribution. Correlations among parameters and with socio-demographic data are exploited to reduce the number of independent parameters to three per district. The model quality is assessed by out-of-sample calculations based on Monte Carlo simulations of losses in daily and annual resolution. We demonstrate good agreement between annual model results and empirical values, albeit observing a small potential underestimation of high losses. For the majority of districts we find high correlations between annual loss estimates and data. Absolute daily losses in Germany for the three most severe storms show good predictions of losses across four orders of magnitude.

This article is structured as follows: After a brief discussion of data, we describe motivation and details of the damage function in Sect. 2.3. A simplified parameterization of the damage function is demonstrated in Sect. 2.4. Finally, we present modeled loss estimates and close with the discussion of our results in Sects. 2.5 and 2.6, respectively.

2.2 Data

Insurance loss data from the years 1997 to 2007 were provided by the German Insurance Association (GDV). The data comprise daily losses due to wind and hail for 439 German administrative districts. To eliminate economic influences such as growing market penetration and price effects, loss data were divided by the total insured value of each district to obtain a dimensionless loss ratio. Further description of the loss data is given by Donat et al. (2011b). As the empirical loss data does not differentiate between wind and hail damages, we limit the scope of the analysis to winter months from October through March, during which damages are predominantly driven by high winds.

Data of daily maximum wind speed (3 s gust wind) are publicly available and were obtained from the German Weather Service (DWD) for 78 wind stations across Germany¹. Wind stations that were lacking more than $5 \times n$ measurements for a sampling period of n years were discarded. Typically, measurements were taken at 10 m height above ground.

2.3 Motivation of the Damage Function

A damage function should naturally have a sigmoid shape with steep initial increase and saturation at large wind speeds. Such growth processes are often modelled by a logistic function

$$d(x) = \frac{d_{\max}}{1 + e^{-cx}}, \quad (2.1)$$

where d_{\max} is the asymptotic upper bound and the exponent c determines the steepness of the function. We apply the transformation $x = \ln(v/b_v)$, with maximum daily wind speed v scaled by local constant b_v . Taking the logarithm reduces broadness and skewness of the distribution of daily maximum wind speeds and ensures that $\lim_{v \rightarrow 0} d(v) = 0$. Since recorded data show that for Germany $d \ll d_{\max}$, $d(v)$ can be approximated as

$$d(v) = \frac{d_{\max}}{1 + (v/b_v)^{-c}} \approx \left(\frac{v}{b}\right)^c, \quad (2.2)$$

where constants were combined to the new scaling parameter $b \approx b_v d_{\max}^{-1/c}$.

Figure 2.1 (a) shows the empirical loss data for an arbitrarily chosen district. By inspection we see that the logarithmically binned data reveals a strong increase for wind speeds higher than approximately 13 m s^{-1} and an approx-

¹ Available online at <http://www.dwd.de>

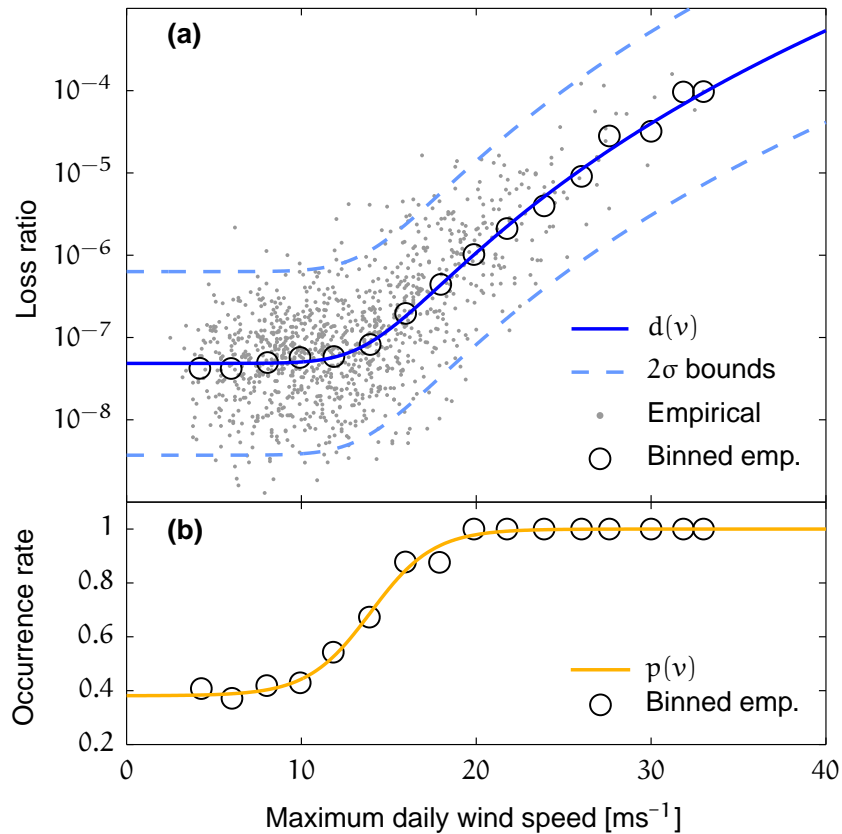


Figure 2.1: Example of the damage function and the occurrence probability for an arbitrary district. In (a) the damage function $d(v)$ is plotted against the maximum daily wind speed v . Confidence bounds of $\pm 2\sigma$ are shown by dashed lines. Grey points represent daily loss data. In (b) the fitted occurrence probability $p(v)$ is shown. Binned empirical data, shown as circles, are given as reference only.

imately constant regime for lower wind speeds. To capture this behaviour an additional constant offset a is introduced, giving

$$d(v) \approx \left(\frac{v}{b}\right)^c + a. \quad (2.3)$$

Calculating the residuals $\hat{\epsilon}$ between empirical data and $d(v)$, we find an approximately log-normal distribution of residuals with nearly constant scale parameter σ . For simplicity, we utilize this finding for modelling statistical deviations ϵ and hence describe losses via a stochastic variable

$$D_\epsilon(v) \sim \mathcal{LN}(\mu(v), \sigma^2), \quad (2.4)$$

where \mathcal{LN} represents the log-normal distribution and $\mu(v) = \ln d(v)$. $\mu(v)$ and σ are the mean and standard deviation, respectively, of the variable's natural logarithm.

So far the analysis accounts for the loss intensity given a loss event, leaving aside the probability of an event. An empirical occurrence rate of loss events

[Fig. 2.1 (b)] was calculated from linearly binned binary data, where a loss event was coded as '1' and days without loss as '0'. While the empirical occurrence rate is approximately 1 at high v , it drops to a constant base rate for $v \rightarrow 0$. Ideally, the occurrence rate could be derived from $D_\epsilon(v)$ as the probability of exceeding a certain loss threshold. We were not able to identify such threshold via censored regression modelling and hence chose to fit the data with an empirical occurrence probability function

$$p(v) = 1 - \frac{\alpha}{1 + e^{\gamma(v-\beta)}} , \quad (2.5)$$

with base probability $(1 - \alpha)$, shift β , and slope γ . Multiplying $D_\epsilon(v)$ with a stochastic weight function $w(v)$ based on $p(v)$, we obtain the complete stochastic damage function

$$\begin{aligned} D_{\epsilon,p}(v) &= w(v)D_\epsilon(v) \\ w(v) &:= \begin{cases} 1, & \text{if } P \leq p(v) \\ 0, & \text{if } P > p(v) \end{cases} \\ P &\sim \mathcal{U}(0, 1) . \end{aligned} \quad (2.6)$$

Maximum likelihood estimation was applied to calculate the parameters of $D_\epsilon(v)$ in an iterative process, alternating between computing parameters a , b , and c while keeping the scale parameter σ constant and vice versa (see pseudo-likelihood algorithm by Ruppert et al., 2003). A least-squares approach was used to fit the parameters of $p(v)$.

As some wind stations may not be representative for a given district, the wind station featuring the highest predictive power was chosen from a set of 5 wind stations closest to the geographical centre of the district. The coefficient of determination for non-linear regression models, generalized R^2 , was chosen as a measure of predictive power. For the given shape of the damage curve $d(v)$, R^2 values related to nearby wind stations indicate the level of variance inherent to the specific combination of district loss and wind data. Due to the high level of statistical deviation around $d(v)$ low R^2 scores would be expected for any smooth damage curve. In fact, all estimated R^2 scores lie within the interval $[0.2, 0.6]$, with an average of 0.42. High R^2 is seen for north-western coastal regions which often experience high winds. Regions with an R^2 score of 0.4 and below largely coincide with German low mountain ranges (Mittelgebirge) and along the southern alpine border. Best scores are hence generally obtained for regions with homogeneous elevation and high frequency of strong winds.

The spatial distribution of the exponent c estimated for all German districts is shown in Fig. 2.2. We find a slightly right-skewed distribution with mean 9.8. 80% of values are contained within the interval from 8.3 to 11.8. Values of 15 and beyond can be conceived as outliers, occurring in districts where wind measurements insufficiently differentiate losses even at high wind speeds.

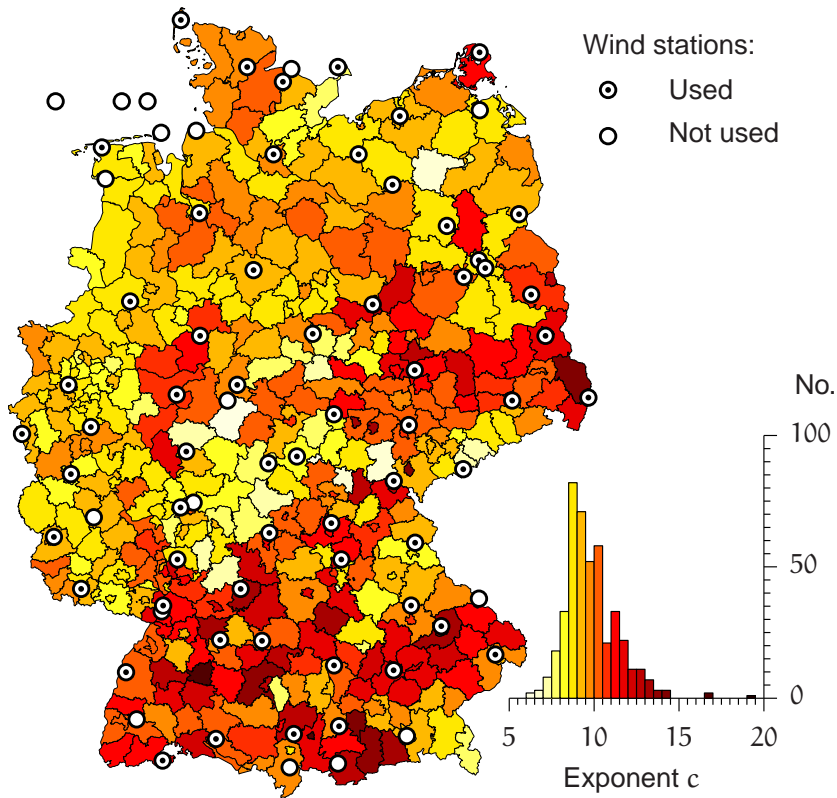


Figure 2.2: Spatial distribution of exponent c and DWD wind stations. The color code indicates the local values of c , summarized in the histogram inset. Markers indicate DWD wind stations that were used for calculations or excluded due to inhomogeneities or missing data.

Geographically, values of c below 10 predominate in Western, Central, and Northern Germany, while values above 10 are most often found across Southern Germany and the southern districts of East Germany.

Our analysis is based on the assumption that maximum wind speed is the dominating criterion for the occurrence and severity of storm damages. It was not feasible to quantify the effects from other potential factors (e.g. storm duration, precipitation, or turbulent winds). However, the presence of systematic large-scale deviations should be reflected in spatial correlations of the statistical deviations ϵ . In fact, calculations of Spearman's correlation coefficient from normalized residuals $\ln(\hat{\epsilon})$ showed significant spatial rank correlations between districts, ranging from -0.30 to 0.67 . While insignificant for the estimation of loss in single districts, these correlations must be accounted for when spatially accumulating loss across Germany. In order to reproduce the spatial correlations during the Monte Carlo calculations, the empirically estimated rank correlations were enforced on the random deviations ϵ of D_ϵ . The algorithm was implemented as follows:

- Determine pairwise Spearman's correlation coefficients $\rho_{i,j}$ of $\ln(\hat{\epsilon})$ between every possible combination of districts and thus populate matrix $\hat{\mathbf{M}} = [\rho_{i,j}]_{439 \times 439}$
- Determine the nearest positive-definite correlation matrix \mathbf{M} using the algorithm derived by Higham (2002)
- Use the iterative procedure by Iman and Conover (1982) to create spatially correlated random deviations $\ln(\epsilon)$.

We assume two main processes giving rise to the statistical deviations being found in Fig. 2.1 (a). Firstly, the correlation between wind speed measurements at separate sites is known to decrease significantly with growing distance. To assess the significance of this effect on small scales, we compared two closely situated wind stations within the same district (Berlin Tempelhof and Berlin Tegel, distance ≈ 11 km). From the empirical distribution we estimate that 75 % of statistical deviations lie within the interval $[-1.5 \text{ m s}^{-1}, 1.4 \text{ m s}^{-1}]$, while roughly 5 % exceed $[-3 \text{ m s}^{-1}, 2.9 \text{ m s}^{-1}]$. Hence a significant part of the observed deviations may be attributed to such source of error. Secondly, insurance data may be subject to statistical fluctuations caused by incorrect or delayed reporting of losses. We however expect that for large losses the latter errors are small and negligible.

2.4 Parametric Simplification

In order to simplify the parameterization of the damage model, we identified global statistical relationships and reduced the number of local fitting parameters. As additional predictors we used the number of residential buildings per district h , long-term damage rate δ defined as the share of days with recorded damages during the observation period, and the wind speed $v = ba^{1/c}$ at the intersection of the constant a and the power-law term in $d(v)$. The raw data for the 439 districts and the corresponding least-square fits are shown in Fig. 2.3 (a–c). Parameters a , α , and β could hence be replaced with the fitted global relationships

$$a = (2.05 \pm 0.58)h^{-0.99 \pm 0.03} \quad (2.7)$$

$$(1 - \alpha) = (0.92 \pm 0.01)\delta^{1.47 \pm 0.02} \quad (2.8)$$

$$\beta = (0.96 \pm 0.01)v + (0.58 \pm 0.24)\text{m s}^{-1} . \quad (2.9)$$

Intuitively, the inverse proportionality between loss offset a and number of building h (Eq. 2.7) follows from the definition of the loss ratio, defined as the absolute loss divided by the insured value, since the insured value scales linearly with the total number of houses. This suggests a common minimum noise level for all districts. Furthermore, the approximate direct proportionality between v and β in Eq. 2.9 hints at a common threshold that separates the

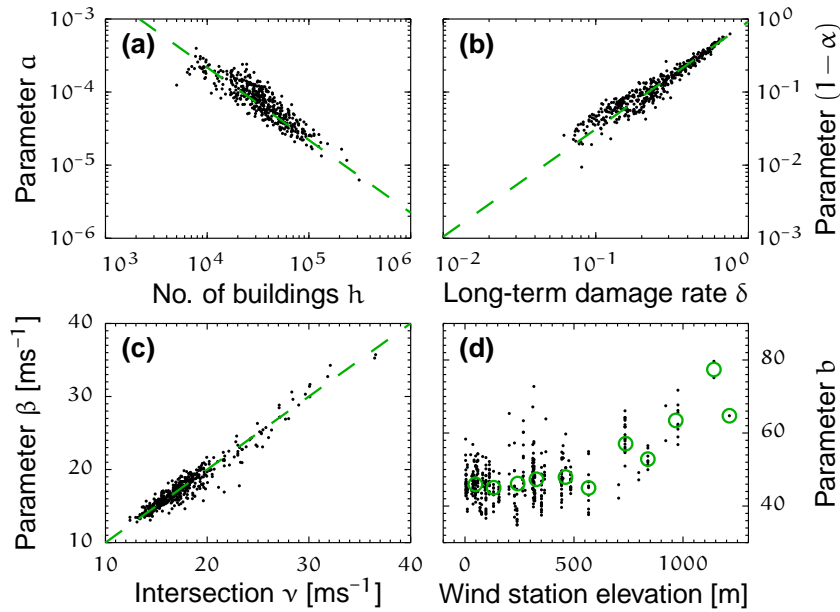


Figure 2.3: Correlations among model parameters and external factors. Scatter plots (a)-(c) show the correlations found for model parameters α , α , and β , respectively. Dots represent individual districts and dashed lines indicate fitted curves (cf. Eqs. 2.7-2.9). (d) shows the parameter b versus the elevation (above MSL) of the used wind stations. Circles denote binned data.

regime of noise at lower wind speeds from storm-driven losses at high wind speeds. In line with this proposition, we interpret $(1 - \alpha)$ as the probability of a random loss event in the noisy regime of the curve. Accordingly, Eq. 2.8 shows that the regional differences of the long-term damage rate δ are dominated by random loss events. The remaining third parameter of $p(v)$, γ , could furthermore be replaced by its mean value over all districts, $\bar{\gamma} = 0.46$. As $p(v)$ generally increases rapidly from $(1 - \alpha)$ to 1, results were insensitive to the error induced by this replacement.

In summary, the above global relationships can be used to reduce the model parameterization to three local parameters (exponent c and scaling parameters b and σ). Additionally, we observe a weak dependence of scale parameter b on the elevation of the respective wind stations above mean sea level [Fig. 2.3 (d)]. However, it is expected that b comprises a multitude of scaling effects due to orography or land use, and that hence the altitude dependence is not sufficient for a robust approximation.

In the following, all calculations are based on the full parametric model unless we refer to the *reduced model*.

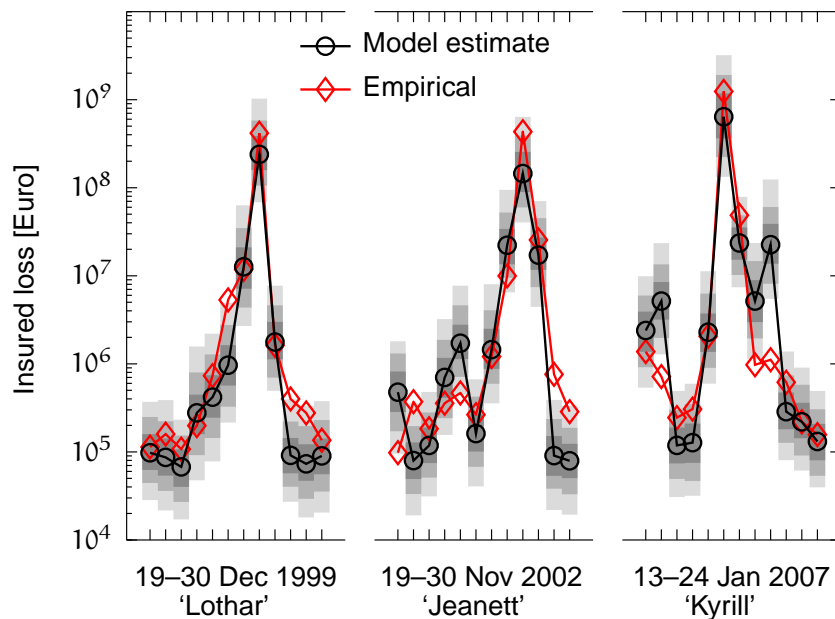


Figure 2.4: Out-of-sample calculations for daily German absolute losses during three severe winter storms (Lothar, Jeanett, and Kyrill). Circles denote the median of the damage distribution and diamonds empirical values. 50%, 80% and 95% confidence bounds are shaded from dark to light grey, respectively.

2.5 Modelling Results

In order to assess the predictive power of the proposed damage function, calculations of regional and countrywide loss figures were compared to empirical values. Due to the availability of only 11 years of spatially resolved loss data, an out-of-sample test algorithm was implemented as follows:

- Exclude year x from empirical damage data
- Train the storm damage model on the remaining data
- Predict countrywide daily and cumulated damages for year x based on daily maximum wind speeds
- Vary x and repeat all calculations.

In order to estimate the distribution for daily losses, the Monte Carlo method was used and 500 realizations of daily loss estimates were calculated.

Figure 2.4 shows daily loss predictions in Germany for the time periods around the three major storm events named Lothar (24.-27.12.1999), Jeanett (26.-29.10.2002), and Kyrill (17.-19.1.2007). These storms are of particular interest, as they caused the largest insurance losses during the period under consideration. For most days empirical values lie within the uncertainty bounds of the model estimates. Peak empirical losses of storm events Lothar and Kyrill

are contained within the 80 % uncertainty bound, while Jeanett is found in the 95 % interval. The results demonstrate the model performance for predicting losses over 4 orders of magnitude.

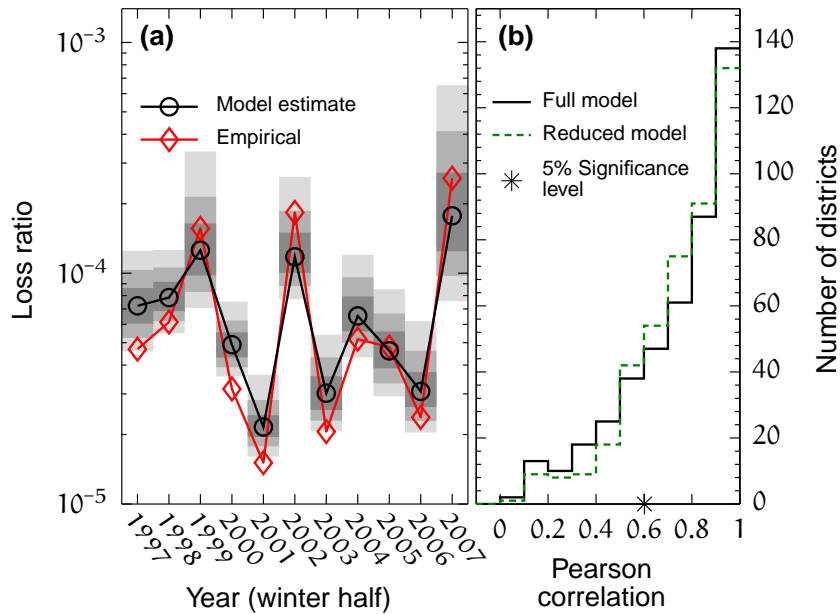


Figure 2.5: Out-of-sample calculations for the annually accumulated loss ratio during winter months (Oct-Mar). Panel (a) shows loss estimates for Germany. Circles denote the median of the estimated damage distribution, while 50 %, 80 % and 95 % confidence bounds are shaded from dark to light grey, respectively. Empirical values are represented by diamonds. Panel (b) shows a histogram of Pearson’s correlation coefficients between annual loss estimates and empirical values for each district. Correlations above 0.6 are statistically significant. The solid and dashed lines relate to the fully parameterized and the reduced model, respectively.

Annual loss estimates during winter months are shown in Fig. 2.5(a). Regarding absolute loss figures, we estimate a very high Pearson correlation of 0.99 between the model estimates (median) and the empirical values, which indicates a good reproduction of the annual progression of empirical storm loss data. Annual losses are dominated by the storm events Lothar, Jeanett, and Kyrill in the years 1999, 2002, and 2007, respectively. Loss estimates for these years hence reflect the peaks seen in Fig. 2.4. Additionally, we observe a small positive bias for years with loss ratio below 10^{-4} , which may be due to ignoring correlations in the estimation of $p(v)$ (Eq. 2.5). In total, we find approximately 12 % underestimation of absolute loss accumulated over 11 years.

Figure 2.5(b) summarizes the correlation per district between the median of the annual loss estimates and the empirical values. Approximately 1/3 of all districts show high Pearson correlation coefficients above 0.9. The mean

correlation over all districts is 0.74. The correlations allow for a comparison of the full model and the reduced model with only three fit parameters per district. The histogram shows an increase of correlations between 0.5 and 0.9, while the number of correlations with values above 0.9 is slightly decreased. Together with a slight increase of mean correlation to 0.76 this demonstrates the sufficiency of the three remaining fit parameters. Since both the original and the reduced model produce nearly identical quantitative loss estimates for Germany, we show results for the original model only.

2.6 Discussion

Empirical data of daily insurance losses across German administrative districts show a strong increase of losses with maximum daily wind speed. We find that these losses are well described by power-law damage functions with regionally varying exponents that typically range between 8 and 12 (cf. Fig. 2.2). For the out-of-sample calculations we generated successive parameter fits based on varying time slices of the available data. The estimated parameters were insensitive to these variations, thus demonstrating model robustness even under exclusion of the major loss events.

While these results are in contrast to damage functions published before, a direct comparison of the exponents may be misleading. In fact, excess-over-threshold models, as applied by Klawns and Ulbrich (2003) and Heneka and Ruck (2008), imply a much steeper increase of loss in the threshold vicinity than pure power-law models of absolute wind speed (e.g. Munich Re, 1993, 2001). The basic conjecture of our approach is a monotonous relationship between insured loss and maximum wind speed applicable to both small and extreme storm loss, which enables us to exploit information from a wide range of recorded losses. Since we found a universal power-law increase of loss for all districts, we think that the use of damage functions with differing asymptotic shape may result in significant extrapolation error.

In Fig. 2.4 we demonstrate in an out-of-sample test that daily modelled losses across Germany closely match empirical values ranging over four orders of magnitude. Judging from the comparison of median loss estimates and empirical data, peak losses may be slightly underestimated while still being within the uncertainty bounds of the model. Next to being a purely statistical effect (e.g. insufficient length of time series), this may be due to other aspects such as under-determination of the model based on maximum wind speed only. Where available, empirical data regarding such aspects as the temporal wind profile, storm duration, or gustiness may be used to improve loss estimation. Socio-economic effects such as demand surges (see, e.g., Olsen and Porter, 2011) are expected to play a minor role.

Inspired by other studies, the proposition of an exponential damage function was tested but rejected due to strong overestimation of damages for large wind speeds. Bearing in mind that the damage function was fitted on the whole range

of available loss data and thus not specifically calibrated to extreme losses, we conclude that the model results demonstrate good reproduction of both daily and annual extremes.

Strong countrywide correlations of model parameters support the universal applicability of our damage function and permit the separation of the damage curve into a approximately constant noisy regime and a physical power-law regime.²

Employing these correlations, the model parameterization was successfully reduced to three independent parameters determining the basic shape of the damage curve. While the power-law exponent determines the curve's steepness, the scale parameter accounts for regional variation between districts and wind stations (e.g. distance and orography). The third parameter specifies the width of the log-normal loss distribution around the central curve and thus relates to the expected level of statistical deviations. In particular, the value of the exponent may be interpreted as an indicator for regional vulnerability to extreme winds. Its spatial distribution indicates reduced vulnerability within Western and Northern Germany. As these regions, and especially the coastal regions, are highly exposed to extreme winds, the relatively low values of the exponent suggest a greater level of adaptation to the current wind climate than for Southern Germany.

All model calculations were deliberately based on raw measurements of maximum wind speed as provided by DWD. While most wind stations are known to be subject to inhomogeneities due to change in measurement apparatus, location, or surrounding surface roughness, they may nonetheless possess predictive power for neighbouring districts. Due to the selection criterion of maximizing generalized R^2 , wind stations with inhomogeneities causing significant additional variance were excluded. Unlike temperature or pressure data, correction of inhomogeneities in maximum wind speed data would require case-specific non-linear transformations that are beyond the scope of this study.

Additional insight, in particular regarding the significance for extreme loss modelling, could be gained from a dedicated model intercomparison on the basis of common meteorological and insurance loss data. In further work we moreover intend to apply our model to loss data for other European countries

² *A side note on the originally published paragraph:* When relating the model parameters that were obtained for individual districts with socio-demographic data, strong correlations were observed as seen in Fig. 2.3 (a–c). The presence of these correlations indicates a meaningful parameterization of the damage function. Worse correlations, i.e. a more random parameterization, would have been expected, if the damage function did not fit the wind–loss relation. As described in the succeeding paragraph of the main text, the correlations can be used to determine certain model parameters and to simplify the parameterization of the model. This has, however, negligible effect on the damage estimates itself. Quite different is the effect of the spatial correlations between the residuals of the loss estimates for different districts, which represent unaccounted storm variations, e.g. in duration or precipitation. Of course, these correlations cannot influence the expected loss, but have a widening effect on the uncertainty intervals.

and regions. A cross-national comparison of model parameters could enable the identification of clusters of similar vulnerability and reveal regional adaptation potential.

Acknowledgements. We thank the German Insurance Association (GDV) and the German Weather Service (DWD) for providing the data. This work was further supported by the German Federal Ministry for Education and Research under grant number 31SZ191B (PROGRESS) and by the Baltic Sea Region Programme 2007-2013 (BaltCICA project).

III

Comparison of Storm Damage Functions and their Performance

Abstract. Winter storms are the most costly natural hazard for European residential property. We compare four distinct storm damage functions with respect to their forecast accuracy and variability, with particular regard to the most severe winter storms. The analysis focuses on daily loss estimates under differing spatial aggregation, ranging from district to country level. We discuss the broad and heavily skewed distribution of insured losses posing difficulties for both the calibration and the evaluation of damage functions. From theoretical considerations, we provide a synthesis between the frequently discussed cubic wind–damage relationship and recent studies that report much steeper damage functions for European winter storms. The performance of the storm loss models is evaluated for two sources of wind gust data, direct observations by the German Weather Service and ERA-Interim reanalysis data. While the choice of gust data has little impact on the evaluation of German storm loss, spatially resolved coefficients of variation reveal dependence between model and data choice. The comparison shows that the probabilistic models by Heneka et al. (2006) and Prah1 et al. (2012) both provide accurate loss predictions for moderate to extreme losses, with generally small coefficients of variation. We favour the latter model in terms of model applicability. Application of the versatile deterministic model by K1awa and Ulbrich (2003) should be restricted to extreme loss, for which it shows the least bias and errors comparable to the probabilistic model by Prah1 et al. (2012).

This chapter has been published as:

Prah1, B. F., Rybski, D., Burghoff, O., and Kropp, J. P. (2015). Comparison of storm damage functions and their performance. *Nat. Hazards Earth Syst. Sci.*, 15(4):769–788, doi: 10.5194/nhess-15-769-2015.

© Author(s) 2015. CC Attribution 3.0 License.



3.1 Introduction

As a major contribution to natural-hazard damages, windstorms are responsible for an average of 39% of world-wide economic losses during 1980–2011 (Munich Re, 2013). Across Europe losses from meteorological events are mainly caused by winter storms and comprise 68% of total insured loss caused by natural catastrophes. The largest event so far, winter storm Daria in 1990, totalled \$8.6 billion of insured loss in 2013 values (Swiss Re, 2014).

Recent climatological studies by Schwierz et al. (2010) and Held et al. (2013) have indicated that the severity of winter storm-related loss is likely to increase markedly in the course of the 21st century. While there is no consensus on changes of winter storm frequency, a growing body of research supports a future increase in storm intensity (Feser et al., 2015). With this development in mind, it is questionable whether the anticipated damages will remain within the limits of insurability. Even though Held et al. (2013) come to a positive conclusion for the German insurance market, such analyses hinge on the choice and quality of the employed damage function.

A storm damage function describes the relation between the intensity of a storm and the typical monetary damage caused. While on the continental scale storm intensity can be best described by complex storm severity indices (Deroche et al., 2014; Roberts et al., 2014), local losses are ultimately caused by surface winds. As the magnitude of storm loss is highly sensitive to changes in wind speed, even small variations between potential damage functions could have severe implications for the reliability of loss estimates and their validity for economic and political decision making.

The work in hand tackles this issue by providing a model intercomparison of storm damage functions for the residential sector in the context of European winter storms.

In the discussion of storm damage functions it is often assumed that loss should increase as the square or cube of the maximum wind (gust) speed. These presumptions originate from the following:

- the consideration of wind loads, which are approximately proportional to the exerted pressure and, hence, to the square of the wind speed (e.g. Simiu and Scanlan, 1996);
- the concept of proportionality between structural damage and the dissipation rate of the wind kinetic energy that scales with the third power of wind speed (recently: Emanuel, 2005; Powell and Reinhold, 2007; Kantha, 2008).

In particular, the notion of a cubic relationship is backed by empirical analysis of insurance records, which appear to exhibit cubic or quartic behaviour depending on the storms under scrutiny (Munich Re, 1993, 2001). However, recent literature provides evidence for a much stronger increase of insured storm loss with wind gust speed (Huang et al., 2001; Heneka and Ruck, 2008). For the

insurance data set that we employ here, Prah1 et al. (2012) found a power law with regionally varying exponents that approximately range between 8 and 12.

We reason that the apparent contradiction results from the negligence of a potential loss threshold due to insurance deductibles or similar economic effects. Thus, we schematically demonstrate the transition from very steep loss increase to a more modest cubic power-law.

The comparison of storm damage models is generally impeded by inconsistencies for reasons of (i) differing temporal or spatial resolution of meteorological data, (ii) deviating building codes and enforcement practices, and (iii) differing insurance policies and claims settlement practices (Walker, 2011).

In order to circumvent such inconsistencies, three recently developed damage functions (Klaw1 and Ulbrich, 2003; Heneka and Ruck, 2008; Prah1 et al., 2012) are applied to a common data set of wind gusts and insurance loss data for Germany. These damage functions are complemented by a simple exponential model inspired by recent US hurricane loss models (Huang et al., 2001; Murnane and Elsner, 2012), yielding four mathematically distinct modelling approaches. For simple referencing, we assign the acronyms X and K to the deterministic exponential model and the model by Klaw1 and Ulbrich (2003), respectively. The probabilistic models by Prah1 et al. (2012) and by Heneka and Ruck (2008) are referred to via the letters P and H, respectively.

The theoretical foundations and the implications of each model are discussed in order to mainstream terminology and conceptual structure of storm damage functions. Quantitative results are obtained from numerical estimation and allow a direct comparison of model performance under varied spatial aggregation, relating to either daily loss or particular major storms. During summer months the employed loss data inseparably includes both wind and hail damages. Since the employed damage functions concern wind damage only, we limit the work in hand to days within the winter half-year (WH), comprising the months October through March.

We address the validation of countrywide loss estimates by applying a novel pairwise binomial test metric in conjunction with the relative metrics mean percentage error (MPE) and mean absolute percentage error (MAPE). Furthermore, a coefficient of variation (CV) is employed to assess the predictive uncertainty on district level at daily resolution.

The overall model estimation is based on annual cross validation, an iterative procedure for the sampling of the training data, safeguarding that loss estimates within any given year are obtained from independent training samples. We furthermore assess model robustness by employing a *jackknife* method for the systematic resampling of training data. Selectively excluding parts of the training sample, the jackknife method allows us to assess the dependence of model estimates on the training data. Probabilistic model results are obtained from a Monte Carlo simulation with a sample size of 1000.

In the following section, we give overviews of the employed wind gust and insurance data sets and of the model estimation procedure. In Sect. 3.3 a brief introduction of storm damage functions is followed by a detailed view on each

of the compared models. The numerical modelling results are discussed in Sect. 3.4. In Sect. 3.5 we attempt a synthesis between a cubic wind–damage relation and the considerably steeper damage functions reported for German winter storms. The concluding synopsis and discussion of the theoretical and numerical aspects of the impact model intercomparison are given in Sect. 3.6.

3.2 Data and Methods

3.2.1 Insurance Data

In this work, the employed damage functions are calibrated against detailed insurance loss data obtained for storm damages to residential buildings. The German Insurance Association (GDV) provided loss data relating to the “comprehensive insurance on buildings” line of business resolved for 439 German administrative districts (as of 2006).

The data set comprises the magnitude of absolute losses and insured values as well as the number of claims for the years 1997 to 2007 on a daily basis. With its high spatio-temporal resolution and countrywide coverage, the GDV data set has been successfully applied for the calibration of different damage functions (e.g. Donat et al., 2011b; Prahel et al., 2012; Gerstengarbe et al., 2013).

In order to eliminate price effects and time-varying insurance market penetration, we consider relative figures for the amount of loss and claims throughout. The following definitions are applied:

- loss ratio (LR): the amount of insured loss per day and district, divided by the corresponding sum of insured value;
- claim ratio (CR): the number of affected insurance contracts per day and district, divided by the corresponding total number of insurance contracts.

These definitions are based on the assumption that insured buildings are randomly distributed in each district and are representative of the overall residential building stock. With data coverage of up to 13.4 million insured buildings and in excess of 90 % market coverage (GDV, 2013) we expect the assumptions to hold.

The highly skewed and heavy-tailed distribution of daily losses during the winter half-year is illustrated in Fig. 3.1. More than 50 % of total loss is recorded for the top 6 out of 2000 loss days. The shaded area in Fig. 3.1 highlights the upper 10 % of loss days, comprising in excess of 90 % of total loss. For economic relevance our work focusses on this loss segment, with a sub-division into three distinct loss classes, as shown in Table 3.1.

The vast number of days exhibiting negligible insured loss appears to be due to a random scattering of small losses across time and districts. Supporting the attribution to noise, Prahel et al. (2012) found a direct proportionality between the magnitude of the temporally scattered losses and the number of insured contracts in a given district.

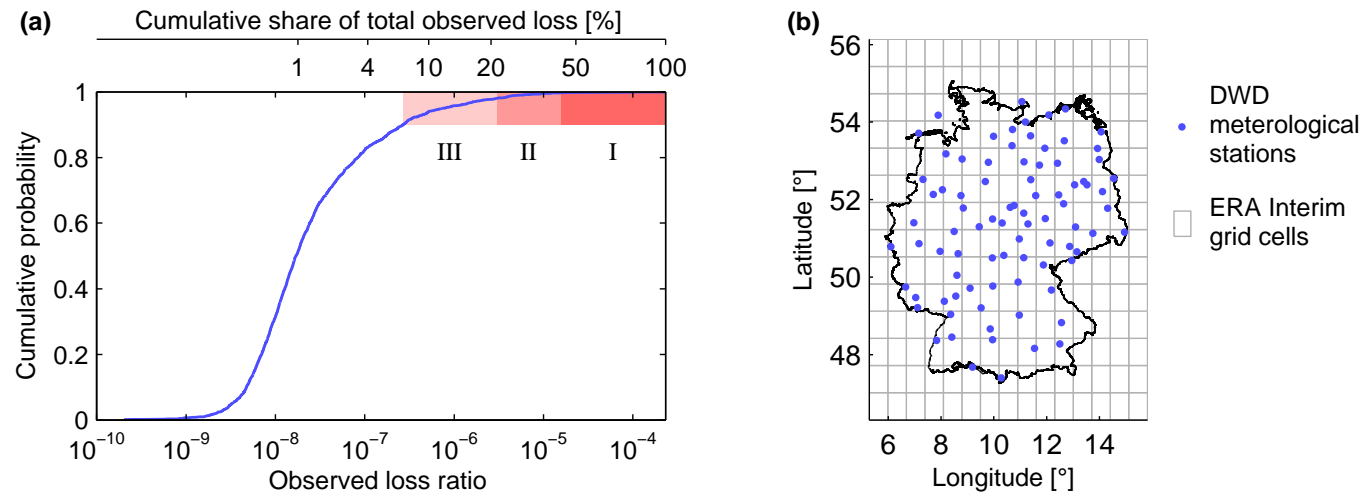


Figure 3.1: (a) shows the empirical cumulative distribution function of loss days in Germany during the winter half-year. The observations comprise 2000 loss days, which exhibit a steep increase of loss at the upper end of their distribution. The shaded area indicates the days within the upper 0.1 quantile, subdivided into the three loss classes defined in Table 3.1. The top scale shows the share of total loss that is accumulated for all losses smaller than or equal to a specific loss ratio. (b) shows the spatial distribution of the employed DWD stations and the ERA-I grid cell resolution.

Loss class	Description	No.	Quantiles of daily losses	Loss share
I	Extreme	6	0.997–1.000	54.9 %
II	Large	34	0.980–0.997	23.4 %
III	Moderate	160	0.900–0.980	15.0 %

Table 3.1: The three loss classes defined for the winter half-year. Given are the number of observations, the related quantiles, and the accumulated loss share for the period 1997 to 2007.

3.2.2 Wind Gust Data

Two sets of meteorological data were employed. The first set comprises daily maxima of the 3 s wind gust measured by the German Weather Service (DWD)¹. Applicable meteorological stations were selected according to the following criteria:

1. Missing values may not exceed 20 days for each year.
2. Average missing days per year may not exceed 10 for the period 1996 to 2008.
3. Stations should exclude mountainous stations above 1400 m a.s.l.

Based on the selection criteria, 85 meteorological stations were selected. Measurements obtained at anemometer heights other than 10 m were adjusted using the simple wind-profile power law

$$v(10) = \left(\frac{10}{h}\right)^\lambda v(h), \quad (3.1)$$

with wind velocity v , anemometer height h , and an exponent $\lambda = 1/7$ as discussed in Wan et al. (2010).

Inhomogeneities in meteorological time series can be identified by finding an optimal solution to the multiple breakpoint problem. Standard methods are available, in particular, for finding inhomogeneities in monthly climatic time series (Venema et al., 2012). Application to daily time series is however subject to ongoing research (e.g. Wang, 2008; Mestre et al., 2011).

In the case of daily block maxima of climatic data, the relatively small change at the breakpoint as compared to the data's variance and the presence of long-term persistence adversely affect the capacity to identify breakpoints correctly. With a low signal-to-noise ratio, the presence of long-term correlation can lead to false identification of breakpoints (Rybski and Neumann, 2011; Bernaola-Galván et al., 2012).

¹ Data available at: <http://www.dwd.de/webwderdis>.

We attempt to avoid over-detection by applying a conservative testing scheme based on multiple cross-comparison of neighbouring stations and the examination of metadata, e.g. about relocation of stations. The testing scheme employs the R implementation of the PMFred algorithm developed by Wang (2008) to identify potential breakpoints in time series of differences between daily gust maxima of any pair of meteorological stations. We reduced the skew of the distribution of gust speeds by applying a logarithmic transformation and hence improved the normality of the data, which constitutes a basic assumption of the PMFred algorithm.

To begin with, we chose a control group of 39 stations whose individual time series showed no significant inhomogeneities in the test algorithm. Subsequently, we paired each of the 85 stations with the 10 closest of the control group and performed the PMFred algorithm on the time series of their differences. If within a 60 day window at least three pairwise tests indicated a breakpoint that could be backed by metadata, the inhomogeneity was corrected. Furthermore, if all 10 pairwise comparisons suggested a significant and otherwise undocumented breakpoint it was also corrected. All corrections were performed using a quantile-matching algorithm (Wang et al., 2010).

Overall, we took a conservative stance on artificial manipulations of the raw time series and corrected only three significant breakpoints in total, two of which were documented in metadata.

The second wind gust data set was obtained from the ERA-Interim reanalysis² (ERA-I, Dee et al., 2011). We use the daily maxima of the 3-hourly values of the 10 m wind gust.

Both sets of wind gust data, DWD and ERA-I, require a downscaling to match the resolution of the insurance data. Prahla et al. (2012) demonstrate that wind gust observations from neighbouring meteorological stations provide sufficient information for the calibration of a storm damage function. Higher precision may be attained via the use of mesoscale climate models for the computation of detailed and physically valid wind fields from reanalysis or observational data (Heneka et al., 2006; Huttenlau and Stötter, 2011). As this is clearly beyond the scope of our work, we limit ourselves to a simple inverse-distance interpolation scheme applied to both DWD and ERA-I data sources. The wind field was interpolated at the centroids of each district, taking into account all locations (stations or grid points) within a certain radius of interaction. Employing leave-one-out cross validation, i.e. iteratively excluding each individual location from the interpolated data set, we calculated the average correlation between empirical and interpolated values at varying radii of interaction. The optimal radius of interaction was chosen as the value at which the average correlation reached its maximum. The estimated radii were 130 and 60 km for DWD and ERA-I, respectively.

² ERA-I data were obtained from: http://data-portal.ecmwf.int/data/d/interim_full_daily.

3.2.3 Model Calibration

The analysis of daily insurance loss data of the winter half-year reveals an extremely broad and strongly skewed loss distribution. Relating loss and wind gust data, a pronounced heteroscedasticity is revealed (cf. Fig. 6 in Heneka and Ruck, 2008), with uncertainty resembling a log-normal error (Prahl et al., 2012). In conjunction with such pronounced heteroscedasticity, the scarcity of extreme events in the tail of the distribution may cause a bias of traditional regression methods, such as least squares, towards singular extremes present in the training data. While a data transformation, such as the logarithm, may reduce skew and heteroscedasticity, it would put stronger weight on smaller loss events and hence counteract the focus on extremes. In practice, potential data transformation and curve fitting methods are dependent on the specific damage model and are hence discussed in conjunction. Calibration issues that arise from the properties of the loss distribution are discussed alongside the mathematical model concepts in Appendix 3.A.

3.2.4 Model Estimation Procedure

Since damage functions are typically employed as predictive models, it is of key importance how accurately they perform in practice. In addition to choosing the optimal model, there is the risk of overfitting to a training data which may not represent the high variability of weather extremes. In order to assess the predictive performance of the employed models, a k-fold cross validation scheme (Kohavi, 1995) is employed in conjunction with a jackknife procedure (Miller, 1974).

For annual cross validation, the 11-year data set is partitioned into annual subsamples. Iteratively, each individual subsample is retained for evaluation, while the model is trained in the 10 years remaining. This process ensures that each year is used exactly once for evaluation.

The employed cross validation enables out-of-sample prediction for each day and allows for the assessment of the model fit with regard to the range of frequently occurring losses.

However, for very scarce extreme events the evaluation of model robustness requires additional resampling of the training data. The resampling is performed via a jackknife procedure, where each individual annual subsample is excluded consecutively from the 10-year training sample.

For the joint analysis of deterministic and probabilistic models, two different schemes for loss aggregation are employed. Generally, we consider the daily district-wise loss estimates as independent random variables dependent only on the maximum gust speed. In the case of deterministic models, the model estimates are interpreted as expected values and were simply summed up over time or space. For the probabilistic models, we employed a Monte Carlo approach, where results of 1000 independent random realisations were aggreg-

ated. The expected value and distribution quantiles were then calculated from the distribution of Monte Carlo estimates at the desired level of aggregation.

3.2.5 Validation Metrics

The broadness and skew of the loss distribution also play a role for the validation of model estimates, as they have significant impact on the applicability of evaluation metrics. Heteroscedastic dependence between prediction error and loss magnitude invalidates traditional moment-based metrics such as R^2 or, equivalently, Pearson's ρ . In particular, very extreme events may attain the character of singularities and dominate absolute performance metrics. Alternatively, relative metrics such as mean percentage error or mean absolute percentage error may be employed over well-defined loss ranges (Hyndman and Koehler, 2006). However, these metrics fail if predictions comprise both days with and days without loss, which is often the case for daily resolved data. Moreover, such zero values prevent the use of common transformations (e.g. power transformations such as Box–Cox Transformation, see Box and Cox, 1964) to increase the normality of the loss distribution required for most statistical metrics.

In order to eliminate the effects of scale of the loss distribution for model comparison, we propose a simple pairwise statistical test based on binomial statistics. The null-hypothesis is that both models have equal predictive skill and, hence, that their predictions are equally likely to be closest to the true observations. Successes (i.e. closer prediction) can be represented by independent Bernoulli trials with probability 0.5. In a one-tailed test the binomial distribution then expresses the probability for a given success rate.

In order to apply the binomial test, the share of predictions where one or the other comes closer to the observation is estimated for each pairing of models. Significance is obtained from the binomial distribution with probability 0.5 and n independent trials, where n equals the total number of loss days for each loss class.

As the binomial test itself does not disclose why any specific model outperforms a competitor, we interpret the results of each model in conjunction with traditional relative metrics relating to a multiplicative error. For the employed data, Prahm et al. (2012) found a variability that is approximately symmetric on the log-scale, such that the assumption of a multiplicative error seems viable.

The employed multiplicative metrics are the MAPE (i.e. the mean of the moduli of deviations between model estimates and observations in percent) and the MPE (i.e. the mean of the deviations between model estimates and observations in percent). While MAPE gives an estimate of the variability of model results, MPE provides an indication for systematic bias.

3.3 Storm Damage Models

A damage function describes the relation between the intensity of a specific hazard and the typical monetary damage caused with respect to either a single structure (*microscale*) or a portfolio of structures (*macroscale*).

Microscale models can be empirical (i.e. statistically derived from data), engineering-based, or a mixture of both. On the macro scale, damages may be either aggregated from microscale models or obtained from statistical relationships based on empirical data (cf. Merz et al., 2010).

Due to the minimum resolution of our data (i.e. districts), our analysis is constrained to the macroscale models of the latter kind. Nonetheless, some of the damage functions under scrutiny contain assumptions on the nature of microscale damage. As there are no publicly available engineering-based models for our region of interest, only statistical models are considered.

For a general overview of modelling approaches, both statistical and engineering-based, we refer the reader to Walker (2011) and, with a focus on hurricane damage, to Pita et al. (2013). In the following, we present each of the four employed damage functions.

3.3.1 Generic Exponential Damage Function

The choice for an exponential damage function is motivated by empirical observation, showing quasi-linear increase of the logarithm of the loss ratio versus maximum wind (gust) speed over a wide range (e.g. Prettenthaler et al., 2012; Murnane and Elsner, 2012).

It is a non-physical damage function in the sense that it does not saturate with increasing wind gust speed and thus ignores an upper limit of physical damage. However, average loss levels reached during European winter storms typically range below or around a few tenths of a percent of insured value, such that loss saturation does not become an issue.

The damage function relates the loss ratio L to the exponential of the gust speed v ,

$$L_X \propto e^{\mathcal{X}_1 v}. \quad (3.2)$$

The absolute gust speed is rescaled via a linear transformation governed by parameter \mathcal{X}_1 . Primarily, the parameter reflects the particular vulnerability to wind damage. Additionally, rescaling of wind gust observations may be required for reasons such as:

- Variations of scale due to mismatches in altitude or location of the geographical reference of the gust data and the building portfolio
- Loss being dependent on a differing wind predictor with approximate proportionality to the maximum gust speed
- Systematic bias caused by the interpolation of wind gust data.

The exponential damage functions focuses on wind-dependent losses only. Typically, these are large losses within the upper tail of the loss distribution. For the employed insurance data, small losses that occurred at days with maximum gust speed beneath the 95th percentile show a predominantly random behaviour not captured by Eq. 3.2 and were hence neglected during calibration. This aspect is also seen exemplarily in Fig. 3.2, showing the independently trained damage function in the context of empirical loss data.

Further details about the calibration of the damage function are given in Sect. 3.A1.

3.3.2 Probabilistic Power-Law Damage Function

In the literature, there are several proponents for power-law-based storm damage functions (e.g. Dorland et al., 1999; Nordhaus, 2010; Bouwer and Wouter Botzen, 2011).

For winter storms affecting Germany, Prah et al. (2012) developed a macroscale damage function based on the presumption of a power-law-based sigmoid curve. Considering the typical loss range of winter storms, the sigmoid curve can be approximated by a simple power-law term. For the general case, their damage function comprises two key components. The first component describes the probability for the occurrence of damage within the portfolio, while the second component models the intensity of loss if a damage has occurred. In conjunction with the introduction of a noise constant, this two-part structure enables the modelling of the entire range of damages, thus not excluding information from the bulk of small losses that may provide additional support for the calibration of the damage function.

For an arbitrary district, Fig. 3.2 shows the curve fits for both components of the damage function as well as the resulting expected value for storm loss. The left-hand panel demonstrates that the predicted 95 % confidence bounds encompass the majority of loss observations and the right-hand panel shows how the probability of occurrence is inferred from the empirical occurrence rate (training data).

The model can be simplified for large wind gust speeds. In this case, the expected value of loss L is approximately proportional to the gust speed v raised to the power \mathcal{P}_1 ,

$$\mathbb{E}[L_p] \propto v^{\mathcal{P}_1}. \quad (3.3)$$

The exponent \mathcal{P}_1 is the key parameter and expresses the vulnerability of the building portfolio. Additional important parameters adjust the scale of the employed wind gust data and control the spread of the loss probability distribution (see Sect. 3.A2 for details). Concerning the scale of the employed gust data, the observations may require a rescaling to relative values (cf. Sect. 3.3.1).

The original model published by Prah et al. (2012) incorporates correlations between district losses caused by the same storm event. Due to the complexity

of the employed modelling scheme, it was not feasible to include these correlations in this paper. However, the effect of correlations is perceived as minor to the overall performance of the damage function and their inclusion would lead primarily to a widening of confidence intervals.

Please refer to Sect. 3.A2 for further details of the mathematical derivations and of the fitting procedure.

3.3.3 Cubic Excess-Over-Threshold Damage Function

Klawa and Ulbrich (2003) proposed a macroscale damage function for German storm loss based on the hypothesis that storm damages grow with wind gust speed in excess of a specific threshold. The approach has since been applied to other European locations (e.g. Leckebusch et al., 2007; Etienne and Beniston, 2012; Cusack, 2013) and was recently refined to the scale of German districts by Donat et al. (2011b).

At the core of the damage function is the definition of a damage proxy D based on the regional wind gust speed v and its 98th percentile,

$$D = \begin{cases} \left(\frac{v-v_{98}}{v_{98}} \right)^3 & \text{if } v \geq v_{98} \\ 0 & \text{if } v < v_{98} \end{cases} . \quad (3.4)$$

The damage function is calibrated by performing a linear regression of loss observations against the damage proxy, thus involving two regression parameters (a scaling coefficient and an offset). In the upper limit, the damage function increases without bounds and hence ignores damage saturation at high gust speed.

The scaled damage proxy is shown exemplarily for an arbitrary district in Fig. 3.2. Since the additive offset parameter rather describes the bulk of loss that may occur below the 98th wind gust percentile, it is not directly attributable to any specific event and hence indicated via a dotted line in Fig. 3.2.

The employed wind gust percentile was empirically found by Klawa and Ulbrich (2003) and may be considered as a third parameter. Since the introduction of the European Standard EN 1991-1-4 describing the wind action on land structures, the 98th wind gust percentile has become a crucial factor for the reinforcement of buildings against wind damage. Even before its legal implementation during the first decade of the 21st century, it may be reasonable to presume an autonomous adaptation³ to the wind climate and hence argue for the applicability of a wind percentile as a proxy for such adaptation.

The cubic relationship of the damage function has been repeatedly put into context with the advection of kinetic energy (Leckebusch et al., 2007; Pinto et al., 2007; Cusack, 2013). As a matter of fact, this line of reasoning is problematic due

³ Structures are reinforced to withstand frequent low-impact events, while adapting to the rare extremes may be too costly. A balance between the individually perceived (monetary) risk and tolerable adaptation cost is maintained.

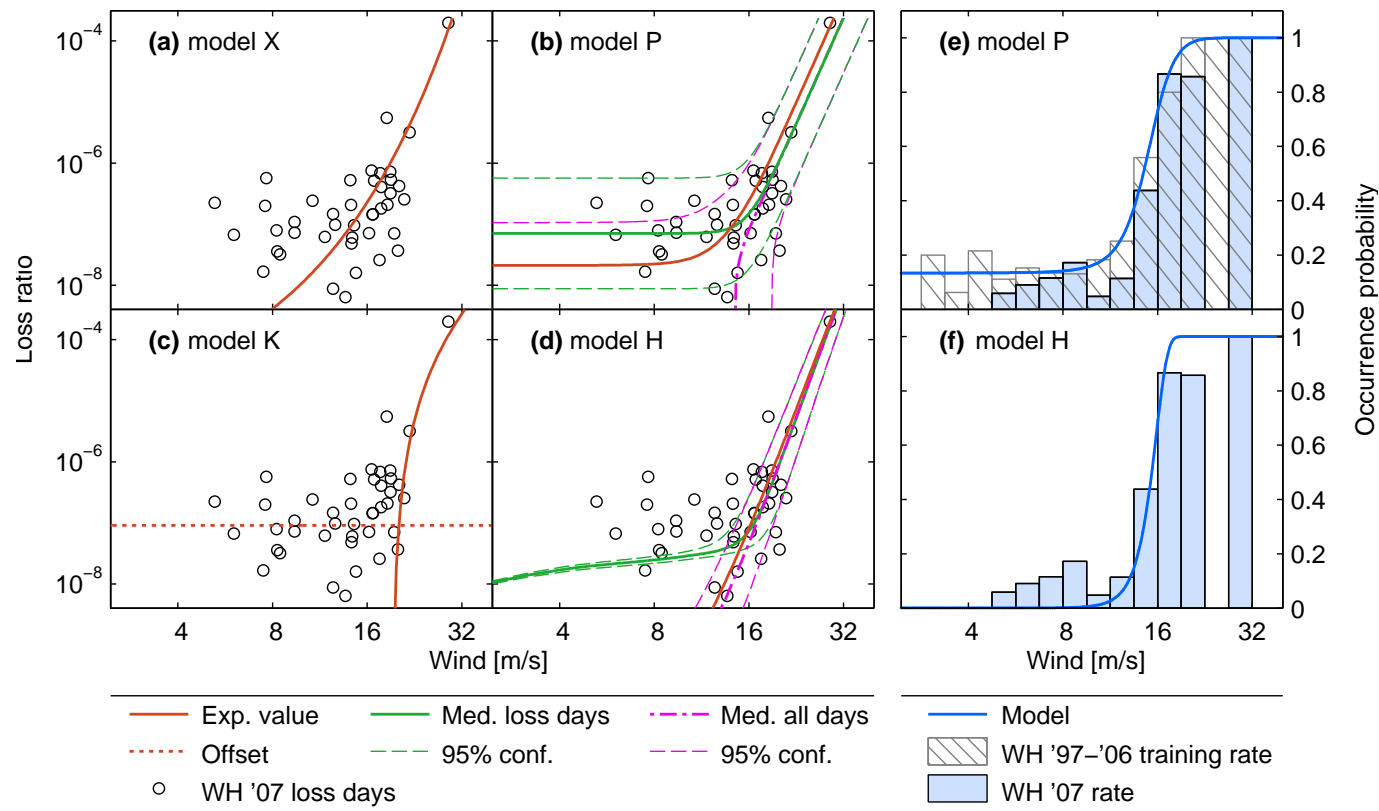


Figure 3.2: Example of model predictions for a single district obtained from DWD data for the training period 1997–2006 and set in contrast to year 2007 empirical data, all limited to the winter half-year. (a)–(d) show the expectation values of the loss ratio versus wind gust speed on a log–log scale, circles denote observed losses during 2007. For probabilistic models P and H, the median and 95% confidence bounds are given. Additionally, we show for model P the median and confidence bounds of the curve fit to actual loss days and for model H an analogous but implied curve. (e) and (f) show the fitted and implied occurrence rate probability for models P and H, respectively. Year 2007 observed occurrence rates are indicated by blue bars. For model P, training data (shaded bars) is displayed as reference.

to the subtraction of the 98th percentile threshold, and hence the resulting damage function is inconsistent with the purely cubic dependence on gust speed. As a consequence, the gradient of the damage function is much steeper than that of a simple cubic gust relationship over the entire range of historical wind gust speeds. Only in the upper asymptotic limit, as the gust speed approaches infinity, does the damage function converge to the simple cubic dependence.

In Sect. 3.A3, we demonstrate that on the basis of the employed data the increase of the loss curve for extreme winter storms is comparable to that of a power law with a steep exponent of approximately 10.

Although Klawa and Ulbrich (2003) developed their damage function for winter storms, the function can be applied to the entire loss range, in which case the regression offset parameter serves as baseline loss resulting from wind gusts beneath the defined percentile threshold. Figure 3.6 illustrates that there is a strong relation between loss and gusts below the 98th wind gust percentile, suggesting that the damage function could potentially utilize a lower wind percentile. Further mathematical details and the fitting procedure are described in Sect. 3.A3.

3.3.4 Probabilistic Claim-Based Damage Function

Heneka et al. (2006) put forward an integrated approach for modelling storm loss, combining a probabilistic description of affected buildings with a micro-scale damage relationship.

Within their theoretical framework, a building damage occurs if a critical wind gust speed, particular to that building, is exceeded. A continuous probability density function is employed to describe the probability of critical gust speeds within the overall building stock. For modelling purposes, Heneka et al. (2006) assumed a Gaussian distribution for critical gust speeds, which is non-physical in a sense as it yields finite probability for negative wind gust speeds. The claim ratio follows naturally as the cumulative distribution function of critical gust speeds, describing the fraction of buildings for which wind gust speed exceeds the critical threshold.

If an individual building i is affected, the damage D_i is assumed to rise as the square of the gust exceedance above threshold until complete destruction is reached at maximum exceedance level \mathcal{H}_1 . Heneka et al. (2006) (see also Heneka and Ruck, 2008; Heneka and Hofherr, 2011) argue that the square term of their microscale damage relationship,

$$D_i = \left(\frac{v - v_c}{\mathcal{H}_1} \right)^2, \quad (3.5)$$

corresponds to proportionality between damage and wind force. Repeating the reasoning given in Sect. 3.3.3, we argue that such proportionality is violated due to the inclusion of the critical threshold v_c which is inconsistent with the wind force being proportional to the square of the untranslated wind gust speed (e.g. Simiu and Scanlan, 1996).

In contrast to the other discussed damage functions, model fitting and loss estimation requires numerical integration, which makes the application of the damage function computationally more demanding. It was found that the model could not be reliably calibrated on loss data only, necessitating the use of additional data for the number of claims per region and day. Given the additional information from claims data, the damage function would be expected to perform as well or better than the competing models.

Due to its probabilistic description of the building stock, the damage function naturally incorporates an upper limit to the claim and loss ratio and may be applicable to a wide range of losses.

The model requires the calibration of four parameters, describing the wind gust speed at which half of the building stock is damaged and its associated standard deviation, the standard deviation of critical wind gust speeds, and the gust range over which building damages reach complete destruction. Further description of the mathematical details and the three-step calibration procedure is given in Sect. 3.A4.

For an exemplary district, Fig. 3.2 shows the expected value and 95 % confidence bounds of the damage function. For better comparison with the probabilistic power-law damage function, we further decomposed the damage function into the implied components for the occurrence probability and the loss intensity, both shown in Fig. 3.2.

3.4 Comparison Results


Bringing together the four different models, the two wind gust data sources, and the modelling procedure (Sect. 3.2.4), model predictions were obtained for 2004 days (consisting of the winter halves of 11 years) and for each of the 439 administrative districts.

Due to the high level of detail, the presentation of results is focused on three distinct aggregation levels: (i) daily loss per district, (ii) daily country-wide losses, and (iii) countrywide losses caused by the six most severe storm events during their entire passage duration.

In case of models K and H, different setups for model calibration were possible (cf. Appendix 3.A). For greater clarity, only those results that relate to the best-performing setup are reported, while additional results are provided in the Supplement (see Sect. 3.B2).

The circumstances of comparing two deterministic and two probabilistic models require the choice of a common metric. The output of the deterministic models is hence considered equivalent to an expected value obtained from the probabilistic models and forms the basis of the model intercomparison.

	North	East	South	West	All
DWD	231	342	436	228	331
	248	384	580	255	385
	266	403	911	290	508
	290	552	997	352	578
ERA Int.	356	327	417	286	376
	401	333	469	299	387
	515	342	738	305	458
	842	580	745	527	665



Model color code

X	H	P	K
---	---	---	---

Table 3.2: Spatial averages of the coefficient of variation for each model. For ease of comparison, values are sorted in ascending order. The respective model is indicated by the colour code. The spatial extent is defined by the four geographic regions (North, East, South, West) depicted in the map inset.

3.4.1 Daily Loss per District

While temporal or spatial aggregation generally leads to a convergence of model estimates and observations, strong variability is expected for daily storm loss estimates on the fine district scale.

On the basis of root-mean-squared error (RMSE) we define a coefficient of variation (cv),

$$CV_{\text{RMSE}} = \frac{1}{\bar{x}} \left(\frac{1}{n} \sum_{i=1}^n (x_i - \hat{x}_i)^2 \right)^{\frac{1}{2}}, \quad (3.6)$$

where, for n samples, x and \hat{x} denote the observations and estimates of the expected value respectively. Values are normalized to the mean of the observations \bar{x} .

Table 3.2 shows regional averages of the cv for each of the four competing models. These results highlight the interdependence between model and wind gust choice. While model H mostly outperforms the competing models for DWD wind gust data, it appears less suited for ERA-I wind gust data, whose distribution properties are distinctly different from those of the DWD data. Of particular interest is the fact that, irrespective of the wind gust data source, model H performs best across southern Germany. With relatively complex terrain and less frequent storm events, this region poses the greatest challenge to the damage

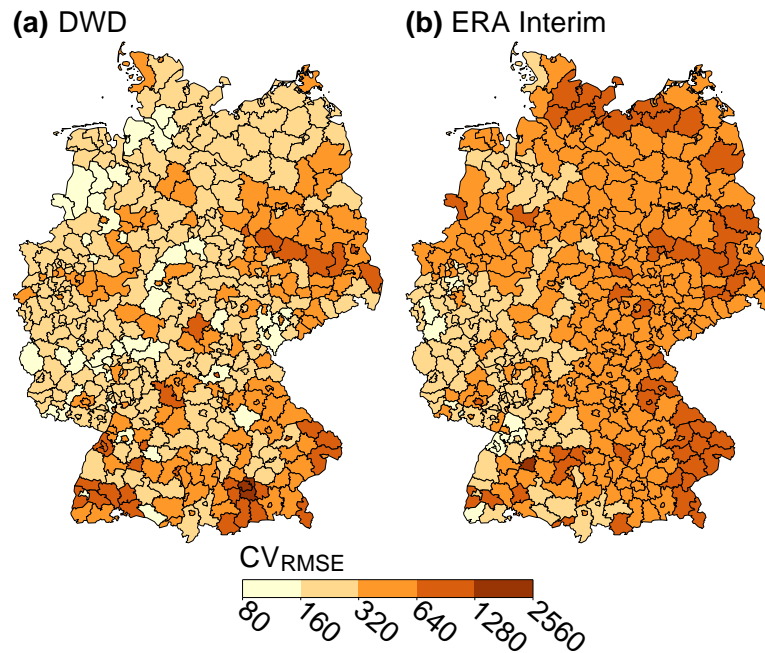


Figure 3.3: Coefficients of variation of the root-mean-squared error per district, evaluated for the entire 11-year modelling period. Depicted is the minimum value of CV_{RMSE} found for any of the four models. (a) and (b) show results obtained from DWD and ERA-I wind gust data, respectively.

models, resulting in a wide spread of cv values between different models. In contrast, model K appears to be least reliable in the south. While the exponential model X fares worst overall, it scores best for DWD wind gust data over northern Germany. It may be assumed that in this region the probability distribution of the DWD wind gust data are most favourable for the steep exponential model. Overall, models H and P show the least variation throughout. While model K performs well, with the exception of southern Germany, the exponential model consistently generates the largest amount of variation and, hence, modelling error.

Due to the fact that the district resolution exceeds the resolution of sampling points of the wind field, a strong influence of the choice of gust data are expected. Figure 3.3 shows a baseline cv estimated as the minimum value found for any of the four competing models. The DWD-based values show relatively small variation across north-western Germany, while exhibiting stronger variation in southern Germany. In contrast to the DWD-based values, ERA-I-based cv estimates show a marked increase of variation from east to west. The origin of this effect, however, remains unclear.

3.4.2 Countrywide Daily Loss

Our second appraisal of the model performance is based upon countrywide daily losses. The spatial aggregation has the beneficial effects of reducing loss variability and yielding a high number of otherwise spatially separated loss events.

Figure 3.4 shows the model predictions for the countrywide loss ratio plotted against the observations from insurance data. Focusing the initial examination onto results based on DWD wind gust observations [Fig. 3.4 (a)], several important aspects are revealed.

First of all, the loss predictions from all models exhibit a very high variability in the range of few orders of magnitude. Since the variability cannot be significantly reduced by model choice, it may be a consequence of other aspects such as the stochastic nature of the building damage, measurement error of gust speed, or the omission of further explanatory parameters. Secondly, the model variability appears nearly symmetric on the log-scale, indicating a strongly skewed distribution. In this case, expected values may be significantly lower than loss observations that fall into the upper tail of the uncertainty distribution.

Two models, K and P, show a lower bound for the expected value of predicted loss. In the case of K, this is a direct consequence of the model design which involves a constant baseline loss that accounts for any loss beneath the local 98th wind gust percentile. For model P a similar lower bound exists, which reflects the expected value of the noise level present in the loss data at any wind gust speed.

When considering the binned loss ratios (black circles) in Fig. 3.4 (a), both models X and H exhibit an underestimation of small losses, which is more pronounced for model H. A comparison with Fig. 3.2 shows that this behaviour is in line with the rapid convergence to zero of the damage curve for model H. Unsurprisingly, model P shows good agreement of binned loss ratios over a wide range of loss due to the fact that this model is the only one specifically designed to match also the low and medium loss ranges. In comparison, model K maps a considerably larger fraction of losses onto its lower bound (baseline loss) and seems to underestimate losses especially in the region around 10^{-6} . This behaviour is a likely outcome of the wind gust threshold fixed to the 98th percentile. Losses near or below this threshold may be strongly underestimated, an effect that plays a larger role for small-scale storms than for extreme, large-scale storm events.

For ERA-I-driven simulations, Fig. 3.4 (b) shows a similar overall behaviour as for DWD wind gust data. Comparison indicates a stronger variability of model results for ERA-I. Likely causes for this effect are the reduced spatial resolution of ERA-I grid cells compared to the spatial distribution of DWD climate stations and the lack of precise geographical allocation of wind gust values attributable only to entire grid cells.

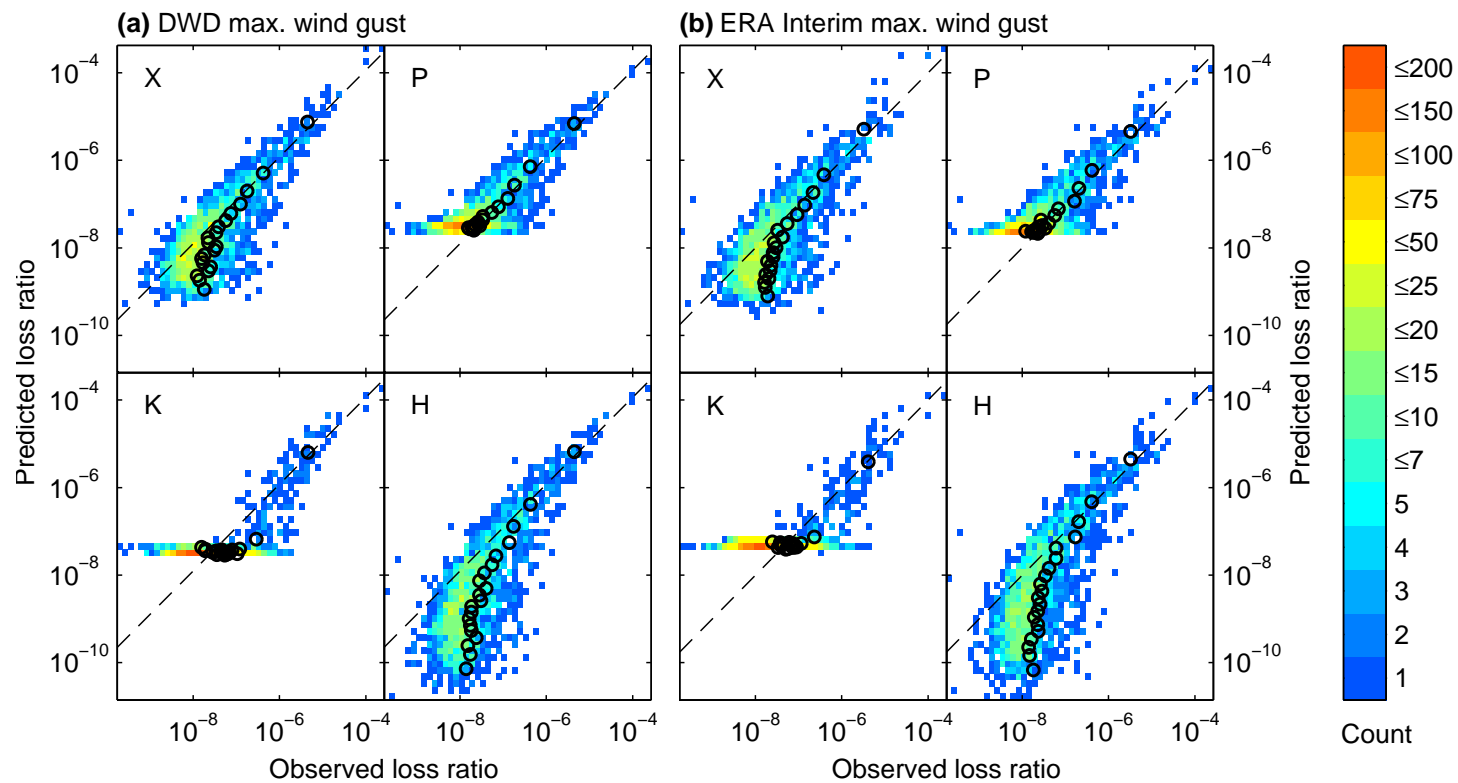


Figure 3.4: On country level, the predicted daily loss ratio (expected value) for each model is plotted versus observed losses using a double-logarithmic scale. (a) shows results based on DWD wind-gust data, ERA-1 wind-gust data are used in (b). The colours indicate the 2-D histogram count. The black circles represent (linear) averages of 100 losses each, binned by descending order of predicted loss. Black dashed lines have unity slope and indicate equality of observation and prediction.

Loss class	Tested against	Share of closest loss estimates in % (p value)			
		X	P	K	H
I	X	—	83 (0.02)	67 (0.11)	50 (0.34)
	P	17 (0.89)	—	17 (0.89)	67 (0.11)
	K	33 (0.66)	83 (0.02)	—	50 (0.34)
	H	50 (0.34)	33 (0.66)	50 (0.34)	—
II	X	—	68 (0.01)	24 (1.00)	62 (0.06)
	P	32 (0.97)	—	24 (1.00)	35 (0.94)
	K	76 (0.00)	76 (0.00)	—	76 (0.00)
	H	38 (0.89)	65 (0.03)	24 (1.00)	—
III	X	—	53 (0.24)	25 (1.00)	35 (1.00)
	P	48 (0.71)	—	35 (1.00)	47 (0.76)
	K	75 (0.00)	65 (0.00)	—	71 (0.00)
	H	65 (0.00)	53 (0.19)	29 (1.00)	—

Table 3.3: Results from a binomial test for the prediction accuracy of the different models based on daily loss estimates calculated from DWD wind gust data. The model of each column is tested against each row of competing models and across loss classes (as defined in Table 3.1). Bold results indicate superiority of the tested model with statistical significance greater than 95 %.

The similarity of results drawn from DWD and ERA-I wind gust data prevails for all further model results, and we hence focus the subsequent discussion on DWD-based model estimates. The quality (performance) of wind gust data in the context of storm damages is beyond the scope of the work in hand. For special interest we provide results corresponding to ERA-I in the Supplement (see Sect. 3.B3).

It is evident from an economic (or insurance) point of view that the performance for small and mid-range damages should be disregarded in case better performance is achieved for large loss events. In our further analysis we accommodate for this aspect by applying the loss categories defined in Table 3.1.

In order to compare model results over different loss ranges, we apply a simple scale-independent pairwise statistical test based on binomial statistics. For each pair of models, Table 3.3 provides the share of predictions where one or the other comes closer to the observation. Values with a statistical significance greater than 95 % are set in bold.

As the binomial test itself does not disclose why any specific model outperforms a competitor, we interpret the results of each model in conjunction with the mean absolute percentage error (MAPE) and the mean percentage error (MPE). Table 3.4 summarizes the results both for MAPE and MPE.

Loss class	Model MAPE (MPE) in %			
	X	P	K	H
I	56 (49)	17 (−5)	27 (−1)	26 (11)
II	67 (27)	51 (27)	79 (33)	55 (16)
III	75 (6)	97 (43)	85 (−51)	75 (−6)

Table 3.4: Estimates of the MAPE and MPE for each of the competing models and across loss classes (as defined in Table 3.1) based on DWD wind gust data. Best values for each class are emphasized in bold.

For extreme losses in loss class I the binomial test gives prevalence to the model P, whose estimates exhibit the lowest MAPE. There appears to be indifference between models H and P, although MPE shows that model H tends to overestimate extreme losses, while model P shows a small downward bias. Model K exhibits the least bias and yields the lowest MPE.

Considering loss class II, all models show a strong tendency to overestimate large losses. Here, the smallest bias is produced by H with an MPE of 16%. Results from P exhibit the least variability of the four models, so that the model can outperform the competitors in the binomial test.

In contrast, moderate losses in class III illustrate a completely different behaviour. The biggest change arises for K, which converts from significant overestimation to strong underestimation indicated by a negative bias of −51%. While the upward bias of P increases for moderate losses, models X and H exhibit only small bias and generally the smallest MAPE.

All above metrics were based on model estimates obtained from DWD wind gusts [cf. Fig. 3.4(a)]. Tables related to ERA-I wind gusts generally show the same tendencies and are given in the supplementary material in Sect. 3.B3. In Sect. 3.B1, we also provide an additional diagram showing results of the binomial test for small and minor losses below the 0.9 quantile.

3.4.3 Most Severe Storm Events

Having so far considered only single loss days, Fig. 3.5 shows the aggregated loss ratios for the six most severe (in terms of loss) winter storms during the observation period. The daily loss estimates were accumulated for the entire passage duration of the respective cyclones, whose start and end dates are given in Table 3.5.

In addition to the expected value obtained from the full training sample, estimates of the expected value obtained from the jackknife resampling give an indication of the robustness of the model fit. A large spread of jackknife estimates, e.g. as seen for the model X, indicates a strong dependence on the training sample.

Storm	Start date	End date
Anatol	2 Dec 1999	5 Dec 1999
Lothar	24 Dec 1999	27 Dec 1999
Jennifer	25 Jan 2002	30 Jan 2002
Anna	25 Feb 2002	1 Mar 2002
Jeanett	26 Oct 2002	29 Oct 2002
Kyrill	17 Jan 2007	19 Jan 2007

Table 3.5: Dates of the six most severe winter storms during the period 1997–2007 (Donat et al., 2011b).

Robustness is of particular concern, since the short training period may not always contain very severe storms, and, hence, the storm damage function must reliably extrapolate beyond its support. Empirically, this aspect is illustrated most prominently for winter storms Jeanett and Kyrill, both affecting approximately the same geographical region.

In the case of model K, the outliers of the jackknife estimates for these storms relate to a training sample containing neither one as benchmark. It becomes apparent that the linear regression employed for model K straps the otherwise highly constrained damage function to the maximum level of losses present in the training sample.

With the exception of winter storm Lothar, model P exhibits the least spread of expected values. Even though there are no constraints on the exponent of the damage function as for model K, the model demonstrates robustness due to its larger support from the entire range of observed losses.

A similarly robust behaviour is shown by model H, albeit there appears to be some sensitivity to the training sample for winter storms Jeanett and Kyrill. In contrast to model P, the robustness of model H is likely to originate from the strong constraints imposed on the damage function by the choice of distribution function for the critical gust speed.

The least constrained model X appears not only to be sensitive to the training sample used, but also generates significant overestimation for the three most severe winter storms. Although a verdict may not be based on three events only, the exponential approach appears less reliable for extreme winter storms than the competing models.

Finally, Fig. 3.5 also shows the probability density contours for the probabilistic models P and H derived from Monte Carlo calculations, convolving all 10 jackknife model fits with 1000 realizations each. While a judgement on the adequacy of the distributions cannot be made due to the scarcity of extreme events, some observations can be made. Model P, which assumes a log-normal uncertainty distribution with constant scale parameter generates heavily skewed loss distributions that by inspection seem too wide. In contrast, the

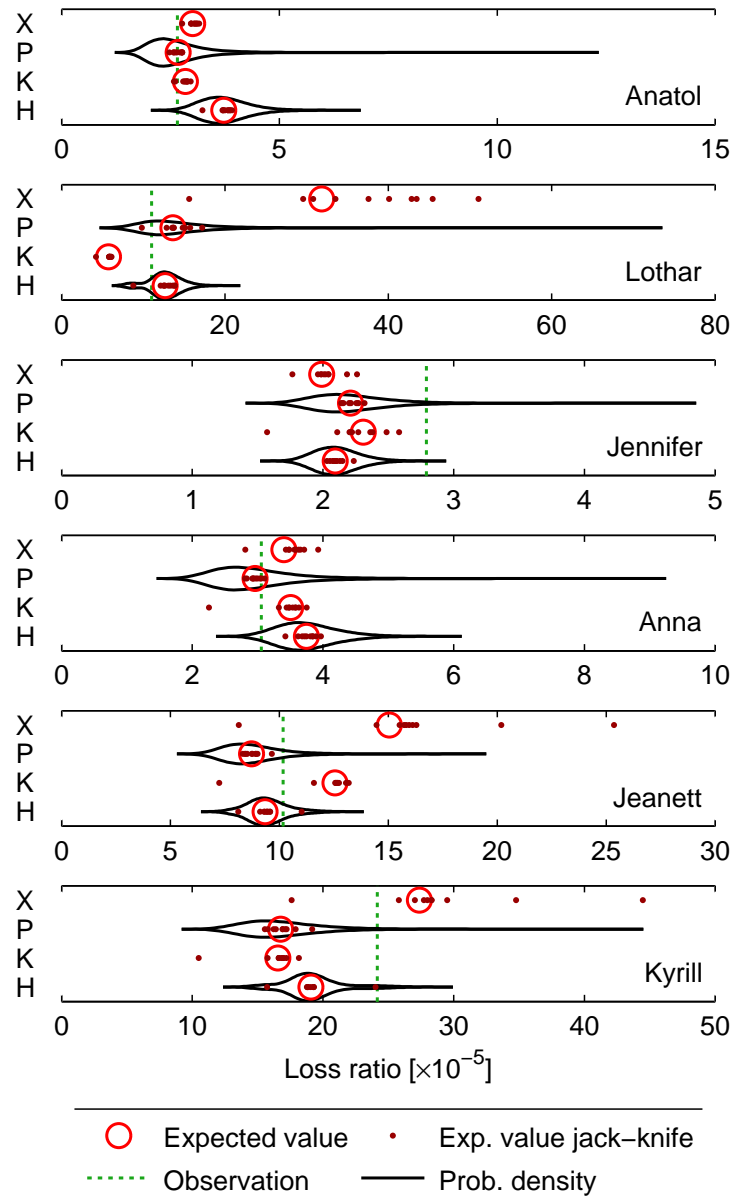


Figure 3.5: Model estimates for the six most severe winter storms in the period 1997–2007 based on DWD data. Red circles indicate the expected value obtained from models trained on the full 10-year data, while the red dots represent expected values from the 9-year resampled (jackknife) training periods. For models P and H, the black contours represent the probability distribution of predicted storm loss for the 10-year training data. Empirical insured loss is marked by green dashed lines.

less-skewed loss distribution produced by H appears more reasonable. In general, both models yield loss distributions that encompass empirical observations.

3.5 Towards a Synthesis of Storm Damage Functions

All of the four different damage functions discussed herein exhibit a loss increase that is much more rapid than a cubic power law derived from physical considerations about the kinetic energy of the wind mass. In this section, we propose a simple mechanism to reconcile the steep loss increase with a cubic power law. With our hypothesis we intend to expedite the discussion on the overall shape of the damage curve, since its behaviour beyond the support has strong implications for the extrapolation of loss.

Figure 3.6(a) shows the average loss increase obtained when superimposing data from all German districts. Visual comparison with the power-law guiding lines suggests that both the LR and the CR curves increase significantly faster than the 3rd power of wind gust speed. Moreover, the average LR of affected buildings (i.e. those for which an insurance claim was filed) remains approximately constant over a wide range of wind gust speed. This implies a minimum loss threshold for damage compensation to be claimed. Such a threshold could be caused by insurance deductibles, but may also arise from small damages that either go unnoticed or are fixed autonomously.

We make the hypothesis that the steep loss increase that is observed from the GDV data may be a consequence of the presence of such a loss threshold. Mathematically, when applying a threshold T the expected loss ratio LR_{all} is given by

$$LR_{\text{all}} = \int_T^{\infty} L f_v(L) dL, \quad (3.7)$$

where $f_v(L)$ denotes the probability distribution of the loss ratio L at gust speed v . The claim ratio CR follows from the respective cumulative distributive function, $F_v(L)$, as

$$CR = 1 - F_v(T). \quad (3.8)$$

The loss ratio of affected buildings LR_{affected} is then simply given by

$$LR_{\text{affected}} = \frac{LR_{\text{all}}}{CR}. \quad (3.9)$$

Assuming a log-normal uncertainty distribution, Fig. 3.6(b) illustrates the effect of a loss threshold on the expected LR obtained from a simple cubic loss-wind relationship. As a result, for low wind gust speed LR_{affected} remains close to the threshold value, while LR_{all} steeply increases. The noise level of the GDV

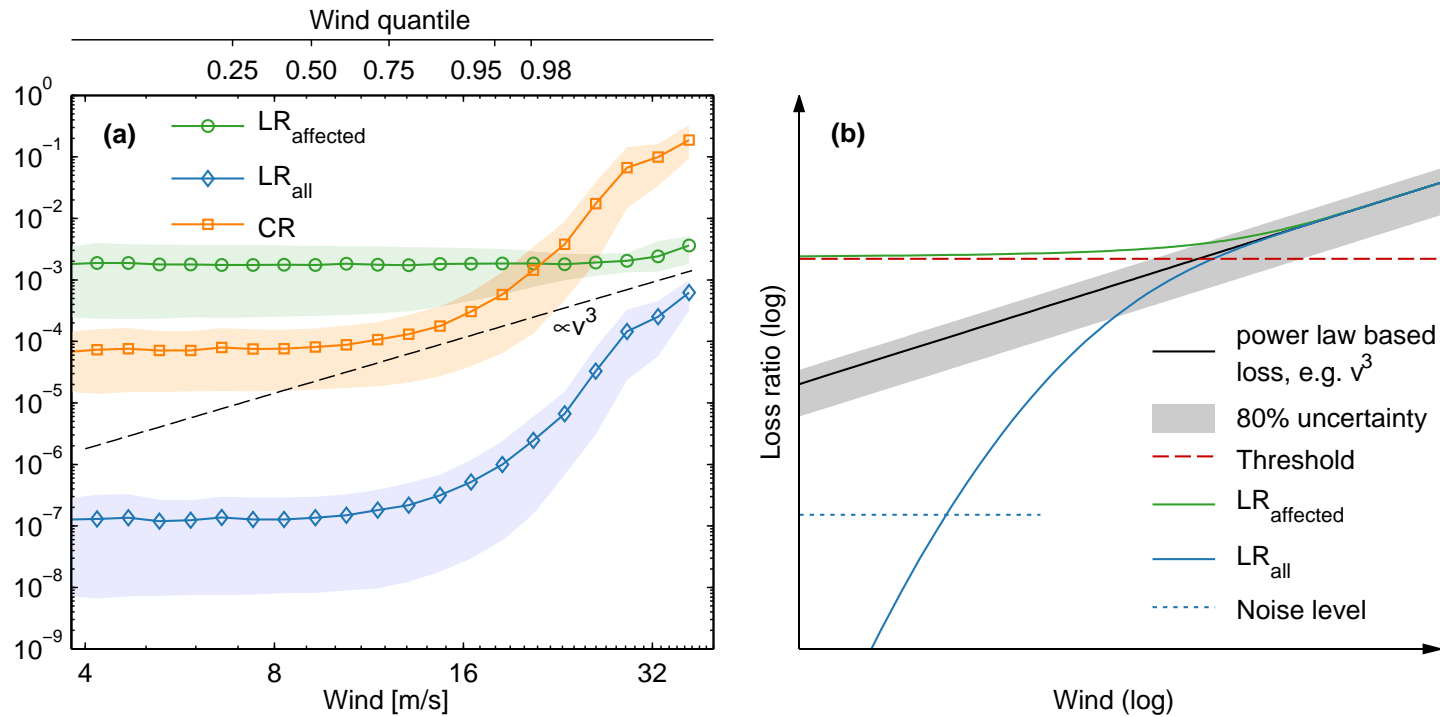


Figure 3.6: (a) shows the overall DWD gust dependence of the loss and claim ratio for all buildings and the loss ratio only of affected (i.e. damaged) buildings. Shown on a log–log scale, the solid curves represent expected values across all available districts and loss days, while the shaded areas indicate an 80 % uncertainty interval for observations. The dashed line provides a guide to the eye representing a power laws with exponent 3. The upper scale indicates the respective wind gust quantiles. (b) shows schematically the decomposition of the loss ratio of a cubic loss–wind relationship subject to a minimum loss threshold. With a lognormal uncertainty distribution, indicated by the shaded 80 % uncertainty bounds, a picture similar to (a) arises.

data however entails a minimum loss level, approximately corresponding to a single damaged building per district portfolio.

To be consistent, both LR curves given in Fig. 3.6 (a) must converge as gust speed increases. However, at these gust levels damages are unlikely to follow an idealized square or cubic relationship, especially with cascading effects in case of a breach of the building envelope and additional damage caused by flying debris. Sparks and Bhinderwala (1994) show that at extreme wind speeds a minor fraction of overall loss is comprised by direct wind damage, while the majority of loss results from interior or non-wind damage that are not captured by the physical considerations above.

3.6 Discussion and Concluding Remarks

The non-linear processes behind wind and non-wind damage as well as the effects of cascading failure of structural components entail that reduced-form approaches as discussed here may only approximate the actual storm damage characteristics. In order to assess the robustness and quality of macroscale storm damage functions, we have analysed and compared the results of four different models applicable to the European winter storm season. As a growing body of climatological research indicates, an increase in future storm intensity (see, e.g., the review article by Feser et al., 2015) could lead to the emergence of new hazard profiles. Conditional on the accurate reproduction of local wind characteristics, gust-based damage functions can provide a flexible tool to assess these changes.

Before we discuss the detailed results of the comparison, it is important to acknowledge the effect of deductibles on the shape of damage functions derived from insurance data. Care must be taken as to what extent physical damage concepts, such as a cubic wind–damage relationship, may be applied to insured storm loss. In this regard, all four compared damage functions exhibit a much stronger increase of loss, which is in good agreement with the GDV data employed herein. However, by introducing a simple loss threshold we could demonstrate how such a steep damage function for winter storm loss could be reconciled with a purely cubic wind–damage relationship. If, as climatological research suggests, future storm intensities increase beyond current levels, the overall shape of the damage function plays a crucial role for the extrapolation of future losses. With our threshold hypothesis we intend to expedite the discussion on the validity of damage functions beyond their original data support.

Storm-related insured losses generally exhibit a very broad distribution with a high dynamic range that spans several orders of magnitude. The loss distribution is highly skewed with very few extreme loss events dominating total annual loss. These two aspects pose severe difficulties for both the calibration and the evaluation of damage functions.

With a focus on the level of extreme losses, least-squares curve fitting has often been employed to calibrate damage curves to loss data. The combination

of skewed loss distribution and heteroscedastic variance seen for the case of GDV data suggests a violation of the basic assumption for least-squares fitting and potentially leads to biased results. Due to the high dynamic range even temporally or spatially aggregated loss figures, as used in the cubic excess-over-threshold damage function by Klawns and Ulbrich (2003) (model K), are subject to this effect as they are still dominated by extreme losses.

The optimal curve fitting procedure remains a matter of discussion. Relying on the assumption of general damage relation valid for a large range of losses, the probabilistic power-law damage function by Prahls et al. (2012) (model P) puts equal weight on all data points. In contrast, the fitting procedure for the probabilistic claim-based damage function by Heneka and Ruck (2008) (model H) has given greater weight to extremes by using averages of binned losses. The comparison between model H and the simple exponential damage function (model X), both of which are calibrated in the same manner, shows that effective calibration relies on a combination of model constraints and curve fitting.

As was seen in Fig. 3.5, model H attains greater robustness against jackknife variations of the training sample due to the presumption of a specific claims distribution. Following a different philosophy, model P achieves robustness by rooting the damage function in the entire range of loss.

Transferability is one of the biggest challenges of empirical damage functions. All of the discussed damage functions require substantial calibration to loss data. On the one hand, Heneka and Hofherr (2011) applied their damage function to Germany by employing a static parameterization originally obtained for the federal state of Baden-Württemberg. Donat et al. (2011a), on the other hand, assume the same vulnerability for nation-wide building stock. In both cases, spatial extension of the model comes at cost of blurring regional vulnerability.

From a practical point of view, model K is most easily calibrated since only a scaling of an otherwise robust raw damage term is required. More elaborate are the calibration procedures for models X and P, which both require detailed loss data. Mathematically, calibration of model H is most demanding and also requires additional data for the number of loss claims.

In order to assess the countrywide performance of the different models, a simple binomial test was devised. In conjunction with the more traditional metrics MAPE and MPE, it was shown that models H and P generally perform best, with some advantage for model P in the large loss class. Most interestingly, the behaviour for extreme losses is indecisive. Model P shows the least variability in terms of MAPE, while model K exhibits the least bias. In terms of the closest model predictions, the binomial test is indecisive between models H and P, whereas both are preferred to models K and X. A summary of the results is given in Table 3.6.

The applicability of model K appears to be focused on extreme losses. Its further behaviour turns from a positive bias for large losses into a strong negative bias for the moderate loss class. In Sect. 3.A3 we showed that for extreme

gust speeds, model K exhibits steepness similar to model P. However the model reaches a lower bound at the 98th wind gust percentile and hence appears to understate losses at speeds in the proximity of this threshold.

Overall, similar behaviour is found for ERA-I-based results which are given in the Supplement (see Sect. 3.B3). A peculiar difference is that for the class of extreme loss days model K performs best in terms of deviation and bias, but fares worse when regarding the losses accumulated for the six largest storms. These contradictory findings can be explained by the imprecise representation of major storms in ERA-I data, especially with regard to the temporal wind profile.

Generally, the obtained results were irrespective of either DWD or ERA-I wind gust data. Not surprising, ERA-I-based results showed greater variance than those based on direct wind gust observations. Interestingly, on district level the estimated coefficients of variation reveal a marked increase of model variance from the west to the east of Germany.

Further analysis of the coefficient of variation emphasized the importance of the interplay between damage function and the particular wind gust distribution (from either DWD or ERA-I). Strong interdependence was seen for model H, performing best with DWD data, and for model K, which showed best results for ERA-I data. While model P showed low variability throughout and appeared most flexible to the different data sources, model X showed the greatest error variance overall.

It is worthwhile to note that the coefficient of variation indicates a strong level of residual error variance even for the best-performing model. The advantage of DWD over ERA-I gust data (cf. Fig. 3.3) suggests a strong influence of uncertainty in wind gust data. However, there are also a number of potential uncertainty sources connected to the employed insurance data. Uncertainties may arise from gradual damage accumulation masking the effect of individual storms, from incentives for insurance holders (e.g. deductibles), and from wealth levels that affect both building quality and insurance taken. While the employed data does not allow a stratification of losses along socio-economic dimensions, our regional calibration implicitly accounts for spatial variations due to regionally differing vulnerability and wealth patterns. An altogether different situation would arise for models calibrated on a national scale, where such effects must be considered explicitly.

In our comparison it would not be meaningful to draw a unique conclusion on the suitability of each model as the performance may crucially depend on the purpose for which it is applied. In the light of this limitation, the exponential modelling approach was found less adequate for the modelling of extremes. In contrast, model K showed its best results for extreme losses, albeit with a calibration procedure that appears less robust than those of the probabilistic models H and P.

Both probabilistic models provided good results over a wide range of loss (moderate to extreme), with their model differences being much smaller than

Criteria	Rank	Model	Description
Extreme loss predictions (loss class I)	1.	P	least error, small bias
	1.	K	small error, least bias
	3.	H	slightly worse error, moderate positive bias
	4.	X	strong error and strong positive bias
Moderate to large loss predictions (loss classes III and II)	1.	H	good prediction, positive bias for ERA-I, smallest bias for DWD
	2.	P	good prediction for large loss, positive bias
	3.	X	decent prediction for large loss, smallest error and least bias for moderate loss
	4.	K	reasonable prediction, strong bias flipping from negative to positive
Variability on district level	1.	H	best for DWD, overall good for ERA-I
	1.	P	very good for both gust data sources
	3.	K	better for ERA-I; best in north-eastern, worst in southern Germany
	4.	X	worst for DWD, large variability for ERA-I
Model applicability	1.	K	simple calibration, also on extreme losses only
	2.	P	requires data for all sizes of loss
	2.	X	requires large training data set
	4.	H	both number of claims and loss data required

Table 3.6: Ranking of the four damage functions according to their prediction quality, variability, and applicability.

the general variability of losses. On the regional level, they yielded smaller coefficients of variation than the two deterministic models. While models H and P exhibited comparable results, a slight preference could be given to model P in terms of robustness and applicability. With regard to the broadly skewed uncertainty of estimates, probabilistic models can give a better picture of potential loss and should generally be preferred. However, uncertainty estimates for extreme loss remain a concern and should be subject to further research.

Acknowledgements. We gratefully acknowledge valuable discussions with U. Ulbrich and M. Boettle. We thank the German Insurance Association (GDV), the German Weather Service (DWD), and the European Centre for Medium-Range Weather Forecasts (ECMWF) for providing the data. This work was supported by the European Community's Seventh Framework Programme under grant agreement no. 308497 (Project RAMSES).

Appendices to Chapter III

3.A Mathematical Model Description and Calibration Setup

3.A1 Generic Exponential Damage Function

The assumption of an exponential damage relationship is not uncommon in the related literature (Huang et al., 2001; Prettenthaler et al., 2012; Murnane and Elsner, 2012) and such models are characterized by a steeper increase than comparable power-law models.

Mathematically, the damage function is comprised of a simple exponential term for the loss ratio,

$$L_X(v) = e^{X_1(v-X_2)}, \quad (3.10)$$

where coefficient X_1 re-scales the wind gust, and offset X_2 adjusts the estimates of the exponential term to the observed loss figures.

Due to the high dynamic range of the loss data and their inherent heteroscedasticity, the damage function cannot be calibrated directly via least squares. Similarly to the approach for model H, training data were truncated below the 95th wind gust percentile in order to discard the noisy lower end of the loss spectrum that would otherwise distort the damage function. Using gust speed, the remaining loss data were averaged in 10 equally spaced bins with a minimum of five losses each. Thus the relative weight of the few extremes compared to the abundance of small losses was increased. Finally, a logarithmic transformation of the loss averages was employed to reduce the dynamic range of loss and Eq. 3.10 was fitted via least squares regression.

3.A2 Probabilistic Power-Law Damage Function

Prahl et al. (2012) advocate a probabilistic damage function based on a power-law approximation to a more general sigmoid curve. The backbone of the damage function is given by the relationship for the median of the loss magnitude M (i.e. the loss ratio, given at least one loss claim),

$$\tilde{M}_v \approx \left(\frac{v}{\mathcal{P}_2} \right)^{\mathcal{P}_1} + \mathcal{P}_3, \quad (3.11)$$

where in addition to the power-law scaling \mathcal{P}_2 and exponent \mathcal{P}_1 a constant noise level \mathcal{P}_3 is included. Based on the observation that for given wind gust speed v the dispersion of insured losses approximately followed a log-normal

distribution, $\text{LN}(\mu, \sigma)$, the stochastic loss magnitude is described as a random variable

$$M_v \sim \mathcal{LN}\left(\ln\left(\widetilde{M}_v\right), \mathcal{P}_4\right). \quad (3.12)$$

The location parameter of the log-normal distribution is related to the median by $\mu = \ln(\widetilde{M}_v)$. The scale parameter $\sigma = \mathcal{P}_4$ describes both the variability due to imprecise gust observation and the aleatory uncertainty regarding the damage caused.

Complementary to the loss magnitude, the probability of loss occurrence (i.e. of receiving one or more loss claims) is given by the relationship

$$p(v) = 1 - \frac{\mathcal{P}_5}{1 + e^{\mathcal{P}_7(v - \mathcal{P}_6)}}. \quad (3.13)$$

The turning point \mathcal{P}_6 relates to the transition from the noisy regime to the regime of physically driven damages. \mathcal{P}_7 determines the sharpness of the transition and \mathcal{P}_5 the noise level. Loss occurrence is described stochastically as a random variable

$$O_v = \begin{cases} 1 & \text{if } P \leq p(v) \\ 0 & \text{if } P > p(v) \end{cases}, \quad (3.14)$$

where random variable P is drawn from the standard uniform distribution, $P \sim \mathcal{U}(0, 1)$.

In conjunction, loss occurrence and loss magnitude yield the stochastic expression for the loss ratio

$$L_P = O_v M_v, \quad (3.15)$$

with an expected value given by

$$\begin{aligned} \mathbb{E}[L_P]_v &= \mathbb{E}[O_v] \mathbb{E}[M_v] \\ &= p(v) e^{\mu + \frac{\sigma^2}{2}} \\ &= p(v) e^{\frac{\mathcal{P}_4^2}{2}} \widetilde{M}_v. \end{aligned} \quad (3.16)$$

For high wind gust speeds $v \gg \mathcal{P}_6$, e.g. beyond the 95th percentile, the noise level becomes negligible and the expression for the expected value of loss simplifies to

$$\mathbb{E}[L_P]_{(v \gg \mathcal{P}_6)} \approx e^{\frac{\mathcal{P}_4^2}{2}} \left(\frac{v}{\mathcal{P}_2}\right)^{\mathcal{P}_1}. \quad (3.17)$$

Equation 3.17 demonstrates that for high wind gust speeds the expected value of the damage function is approximately proportional to the gust speed raised to the power \mathcal{P}_1 .

Both components of the damage function are calibrated separately. The log-normally distributed loss magnitude is fitted via maximum likelihood to the empirical loss. A least-squares approach is used to fit the loss occurrence term against empirical occurrence rates derived from binned data, enforcing parameter constraints such that the loss occurrence probability is bound within the interval $[0, 1]$.

3.A3 Cubic Excess-Over-Threshold Damage Function

Klawa and Ulbrich (2003) developed a simple storm damage function that was subsequently refined for regional application and calibrated to GDV data (Donat et al., 2011a,b). At the heart of the damage function is a cubed power-law term as a proxy for storm damage,

$$D(v) = \begin{cases} \left(\frac{v-v_{98}}{v_{98}} \right)^3 & \text{if } v \geq v_{98} \\ 0 & \text{if } v < v_{98} \end{cases} . \quad (3.18)$$

The damage function

$$L_K(v) = \mathcal{K}_1 D(v) + \mathcal{K}_2 \quad (3.19)$$

is calibrated against loss data via linear regression, where constants \mathcal{K}_1 and \mathcal{K}_2 are the regression coefficients.

Keeping in mind the high dynamic range of loss claims with few dominating extreme losses, the linear regression implicitly puts a strong emphasis on extreme losses ensuring that these are closely matched (cf. Fig. 3.2).

The shape of the damage function is determined by the power-law term, which is influenced only by the 98th wind gust percentile. We chose to determine the 98th percentile from the same training sample as used for calibration of the remaining parameters.

The value of this threshold is of particular interest, as it controls the shape and with it the steepness of the damage function. To clarify this statement, we relate the cubed power-law term of the damage function with a tangent based on a simple power law without threshold. For every gust speed v , the tangency condition requires equality of the function values

$$c_1 \left(\frac{v}{v_{98}} - 1 \right)^3 = \left(\frac{v}{c_2} \right)^\gamma \quad (3.20)$$

and equality of the first derivatives

$$\frac{3c_1}{v_{98}} \left(\frac{v}{v_{98}} - 1 \right)^2 = \frac{\gamma}{c_2^\gamma} v^{\gamma-1} . \quad (3.21)$$

Solving Eqs. 3.20 and 3.21 for the exponent γ yields the simple relationship

$$\begin{aligned}\gamma &= 3 \frac{v}{v_{98}} \left(\frac{v}{v_{98}} - 1 \right)^{-1} \\ &\equiv \frac{3\eta}{\eta - 1}.\end{aligned}\tag{3.22}$$

Equation 3.22 shows that the local steepness of the cubed excess-over-threshold term depends on the ratio $\eta = v/v_{98}$ of the gust speed to its 98th percentile. For the employed DWD data, the average ratio over all districts of the maximum measured gust speed to the 98th percentile is $\bar{\eta}_{\max} \approx 1.50$, implying that for extreme losses the damage curve increases approximately as a power law with exponent $\gamma \approx 9.0$. Repeating the calculation for ERA-I data, we estimated $\bar{\eta}_{\max} \approx 1.41$ and a local power-law exponent $\gamma \approx 10.3$.

Hence, the steepness of the model is dependent on the wind gust data source, which may have a potential impact on the portability of the damage function. Additionally, the high local exponents around 10 indicate a similarity with other models that report exponents of a similar magnitude, e.g. Prahm et al. (2012). In physical terms, the two regression coefficients \mathcal{K}_1 and \mathcal{K}_2 are interpreted, respectively, as a scaling constant and a base loss for losses occurring at wind gusts beneath the threshold. As such, \mathcal{K}_2 must be constrained to be strictly non-negative.

For data-scarce applications, it may be opportune to resolve regional portfolio differences via population density as a proxy for (insured) value and obtain a global parameterization via regression on the national level (e.g. Donat et al., 2011a). In contrast, the finely resolved loss data for our study allowed a local parameterization and the simple summation of loss to the national level.

Finally, Donat et al. (2011a) perform the regression against annual loss aggregates, while Donat et al. (2011b) demonstrate calibration against a selected sample of the 34 most loss-intensive storm passages. We find that the former calibration method produces better results. However, for reference, results from both calibration methods are given in the Supplement (see Sect. 3.B2).

3.A4 Probabilistic Claim-Based Damage Function

Heneka et al. (2006) provide a theoretical framework for the modelling of storm loss. Their model was applied first to the federal state of Baden-Württemberg and subsequently to Germany (Heneka and Hofherr, 2011). Maintaining the key assumptions made by Heneka et al. (2006) as far as possible, the inter-comparison was based on the following considerations for model design and calibration.

The fundamental concept of model H is the idea that buildings sustain damage only above a critical wind gust threshold v_c . The damage sustained by individual buildings is hence dependent on the specific value of the critical

threshold and is formalized by a microscale damage relationship for the fractional damage g ,

$$g(v, v_c) = \begin{cases} 0, & v < v_c \\ \left(\frac{v-v_c}{\mathcal{H}_1}\right)^2, & v_c \leq v \leq (v_c + \mathcal{H}_1) \\ 1, & v > (v_c + \mathcal{H}_1) \end{cases}, \quad (3.23)$$

reaching complete destruction at a wind gust increase of \mathcal{H}_1 above the critical threshold.

For a portfolio of buildings, each with individual critical threshold, a specific density distribution for v_c may be assumed or otherwise estimated. For simplicity, Heneka et al. (2006) idealized the density distribution of v_c by the density of the normal distribution $f(v_c, \mu_c, \mathcal{H}_2)$, with mean μ_c and standard deviation \mathcal{H}_2 . It follows that the claim ratio $C_H(v)$, i.e. the relative share of affected buildings, is given by the integral

$$C_H(v) = \int_{-\infty}^v f(v_c, \mu_c, \mathcal{H}_2) dv_c. \quad (3.24)$$

The loss ratio $L_H(v)$ is then obtained by solving the convolution integral

$$L_H(v) = \int_{-\infty}^v g(v, v_c) f(v_c, \mu_c, \mathcal{H}_2) dv_c, \quad (3.25)$$

combining the density distribution of v_c with the microscale damage function $g(v, v_c)$.

Finally, uncertainty is introduced by assuming a Gaussian distribution $f(\mu_c, \mathcal{H}_4, \mathcal{H}_3)$ for the mean critical wind gust speed μ_c , with mean \mathcal{H}_4 and standard deviation \mathcal{H}_3 . Putting all components together, we obtain an expression for the expected value of the loss ratio,

$$\mathbb{E}[L_H] = \int_0^1 L f(\mu(L), \mathcal{H}_4, \mathcal{H}_3) \frac{d\mu(L)}{dL} dL, \quad (3.26)$$

where we define $\mu_c = \mu(L)$ as the inverse function of Eq. 3.25 with respect to μ_c .

For calibration, Heneka et al. (2006) used least-squares fitting of claims and loss data that was pooled for the entire state of Baden-Württemberg. However, fitting the damage function to individual districts, it was found that least-squares curve fitting was yielding poor results due to frequent overfitting to the few number of "outlying" extreme events and the generally high dynamic range of the data. Furthermore, the model was developed on strong winds and could not deal with the noise present in the GDV data at low wind gust speeds.

For the work in hand, these problems were solved via a three-step fitting procedure. In order to exclude the effect of noise, data below the 95th wind gust percentile were discarded during the fitting procedure.

	Source	\mathcal{H}_4	\mathcal{H}_3	\mathcal{H}_2	\mathcal{H}_1
Absolute gust	Heneka and Ruck	50.5	2.5	7.8	70.0
	DWD	42.3	2.0	6.2	49.7
		(50.5)	(2.4)	(7.4)	(59.4)
	ERA-I	41.6	1.8	5.6	45.5
		(50.5)	(2.2)	(6.8)	(55.3)
	Relative gust	Heneka and Ruck	1.31	0.04	0.20
DWD		2.28	0.09	0.32	2.67
		(1.31)	(0.05)	(0.19)	(1.54)
ERA-I		2.17	0.10	0.29	2.43
		(1.31)	(0.06)	(0.18)	(1.47)

Table 3.7: Comparison of the parameter values obtained for the federal state of Baden-Württemberg with those published by Heneka and Ruck (2008). Accordingly, relative wind gust speed was normalized by its 98th percentile. For easier comparison, the values in brackets are rescaled to match the published value of \mathcal{H}_4 .

In the first step, Eq. 3.24 was fitted to claims data. To overcome the problem of the high dynamic range, claims data were logarithmically transformed. To counteract the downside of the transformation, namely the increased weight of the abundant small damages as compared to the few extremes, the data were binned into 10 equally spaced bins, each containing a minimum of five data points. Using the method of least squares the curve was fitted to the mean values of each bin. In this step, we made the implicit assumption of a multiplicative error term, relating to a symmetric distribution around the mean of the log-transformed claims data (i.e. the geometric mean of the absolute numbers). This assumption is backed by actuarial practice for describing insurance damage claim distributions by log-symmetric distribution such as the log-normal distribution (Lawrence, 1988).

In the second step, the above described fitting procedure is used to calibrate Eq. 3.25 to the loss ratio data.

Thirdly, the parameters of the normal distribution describing the random fluctuation of μ_c are determined via log-likelihood optimization based on loss data at full detail.

Due to the strong deviation from the original least-squares fitting employed by Heneka et al. (2006), it was necessary to validate the parameters obtained from the GDV data set. For this purpose, we pooled the GDV data for all districts in the state of Baden-Württemberg and compared the obtained model parameters against those values published by Heneka and Ruck (2008). The results presented in Table 3.7 show good agreement of the individual parameters across the different sources. As the wind gust data sources are not directly

comparable, the parameters shown in brackets were rescaled according to \mathcal{H}_4 . Regarding these values, only \mathcal{H}_2 , which represents the wind gust range from beginning to total destruction, shows a significant difference of approximately -15% as compared to the original values.

While we report only those results that relate to the best performing model setup, results from applying the Baden-Württemberg calibration to entire Germany (similarly to Heneka and Hofherr, 2011) are included in the Supplement for special interest (see Sect. 3.B2).

3.B Supplementary Material

3.B1 Binomial Test for Model Performance

While the results in Sect. 3.4.2 focus on the upper 10th percentile of the loss distribution, separated into the three defined loss classes, Fig. 3.7 shows the results of the simple binomial test based on a moving-window approach. Here, we apply a 2 and a 10 percentile window to the model estimates which were ranked by descending order of the corresponding empirical loss. This approach enables a full view on the relative performance of the individual models also in medium or low loss ranges.

However, care must be taken when interpreting the behaviour for small loss events, as the limitation of the different models play a deciding role. In particular the lower bounds of the models P and K, observed in Fig. 3.4, lead to a strong signal in Fig. 3.7. For example, pairwise comparisons with model K show an apparently strong performance of model K for a cumulative loss ratio between 10^{-8} and 10^{-7} . However, this effect corresponds to observed losses incidentally matching the lower bound of the model and, hence, does not indicate superior predictive skill. Considering the loss range indicated by the left-hand axis (cumulative loss ratio) it becomes clear that this effect may be rather seen as an artefact at an insignificant loss level.

3.B2 Results for Different Set-Ups of Models K and H

Based on their respective publications, different calibrations options are available for both the model K and the model H. In case of model K, Donat et al. (2011a) perform a regression against annual loss aggregates, while Donat et al. (2011b) demonstrate calibration against a selected sample of the 34 most loss-intensive storm passages. Figure 3.8 shows the results obtained after both calibrations, the annual calibration [K] employed in Chapter III and the storm-based calibration [K storm].

As outlined in Chapter III, our approach to the calibration of model H differs from those originally published by Heneka and Ruck (2008). Whereas we applied a district-wise calibration, Heneka and Ruck (2008) calibrated their model against pooled data, merged from all post-code areas in the federal state of Baden-Württemberg. Following their approach, we have also pooled all district data within Baden-Württemberg. In line with Heneka and Ruck (2008), the model was calibrated against absolute DWD wind gust data [H BW] and against relative DWD data [H BW rel] normalized to the 98th wind gust percentile. All results of the different calibrations are shown in Fig. 3.8.

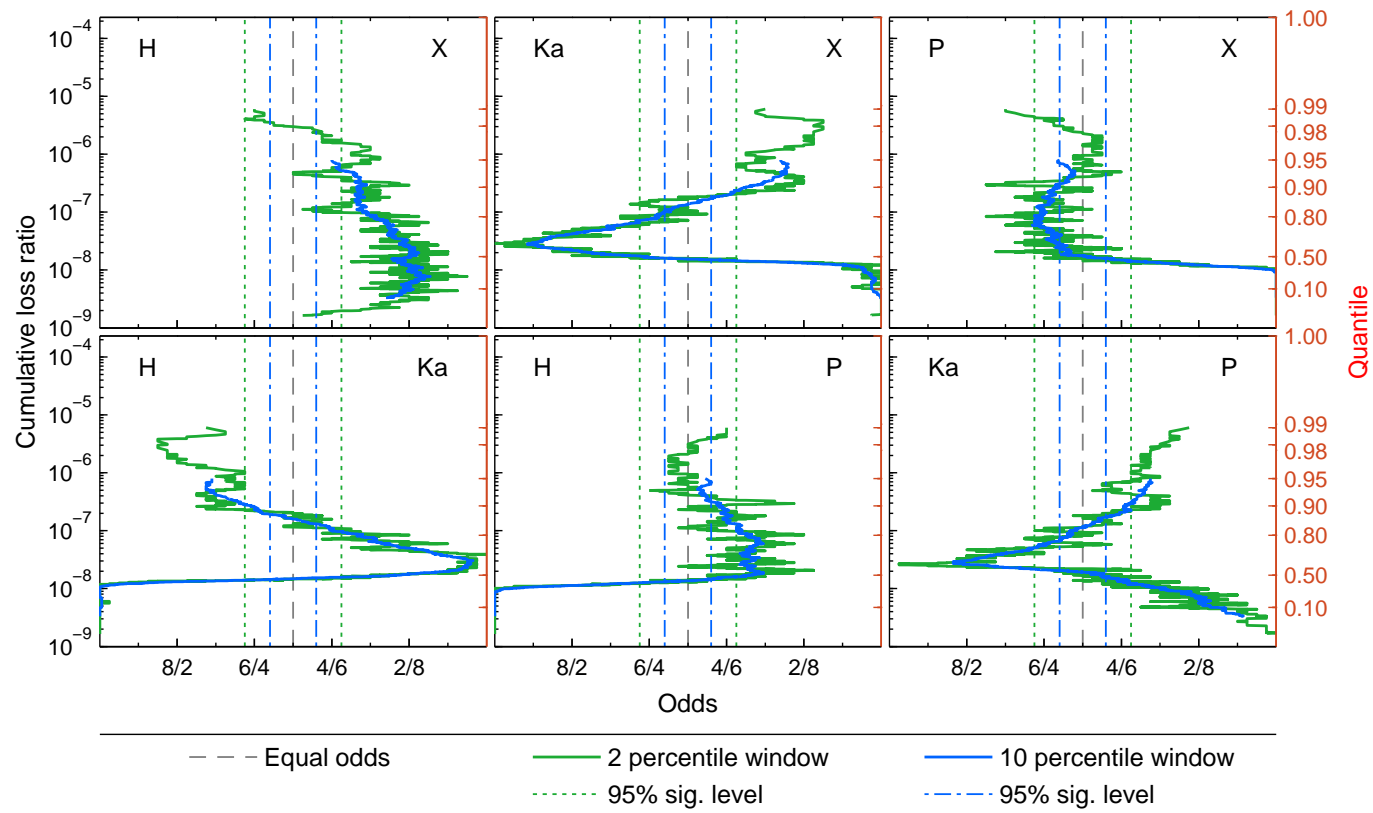


Figure 3.7: The figure shows the odds (i.e. the ratio of the total hits – as being closest to the observation – of each of the models in the pairwise comparison) calculated for the simple pairwise binomial test on varying loss ranges. Estimates were ranked in descending order by the corresponding observed loss amount. Moving 2 and 10 percentile windows were used to estimate the pairwise odds. The results are significant if the odds exceeded the 95% guidelines obtained from the binomial distribution.

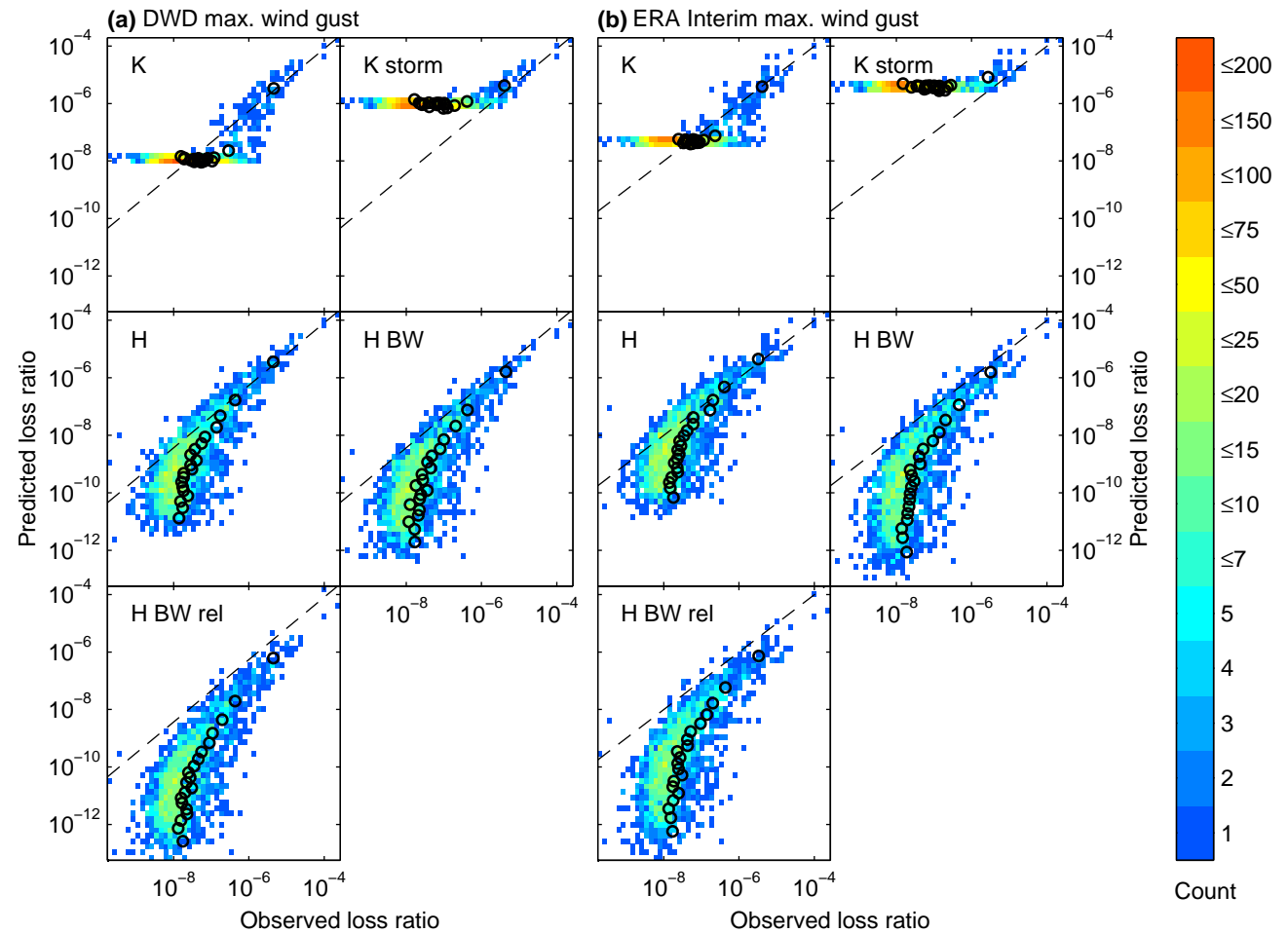
3.B3 Countrywide Results of the Binomial Test and MAPE/MPE Metrics Based on ERA-I Data

The following Tables 3.8 and 3.9 show countrywide results obtained from ERA-I wind gust data. They correspond to the DWD based Tables 3.3 and 3.4 in the main paper. The results based on ERA-I are very similar to those obtained from DWD data, with the exception of loss class one, where model K appears to excel. The results should, however, be interpreted in conjunction with Fig. 3.9, which indicates that the loss accumulated over the entire passage duration of the 6 most severe winter storms (with peaks corresponding to the 6 most severe loss days) is not so well reproduced by model K.

Loss class	Test vs.	Share of closest loss estimates in % (p-value)			
		X	P	K	H
I	X	—	83 (0.02)	100 (0.00)	67 (0.11)
	P	17 (0.89)	—	83 (0.02)	33 (0.66)
	K	0 (0.98)	17 (0.89)	—	50 (0.34)
	H	33 (0.66)	67 (0.11)	50 (0.34)	—
II	X	—	79 (0.00)	29 (0.99)	71 (0.00)
	P	21 (1.00)	—	26 (1.00)	18 (1.00)
	K	71 (0.00)	74 (0.00)	—	71 (0.00)
	H	29 (0.99)	82 (0.00)	29 (0.99)	—
III	X	—	53 (0.24)	34 (1.00)	34 (1.00)
	P	48 (0.71)	—	38 (1.00)	47 (0.76)
	K	66 (0.00)	63 (0.00)	—	64 (0.00)
	H	66 (0.00)	53 (0.19)	36 (1.00)	—

Table 3.8: Results from a binomial test for the prediction accuracy of the different models based on ERA-I wind gust data. The model of each column is tested against each row of competing models and across loss classes (as defined in Tab. 3.1). Bold results indicate superiority of the tested model with statistical significance greater than 95%.

Figure 3.8: On country level, the predicted daily loss ratio (expected value) for each model is plotted versus observed losses on double-logarithmic scale. Left-hand panel **(a)** shows results based on DWD wind gust data, ERA-I wind gust data is used in panel **(b)**. The colors indicate the 2-D histogram count. The black circles represent (linear) averages of 100 losses each, binned by descending order of predicted loss. Black dashed lines have unity slope and indicate equality of observation and prediction.



Loss class	Model MAPE (MPE) both in %			
	X	P	K	H
I	250 (220)	62 (9)	57 (0)	91 (43)
II	133 (84)	90 (45)	108 (46)	102 (49)
III	82 (16)	95 (40)	85 (−51)	86 (19)

Table 3.9: Estimates of the MAPE and MPE for each of the competing models and across loss classes (as defined in Tab. 3.1) based on ERA-I wind gust data. Best values for each class are emphasized in bold.

3.B4 Results for the Six Most Severe Winter Storms Obtained from ERA-I Data

Figure 3.9 shows model estimates for the 6 most severe winter storms during the period under observation. The results are based on ERA-I data and correspond to Fig. 3.5, which is based on DWD wind gust data. Overall, the ERA-I based results show similar relative intervals than those obtained from DWD data. However, there appears to be a general bias in the wind gust data, e.g. shown by the pronounced overestimation for winter storm Anatol and the underestimation of winter storm Anna.

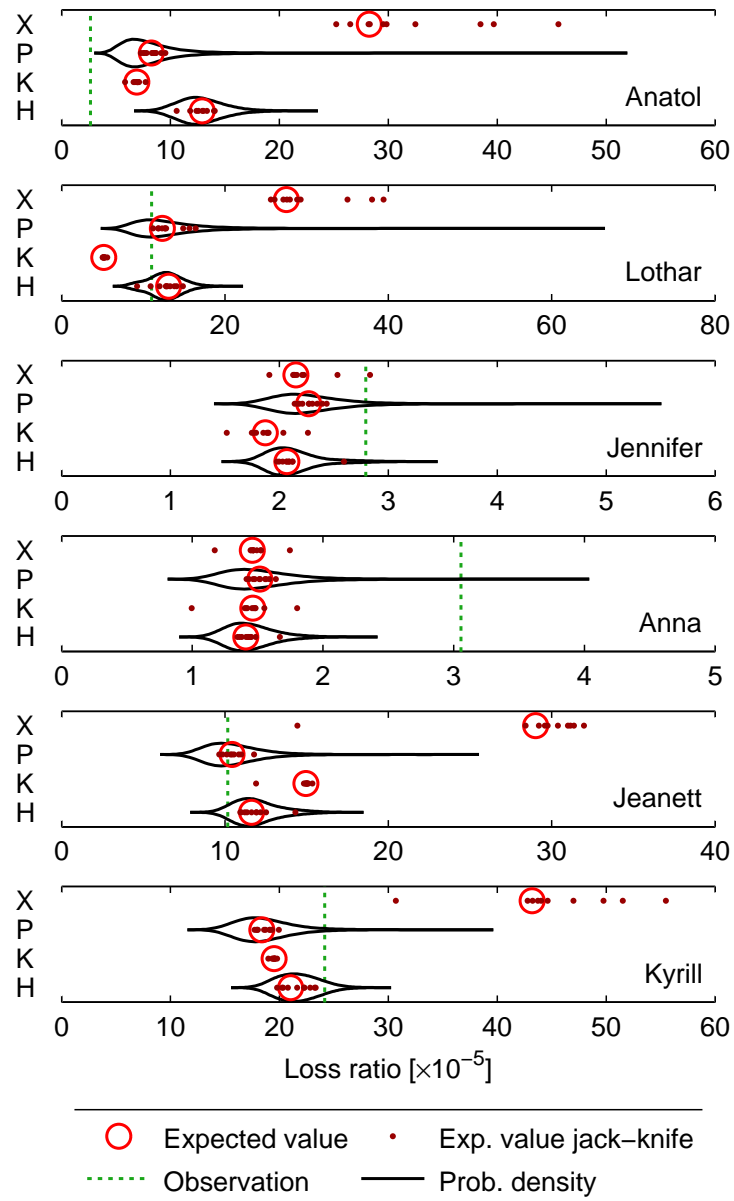


Figure 3.9: Model estimates for the 6 most severe winter storms in the period 1997–2007 based on ERA-I data. Red circles indicate the expected value obtained from models trained on full 10-year data, while the red dots represent expected values from the 9-year resampled (*jackknife*) training periods. For models P and H, the black contours reflect the probability distribution of predicted storm loss for the 10-year training data. Empirical insured loss is marked by green dashed lines.

IV

Damage Functions for Climate-Related Hazards: Unification and Uncertainty Analysis

Abstract. Most climate change impacts manifest in the form of natural hazards. Damage assessment typically relies on damage functions that translate the magnitude of extreme events to a quantifiable damage. In practice, the availability of damage functions is limited due to a lack of data sources and a lack of understanding of damage processes. The study of the characteristics of damage functions for different hazards could strengthen the theoretical foundation of damage functions and support their development and validation. Accordingly, we investigate analogies of damage functions for coastal flooding and for wind storms and identify a unified approach. This approach has general applicability for granular portfolios and may also be applied, for example, to heat-related mortality. Moreover, the unification enables the transfer of methodology between hazards and a consistent treatment of uncertainty. This is demonstrated by a sensitivity analysis on the basis of two simple case studies (for coastal flood and storm damage). The analysis reveals the relevance of the various uncertainty sources at varying hazard magnitude and on both the microscale and the macroscale level. Main findings are the dominance of uncertainty from the hazard magnitude and the persistent behaviour of intrinsic uncertainties on both scale levels. Our results shed light on the general role of uncertainties and provide useful insight for the application of the unified approach.

This chapter has been published as:

Prahl, B. F., Rybski, D., Boettle, M., and Kropp, J. P. (2016). Damage functions for climate-related hazards: Unification and uncertainty analysis. *Nat. Hazards Earth Syst. Sci.*, 16(5):1189–1203, doi: 10.5194/nhess-16-1189-2016.

© Author(s) 2016. CC Attribution 3.0 License.



4.1 Introduction

As climate extremes, natural hazards are an inherent part of the climate system. There is increasing evidence that a changing climate leads to changes in hazard characteristics and can even result in unprecedented extreme weather and climate events (IPCC, 2012). For instance, sea level rise aggravates the intensity of coastal floods such that expected damage increases more rapidly than mean sea level (Boettle et al., 2016).

For a risk assessment of natural hazards, damage functions are employed to translate the magnitude¹ of extreme events to a quantifiable damage. Often the focus is on the modelling of the hazard, while the damage assessment receives less attention (Merz et al., 2010).

Accordingly, the availability of damage functions is very limited. On the one hand, empirical damage functions may not be inferable due to a lack of observations for certain impacts or sites. On the other hand, the correlations between loss and the explanatory variable(s) might be weak and loss estimates could become unreliable due to the high level of uncertainty. This results in the need for a comprehensive damage assessment in order to enable the quantification and comparison of the impacts from different natural hazards and their interactions (Kreibich et al., 2014).

For this purpose, the work at hand provides an investigation into the common aspects of damage functions for different hazards. It considers similarities in damage functions and exposure for coastal flooding (as applied by Hinkel et al., 2014) and windstorms (Heneka and Ruck, 2008). A general derivation of the damage functions reveals that these constitute two facets of a more general approach which we refer to as a unified damage function.

Moving towards a multi-risk assessment, it is shown how this approach can be extended to heat-related mortality. This is of particular concern since heat-related fatalities currently comprise over 90 % of total natural hazard fatalities in Europe and are also a major issue for developing countries (Golnaraghi et al., 2014; Munich Re, 2013).

The unified damage function also provides a platform for the discussion of potential uncertainties. Embedding the damage function in a probabilistic framework, this study investigates the relevance of different uncertainty sources for damage estimation. Excluding considerations about the stochastic nature of extreme events, we consider uncertainties in the damage function subject to a hypothetical hazard magnitude. A variance-based sensitivity analysis (vbsa, see Saltelli et al., 2008) is employed to quantify the influence of uncertainties at different hazard magnitudes. Furthermore, the analysis compares the relevance of uncertainties on the microscale and the aggregated portfolio levels. As a result, the work at hand provides indications for considering relevant uncertainties in damage assessments.

¹ Throughout this chapter the term *hazard magnitude* is used to denote the intensity of the hazard with respect to the damage caused.

In Sect. 4.2, we begin by deriving the basis of the unified damage function in the context of coastal flooding and windstorms and extend the concept to heat-related mortality. The role of different uncertainties is discussed in Sect. 4.3, where we also derive the probabilistic framework for the unified damage function. Two case studies are parameterized in Sect. 4.4 to serve as the basis for the sensitivity analysis conducted in Sect. 4.5. We conclude with a discussion of our key results in Sect. 4.6.

4.2 Unified Damage Functions

Damage functions are an important tool for an impact assessment of climate-related hazards. For example, Fig. 4.1 shows three damage functions that relate to the hazards of coastal flooding, wind storms, and excessive heat. It is the goal of this section to determine a unified damage function that has applicability in each of these fields. For this purpose, the analogies between two existing damage functions for coastal floods and windstorms are analysed and an extension to heat-related mortality is proposed.

Henceforth, we rely on the following definitions. A damage function is defined as the mathematical relation between the magnitude of a (natural) hazard and the average damage caused on a specific item (building, person, etc.) or portfolio of items. The emphasis is on direct monetary damage, but the findings can be generalized to any measurable quantity.

In this context, the microscale level relates to a single item. In contrast, the macroscale level refers to a portfolio of independent items with similar properties (e.g. residential buildings). With this definition, we go beyond similar definitions that define the macro domain solely via the spatial extent (e.g. Merz et al., 2010). In the regional context, the macroscale damage function may refer to a city or otherwise spatially delineated portfolio. Damage can be expressed in absolute or relative terms (Merz et al., 2010). In order to facilitate comparison between different hazards, we consistently employ relative figures for both micro- and macroscale damage.

4.2.1 Coastal Floods – Explicit Threshold Representation

In the following, we give account of a damage function that has been frequently applied for the assessment of coastal flooding (e.g. Boettle et al., 2011; Hinkel et al., 2014).

We begin by defining a microscale damage function g , which relates the relative damage r of an item i to the hazard magnitude x :

$$r_i = g(x - \lambda_i). \quad (4.1)$$

The damage is conditional on the exceedance of the item-specific hazard threshold λ_i . In other words, a single item will suffer damage only if its hazard threshold is exceeded.

The hazard magnitude may be represented by a more or less complex indicator. Frequently the most basic indicator, maximum flood height, is chosen (Hallegatte et al., 2013; Hinkel et al., 2014). Neglecting ancillary damaging effects, such as floating debris, the damage to an individual building is dominated by the inundation. Accordingly, the hazard threshold is identified as the elevation of the building site and the threshold exceedance as the inundation level.

The microscale damage function has a lower bound of 0 for $x < \lambda_i$ and increases monotonically to its upper bound g_{\max} for $x \geq \lambda_i$. Considering relative damages, the upper bound is less than or equal to 1 and represents the potential maximum damage. In general, g can exhibit jumps and may hence not be differentiable.

For a macroscale damage assessment, e.g. for a coastal city, it is assumed that all items in the portfolio are exposed to the same hazard magnitude. Local fluctuations (e.g. caused by obstruction or varying distance to coast) are considered as a source of uncertainty in Sect. 4.3. For now, the fraction of affected items c within a portfolio of n items is given by the number of items for which x reaches or exceeds λ_i . Explicitly,

$$c_{\text{expl}}(x) = \frac{1}{n} \sum_{i=1}^n \mathcal{H}(x - \lambda_i), \quad (4.2)$$

where \mathcal{H} denotes the Heaviside step function, defined as

$$\mathcal{H}(z) = \begin{cases} 0, & \text{for } z < 0 \\ 1, & \text{for } z \geq 0. \end{cases} \quad (4.3)$$

The damage ratio for the portfolio (relative damage) is given by the average damage of the individual items:

$$\begin{aligned} d_{\text{expl}}(x) &= \frac{1}{n} \sum_{i=1}^n g(x - \lambda_i) \\ &= \frac{1}{n} \sum_{i=1}^n r_i. \end{aligned} \quad (4.4)$$

While the above equation assumes equal monetary value for each item, generalization is simple. Different item values can be incorporated by weighting the sum with a normalized asset value v_i (i.e. rescaled such that the average equals 1).

In order to emphasize the similarity to the storm damage function described in the following section, we define a discrete frequency distribution $f(\lambda_j)$ for the portfolio and rewrite Eq. (4.4) as

$$d_{\text{expl}}(x) = \sum_j f(\lambda_j) g(x - \lambda_j), \quad (4.5)$$

where the sum runs over all discretized threshold values λ_j .

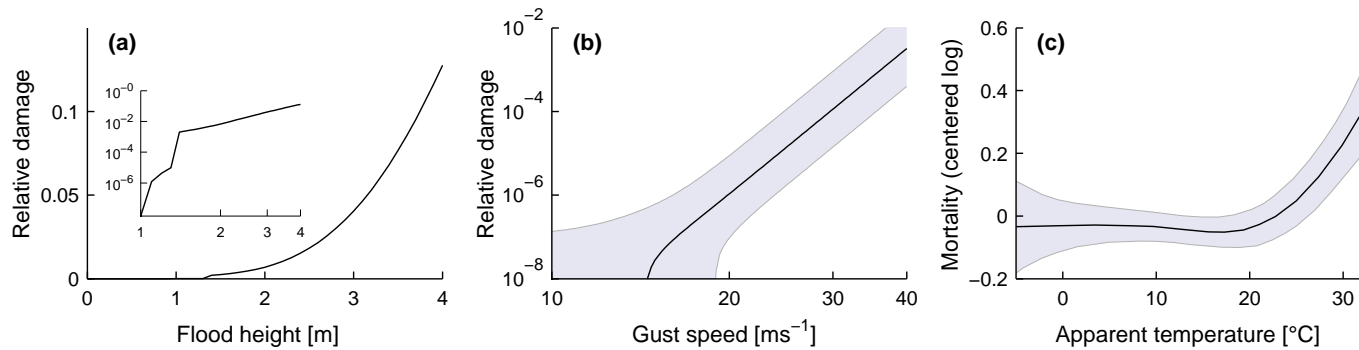


Figure 4.1: (a) Relative flood damage function obtained for the case study of Kalundborg (Boettle et al., 2011), with a log–log inset. (b) Relative storm damage function for a German district (Prahl et al., 2012). (c) Damage function for the city of Bologna, relating mortality increase to apparent temperatures (data extracted from Stafoggia et al., 2006). The shaded areas in (b) and (c) represent uncertainty bands.

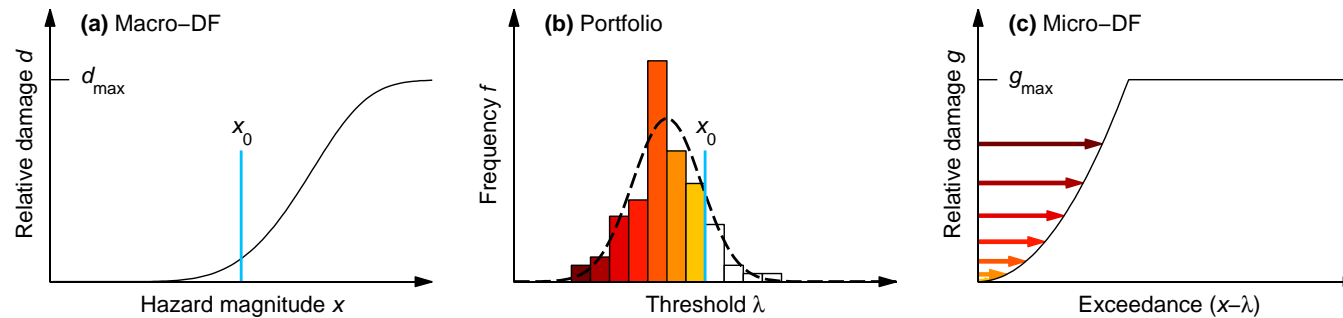


Figure 4.2: Schematically, (a) shows a macroscale damage function based on a building portfolio with a distribution of hazard thresholds as shown in (b), where coloured bars indicate portfolio segments affected at hazard magnitude x_0 . (c) shows the applied microscale damage function. Accordingly, the coloured arrows indicate the damage inflicted on the respective portfolio segments at x_0 .

The relationship between macroscale damage, portfolio composition, and microscale damage function is shown schematically in Fig. 4.2. Given a hypothetical hazard magnitude of x_0 , all colour-coded portfolio segments will be affected since x_0 exceeds their threshold. Accordingly, the coloured arrows in subfigure (c) indicate the damage suffered by each portfolio segment. The sum of these damages amount to the macroscale damage level seen in subfigure (a).

The key characteristic of this approach is the consideration of a granular portfolio of buildings, each with an observable hazard threshold. The approach is reliant on the availability of building-specific information and prior knowledge on the microscale damage function and hence represents a bottom-up approach.

4.2.2 Wind Storms – Implicit Threshold Representation

In this section we give account of a storm damage function that was developed by Heneka and Ruck (2008), which is then set into contrast with the previously discussed coastal flood damage function.

Storm damage functions are typically calibrated to insurance data. The data comprise the fraction of affected buildings (claim ratio) and the damage ratio for a defined region (Prahl et al., 2012).

It can be assumed that buildings have a specific resistance to wind (i.e. threshold wind speed) that depends on their characteristics (Walker, 2011). However, the detailed building characteristics are usually not known and there is no simple proxy for the hazard threshold. In consequence, the hazard threshold must be defined probabilistically, as follows.

In analogy to the coastal flood example, let λ_i denote the hazard threshold of an individual item. From a probabilistic point of view, λ_i constitutes an independent realization of a random variable Λ , whose probability density distribution is given by $f_\Lambda(\lambda)$.

For a given portfolio, $P(\Lambda \leq x)$ represents the expected value of the share of items whose hazard threshold has been attained or exceeded at a given x . Hence, the claim ratio is defined by the distribution of hazard thresholds:

$$\begin{aligned} c_{\text{impl}}(x) &= P(\Lambda \leq x) \\ &= \int_0^x f_\Lambda(\lambda) d\lambda. \end{aligned} \quad (4.6)$$

Having identified the distribution of hazard thresholds, the macroscale damage ratio is given by the convolution of the probability density of the hazard threshold and the microscale damage function $g(x - \lambda)$:

$$\begin{aligned} d_{\text{impl}}(x) &= (f_\Lambda * g)(x) \\ &= \int_0^x f_\Lambda(\lambda) g(x - \lambda) d\lambda. \end{aligned} \quad (4.7)$$

In other words, the potential damage at any hazard threshold λ is weighted with the probability density of λ . Via integration, the macroscale damage comprises all the contributions from hazard thresholds below the hazard magnitude x .

As in the previous case of coastal flooding, the damage function considers a granular portfolio of exposed buildings. The key difference is that in the case of wind storms a direct observation of the hazard threshold is not feasible. Instead, an implicit description of the portfolio is given by the distribution of hazard thresholds. In order to obtain this distribution, the damage function is calibrated against macroscale damage data in a top-down approach.

Simple inspection shows that Eq. (4.7) for wind storm is the continuous analogue to Eq. (4.5) for coastal flooding. Consequently, both approaches – bottom-up in the case of coastal floods and top-down for wind storms – can be understood as different facets of a unified damage function.

4.2.3 Extension to Heat-Related Mortality

Formally, the mathematical relationships derived in the previous sections also hold for other natural hazards such as heat-related mortality.

In general terms, the mortality rate is a measure of fatalities in a given population over a certain period of time. While it is not always possible to attribute fatalities to distinct causes, the effect of excess mortality due to the impact of heat waves has been widely studied (e.g. Gasparrini et al., 2015; Leone et al., 2013). Typically, excess mortality describes the increase of daily mortality in relation to a temperature indicator. An example for excess mortality for the city of Bologna is given in Fig. 4.1 (c). As can be seen, the expected mortality starts to increase just above 20 °C of apparent temperature (Stafoggia et al., 2006). In absolute terms, the increase in mortality can be defined as the daily number of heat-related fatalities divided by the total population.

Although it is a delicate issue to discuss human mortality in a technical language, we believe that it allows for an intuitive and meaningful application of the unified damage function. First, decease is expressed via a Heaviside step function, where 0 and 1 denote life and death respectively. The step function takes the part of the microscale damage function g in the unified damage function. Second, the hazard threshold relates to the maximum heat-wave intensity (e.g. apparent temperature) tolerated by an individual. While this threshold is generally not known and may also fluctuate over time, a statistical description of the distribution of heat-wave thresholds within the population would be feasible.

Extending the regional focus, Leone et al. (2013) and others have shown an influence of local climatic conditions as well as socio-demographic and economic characteristics on the shape of the damage function. However, a comprehensive decomposition of the hazard threshold is yet to be found.

Caution should be taken when considering the uncertainty of the hazard threshold. In contrast to the cases of coastal flood and storm damages, where building portfolios change only gradually, human heat tolerance is subject to continuous biophysical, behavioural, and environmental changes. Hence, a path dependence of the threshold exceedance is expected for ongoing heat waves.

4.3 Uncertainty

While the stochastic occurrence of hazardous events has been subject to ample research, the origin and propagation of uncertainty within the damage function has received less attention. Often, a rough understanding of sensitivity is obtained from estimating alternative scenarios (e.g. Hallegatte et al., 2013; Hinkel et al., 2014). Other studies focus on an empirical description of uncertainty (e.g. Heneka and Ruck, 2008; Merz et al., 2004) but do not provide a comprehensive analysis of potential sources.

To enable a comprehensive sensitivity analysis of uncertainty from different sources, the unified damage function is cast into a probabilistic framework. We begin by defining a taxonomy of uncertainty sources that are relevant in our context.

4.3.1 Brief Taxonomy of Uncertainty Sources

Uncertainties arise at each step along the causal chain, from the modelling or observation of the hazard through the estimation of micro- and macroscale damage to the validation against reported losses. We focus on the propagation of uncertainties within the damage function, linking the microscale with the macroscale behaviour. For this reason, model and parametric uncertainty are excluded. Model uncertainty would arise from selecting an inadequate damage function that deviates from the actual hazard–damage relation. Parametric uncertainty relates to incomplete knowledge about the model parameters (but not the explanatory variables).

It is common to categorize uncertainties into those that are due to statistical variability (aleatory) and those that are due to incomplete knowledge (epistemic) (Merz and Thielen, 2009). While model and parametric uncertainty belong to the latter category, the attribution is not clear-cut for uncertainties in explanatory variables. In principle, all aleatory uncertainty could be addressed as epistemic by raising the level of detail and modelling all minute sub-scale processes. Hence, Bedford and Cooke (2001) state that “the categorization into aleatory and epistemic uncertainties is *for the purposes of a particular model*”.

In order to maintain an intermediate level of detail, the considered uncertainties are classified as aleatory, i.e. statistically tractable. Having excluded model and parametric uncertainty, the remaining sources of uncertainty can be identified from the mathematical description of the damage function. For this

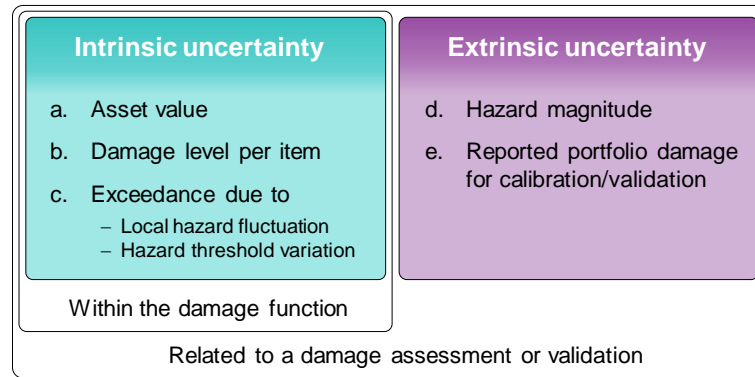


Figure 4.3: Classification of the sources of uncertainty into intrinsic and extrinsic.

purpose, Eq. (4.4) is cast into its most general form, including a variable asset weight v_i and allowing for a local hazard magnitude \tilde{x}_i to fluctuate around x :

$$d_{\text{expl}}(\mathbf{x}) = \frac{1}{n} \sum_{i=1}^n v_i \underbrace{g(\tilde{x}_i - \lambda_i)}_{r_i} e_i \quad (4.8)$$

On the right-hand side of Eq. (4.8), the asset weight v_i , the relative damage r_i , and the exceedance e_i are identified as potential sources of uncertainty. These are *intrinsic* uncertainty sources as they manifest within the damage function. On the left-hand side, the hazard magnitude represents an *extrinsic* source of uncertainty for the damage function. If observations of macroscale damage were available for the calibration or validation, these would represent an additional source of extrinsic uncertainty.

The sources of uncertainty are summarized in Fig. 4.3 and each source is briefly described in the following.

- a. The asset values of affected items can vary significantly (e.g. different house prices). The attribution of values to location is feasible only on a detailed case study level, while large-scale assessment typically relies on by-proxy estimation of average asset value (e.g. Hallegatte et al., 2013; Hinkel et al., 2014). Especially in the latter case, unknown asset values pose a significant source of uncertainty.
- b. Even if structures of similar type are equally affected (i.e. at the same threshold exceedance) their damage can differ considerably. The underlying damaging processes are not well understood and are dependent on construction types and employed materials. The resulting uncertainty could in principle be reduced by modelling all physical processes involved. However, data limitations usually permit no more than a stratification to a few predefined asset classes (Hammond et al., 2015).

- c. The threshold exceedance for an item is subject to uncertainty in the hazard threshold (λ_i) and fluctuations of the local hazard magnitude (\tilde{x}_i). The hazard threshold may either be not directly observable (e.g. for storm damage) or be affected by measurement error (e.g. using elevation models for flood damage assessment). Similarly, the local hazard magnitude is affected by observational or modelling error.
- d. On the macroscale level, the hazard magnitude is typically described by a single indicator (e.g. the maximum flood level or gust speed). For all practical purposes, this indicator is subject to uncertainty, stemming either from imprecise measurement, uncertain model output, or confidence levels estimated from extreme value statistics (Coles and Tawn, 2005). Prah et al. (2012) highlight the relevance of this uncertainty by indicating that variability of reported storm losses could be largely due to uncertainty in wind measurements.
- e. For purposes of calibration and validation, model estimates are often put into comparison with reported figures of damage or economic loss. Like any observation, these figures are subject to uncertainty. For example, reported figures may be affected by gradual damage accumulation masking the effect of individual hazard occurrences, by incentives for insurance holders (e.g. deductibles), and by wealth levels that affect the construction quality and the likelihood of purchasing insurance.

4.3.2 Probabilistic Description of Uncertainty

A quantitative analysis of the aforementioned uncertainties requires an extension of the basic damage function. Here, we derive a comprehensive probabilistic framework for the unified damage function. The framework also forms the mathematical basis for the subsequent sensitivity analysis.

We begin by defining random variables for each of the micro- and macroscale model variables. Microscale variables are the local hazard magnitude \tilde{X} , the hazard threshold Λ , the threshold exceedance E , the inflicted relative damage R , and the relative asset weight V . The asset-weighted damage for a single object is described by L . Similarly, we define the macroscale random variables for the hazard magnitude and its measurement, X and \hat{X} . The macroscale damage for the portfolio takes into account the different weights of the asset values and is described by D . In the following, the probability density function (PDF) of each random variable is denoted as $f_{(\cdot)}$.

The exceedance, $e = \tilde{x} - \lambda$, closely links the uncertainty in the local hazard magnitude with the uncertainty of the hazard threshold. The PDF of the random variable E for the exceedance is hence given by the convolution of the PDFs of X and Λ as follows:

$$f_{E|X=x}(e) = f_{\tilde{X}|X=x}(\tilde{x}) * f_{\Lambda}(-\lambda). \quad (4.9)$$

The distribution of the relative damage caused, $f_{R|E=e}(r)$, is conditional on the level of exceedance. The combination with Eq. (4.9) yields an expression for the distribution of relative damage conditional on the hazard magnitude:

$$f_{R|X=x}(r) = \int_0^{\infty} f_{R|E=e}(r) f_{E|X=x}(e) de. \quad (4.10)$$

We define the asset-weighted damage as the product of relative damage and normalized asset value, $l = rv/n$. In the case that individual asset values are not known, a probabilistic asset weight v is employed. Its PDF, $f_V(v)$, can be obtained by rescaling the PDF of absolute asset values such that the expected value equals 1.

The PDF of l is obtained by combining the PDF of asset weights with Eq. (4.10):

$$f_{L|X=x}(l) = \int_0^{\infty} f_{R|X=x}(nl/v) f_V(v) dv. \quad (4.11)$$

Since the macroscale damage d is the sum of the weighted microscale damages, its PDF is given by the convolution of the density functions for the asset-weighted damages of each of the n portfolio items:

$$D = \sum_{i=1}^n L_i$$

$$f_{D|X=x}(d) = f_{L_1|X} * f_{L_2|X} * \dots * f_{L_n|X}. \quad (4.12)$$

Finally, uncertainty in the true hazard magnitude x (e.g. resulting from measurement or model output \hat{x}) is modelled via PDF $f_{X|\hat{X}=\hat{x}}(x)$. Using Eq. (4.12) it follows that

$$f_{D|\hat{X}=\hat{x}}(d) = \int_0^{\infty} f_{D|X=x}(d) f_{X|\hat{X}=\hat{x}}(x) dx. \quad (4.13)$$

4.4 Case Studies for the Sensitivity Analysis

Based on our taxonomy of uncertainties, we provide an exemplary parameterization of the unified damage function for two separate climate-related hazards: (i) coastal flooding in Lisbon, Portugal, and (ii) winter-storm damage for a German building portfolio comprised of 5000 individual buildings.

The Lisbon case exemplifies a bottom-up approach, where the individual hazard thresholds are known explicitly. Since coastal flooding is not bound by artificial administrative boundaries, we consider a cluster of continuous urban agglomeration in the Lisbon metropolitan area (Fig. 4.4). The cluster extent was kindly supplied by B. Zhou (see Zhou et al., 2013) and had been generated from 2006 data of the CORINE Land Cover (CLC) project (Büttner et al., 2007). It includes several connected suburbs along the shores of river Tejo and the north of the Setúbal peninsula.

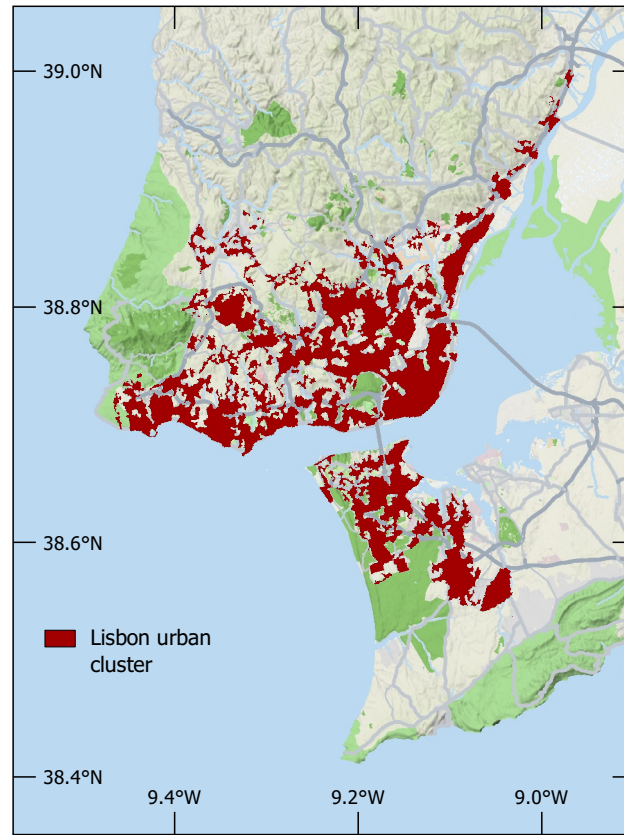


Figure 4.4: The Lisbon urban cluster supplied by B. Zhou (see Zhou et al., 2013). The red-shaded area represents continuous and discontinuous urban fabric as classified in the CLC data (Büttner et al., 2007).

The portfolio of flood-prone buildings within the cluster of Lisbon is based on statistical data provided by the Instituto Nacional de Estatística², the national Portuguese statistics institute. Census data from 2007 on the number of buildings at the highest resolution available (*Freguesia*, i.e. urban quarters) were downscaled via the CLC classes for continuous and discontinuous urban fabric.

The number of buildings within each CLC cell were assigned to elevation levels obtained from the EU-DEM³, a hybrid digital elevation model (DEM) based mainly on SRTM and ASTER GDEM data. A flood-fill algorithm (Poulter and Halpin, 2008) was employed to determine which DEM cells were affected at different flood levels, increasing in steps of 0.5 m up to a maximum of 10 m. All employed data are publicly available. Table 4.1 shows the number of flooded buildings within the Lisbon urban cluster at flood levels up to 10 m.

Microscale building damages in the Lisbon cluster are estimated with the damage function employed by Hinkel et al. (2014), described by a saturating

² Data available from <http://www.ine.pt>.

³ Obtained from <http://www.eea.europa.eu/data-and-maps/data/eu-dem>.

Flood level [m]	Inundated buildings	
	Total	Increase [%]
0.0	0	—
0.5	19	—
1.0	28	47
1.5	36	29
2.0	43	19
2.5	67	56
3.0	107	60
3.5	146	36
4.0	210	44
4.5	453	116
5.0	670	48
5.5	888	33
6.0	1284	45
6.5	1621	26
7.0	1895	17
7.5	2356	24
8.0	2659	13
8.5	3025	14
9.0	3435	14
9.5	3985	16
10.0	4478	12

Table 4.1: The number of inundated buildings within the Lisbon urban cluster at hypothetical flood levels between 0 and 10 m.

power law $z/(z + 1 \text{ m})$. The function implies that relative damage increases proportional to the inundation level for $z \ll 1 \text{ m}$ and saturates at 1 for large z .

A complementary top-down approach is pursued for the German building portfolio, with an implicit description of the hazard threshold by means of a probability density distribution. In the case of storm hazard, the determinants of the hazard threshold are less clear-cut than for flood damages. While they depend strongly on construction type and building age, a strong residual uncertainty remains. Heneka and Ruck (2008) argue for a simple statistical description of hazard thresholds via a normal distribution with mean 55 m s^{-1} and standard deviation 7.8 m s^{-1} . Due to the lack of similar works, we adopt their parameterization to generate a generic portfolio of 5000 residential buildings.

The mean microscale damage caused by severe winds is often described as a power law with an upper bound representing complete destruction (Prah

et al., 2015). Again following Heneka and Ruck (2008), we apply a simple square power law.

Unlike the general features of the damage function, the nature of the uncertainties involved is typically not well understood and their quantification heavily relies on assumptions. Consequently, the required PDFs of the asset value, the microscale damage, the exceedance, and the hazard magnitude were estimated from literature, where available, and otherwise based on own considerations. Tables 4.2 and 4.3 provide a summary of the case study parameterization for each of the case studies, including the employed references. Due to the scarcity of information on uncertainty concerning microscale damage and the asset value, an identical parameterization was used for both case studies. Details on the estimation of uncertainties are given in Appendix 4.A.

Figure 4.5 (a–c) and (d–f) show the derived macroscale damage function, the portfolio composition, and the assumed microscale damage function for both cases respectively.

4.5 Sensitivity Analysis

Going beyond the qualitative description of the involved uncertainties, this section focusses on their potential impact on damage estimates. From a non-linear damage function we expect potential interactions between different uncertainties that may vary with the hazard magnitude. Moreover, the analysis should take the different scales into account, as the macroscale damage is effectively an aggregation of microscale damages.

The influence of the various sources of uncertainty is assessed by performing a sensitivity analysis. Sensitivity analysis usually considers the effect of variation in one or more input variables on the dependent variable. For simple linear models, it may be sufficient to vary only one input variable at a time, since there is no interaction between different input variables. Non-linear models, in contrast, require a global sensitivity analysis, where simultaneous changes of all input variables are considered.

4.5.1 Method

We employ the variance-based sensitivity analysis (vbsa), which estimates the contribution of each input variable to the total variance of the dependent variable (Saltelli et al., 2008). vbsa is a global sensitivity analysis and uses a Monte Carlo approach to sample from the probability distributions of the uncertain variables.

The general algorithm of vbsa is summarized as follows. First, two ($s \times t$) matrices **A** and **B** are defined, where each column vector represents one of the t input variables that has been sampled s times. Initially, the matrices are filled with uniformly distributed random values between 0 and 1. Then, inverse cumulative distribution functions are used to convert the random vectors to the

Table 4.2: Parameterization of the probabilistic damage function for the estimation of damage from coastal flooding in Lisbon. The variables μ and σ denote the mean and standard deviation respectively.

Component	Parameterization	References
Portfolio composition	Frequency distribution for Lisbon	[this paper] see Table 4.1
Microscale damage function	$g(z) = \frac{z}{z+1\text{ m}}$	Hinkel et al. (2014)
Asset value	$\text{Log}\mathcal{N}(\mu = 1, \sigma = 0.5)$	adapted from Ohnishi et al. (2011)
Damage level	$\text{Log}\mathcal{N}(\mu = g, \sigma_{g=0.5} = 0.1)$	[this paper] based on Lawrence (1988)
Threshold exceedance	$\mathcal{N}(\mu = \chi - \lambda, \sigma = 0.2\text{ m})$	Hallegatte et al. (2013) and EEA (2014)
Hazard magnitude	$\mathcal{N}(\mu = \chi, \sigma = 0.1\text{ m})$	Fortunato et al. (2014)

Table 4.3: Parameterization of the probabilistic damage function for the storm damage simulation for a German building portfolio. The variables μ and σ denote the mean and standard deviation respectively.

Component	Parameterization	References
Portfolio composition	$\mathcal{N}(\mu = 50.5\text{ m s}^{-1}, \sigma = 7.8\text{ m s}^{-1})$	Heneka and Ruck (2008)
Microscale damage function	$g(z) = \left(\frac{z}{70\text{ m s}^{-1}}\right)^2$	Heneka and Ruck (2008)
Asset value	$\text{Log}\mathcal{N}(\mu = 1, \sigma = 0.5)$	adapted from Ohnishi et al. (2011)
Damage level	$\text{Log}\mathcal{N}(\mu = g(z), \sigma_{r=0.5} = 0.1)$	[this paper] based on Lawrence (1988)
Threshold exceedance	$\mathcal{N}(\mu = \chi - \lambda, \sigma = 1\text{ m s}^{-1})$	[this paper] based on Mitsuta and Tsukamoto (1989)
Hazard magnitude	$\mathcal{N}(\mu = \chi, \sigma = 1.5\text{ m s}^{-1})$	Prahl et al. (2012) and Hofherr and Kunz (2010)

respective input variables of the model, i.e. the damage function. For each input variable with index i , a new matrix $\mathbf{C}_{(i)}$ is constructed, comprising all columns with index $j \neq i$ from \mathbf{A} and the column $j = i$ from \mathbf{B} .

The total-effect index is chosen as the main metric for sensitivity. It describes the share of output variance that is due to the direct and indirect effects of an uncertain variable. The direct effect (also called first-order effect) measures the lone contribution of varying a single variable, averaged over different realizations of the remaining variables. Indirect effects (higher-order effects) are due to interactions between two or more variables, e.g. a second-order effect may arise from the interaction between the threshold exceedance and the damage level.

The total-effects index TE_i of the damage function $\mathcal{F}(\cdot)$ is evaluated using the recommended Jansen estimator (Jansen, 1999; Saltelli et al., 2010):

$$TE_i = \frac{\frac{1}{2s} \sum_{k=1}^s (\mathcal{F}(\mathbf{A})_k - \mathcal{F}(\mathbf{C}_{(i)})_k)^2}{\sigma^2}, \quad (4.14)$$

with

$$\begin{aligned} \sigma^2 = & \frac{1}{2s} \sum_{k=1}^s (\mathcal{F}(\mathbf{A})_k^2 + \mathcal{F}(\mathbf{B})_k^2) \\ & - \left(\frac{1}{s} \sum_{k=1}^s \mathcal{F}(\mathbf{A})_k + \mathcal{F}(\mathbf{B})_k \right)^2. \end{aligned} \quad (4.15)$$

Note that in Eq. (4.15) we include both matrices \mathbf{A} and \mathbf{B} in order to obtain a closer estimate of the variance than by using matrix \mathbf{A} alone.

The vBSA was applied on three distinct levels: (i) the microscale level related to a single item, (ii) the macroscale level limited to intrinsic uncertainty, and (iii) the macroscale level including extrinsic uncertainty. The sample size s was set to 20 000. At level (i), s random samples of the asset value V , the damage level R , and the exceedance E were drawn from the probability distributions $f_V(v)$, $f_{R|E=e}(r)$, and $f_{E|X=x}(e)$ respectively. At level (ii), the same procedure was applied, albeit for each of the items that sum up the portfolio. Finally, at level (iii), the hazard magnitude X and the macroscale damage D (including the effects of intrinsic uncertainties) were drawn from the distribution functions $f_{X|\hat{X}=\hat{x}}(x)$ and $f_{D|X=x}(d)$ respectively.

In order to evaluate the uncertainty of the sensitivity indices, the bootstrap method was used to obtain uncertainty intervals. Specifically, the s random samples were resampled (i.e. selected randomly with replacement) 1000 times, and each time the sensitivity indices were recalculated. From the resulting distribution, the 95% uncertainty range was estimated.

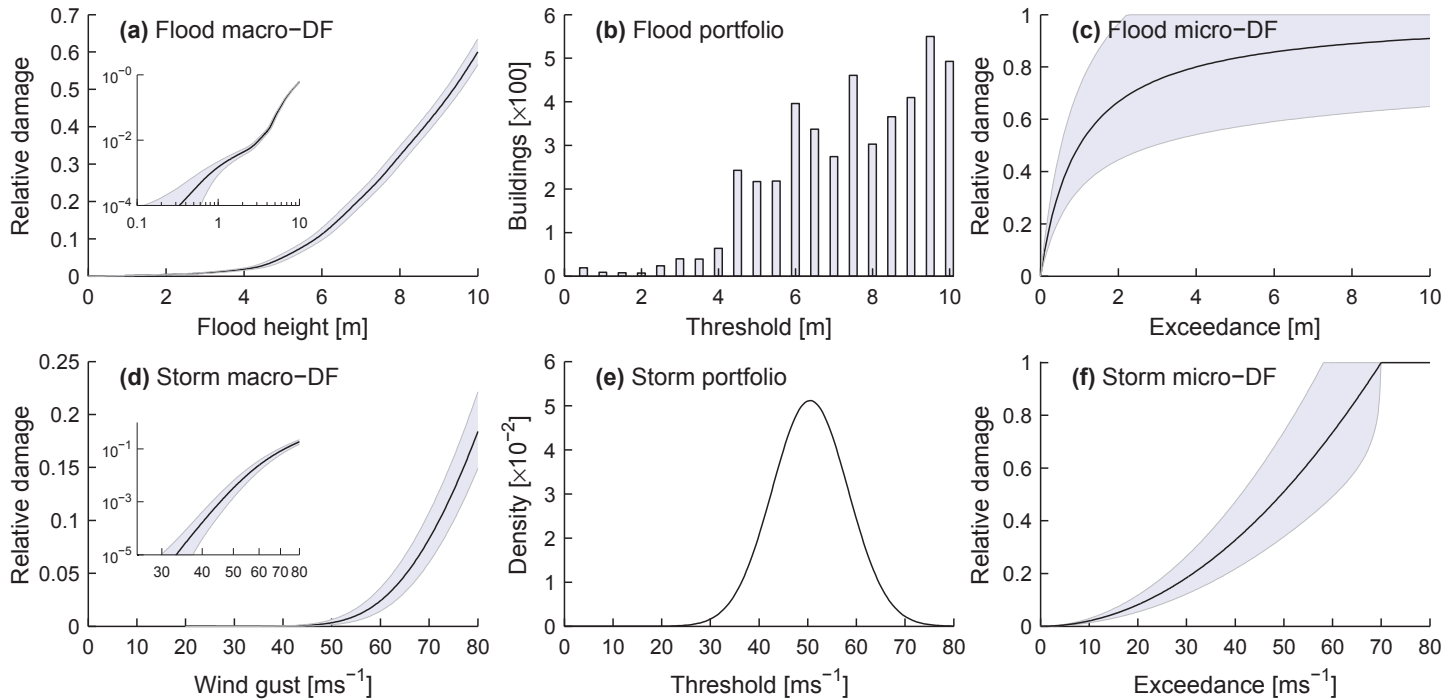


Figure 4.5: (a–c) show the damage function components for the case study of coastal flooding in Lisbon, Portugal. (d–f) demonstrate the methodology for storm damage within a building portfolio of 5000 individual buildings, based on the study by Heneka and Ruck (2008). The shaded areas around the damage functions indicate 95% confidence intervals. The insets in (a) and (d) show the macroscale damage function on a log–log scale.

4.5.2 Results from the Sensitivity Analysis

Figure 4.6 summarizes the vBSA results for the Lisbon case study. Subfigure (a) shows the total-effect index for the intrinsic uncertainties at the microscale level (i.e. concerning a single building). It can be seen that at low inundation levels uncertainty in the threshold exceedance (due to local hazard fluctuations and/or variation of the hazard threshold) dominates. However, at inundation levels beyond 1 m its relevance quickly diminishes and uncertainty in the building asset value dominates. While the effect of the damage-level uncertainty surpasses that of the uncertainty in the threshold exceedance at most inundation levels, it is generally outweighed by the uncertainty in asset value.

The overall behaviour seen for the microscale case also holds true for the accumulated building portfolio of Lisbon. Excluding extrinsic uncertainty, Fig. 4.6 (b) shows the sensitivity of the portfolio damage to intrinsic uncertainties. In contrast to the microscale case, the plot indicates a stronger impact of the uncertainty in the threshold exceedance. This behaviour arises from the fact that there are additional buildings affected as the flood level increases. Hence, the marked bump of the curve above 4 m flood height is explained by the strong increase of affected buildings at that elevation (cf. Table 4.1).

On the macroscale level, Fig. 4.6 (c) shows the effect of the accumulated intrinsic uncertainties and the extrinsic uncertainty in the global hazard magnitude. The complex behaviour of the two curves can be decomposed into two main aspects. Firstly, the relative importance of intrinsic uncertainties decreases with rising flood levels. Secondly, the strong impact of intrinsic uncertainties around a flood level of 2 m results from the low fraction of newly affected buildings, as seen in Table 4.1. Higher fractions at 3 m and in particular beyond 4 m lead to an increased relevance of the uncertainty in hazard magnitude.

This behaviour can be explained as follows. For a fixed number of affected buildings, intrinsic uncertainty outpaces the uncertainty in hazard magnitude. However, an increase in affected buildings reduces the relative magnitude of intrinsic uncertainty due to diversification. This is not the case for the uncertainty in hazard magnitude, which acts as a bias for the entire portfolio.

The sum of the total-effect indices of each variable is equal to 1 only in the absence of higher-order effects. Sums larger than 1 are due to potential double counting, as higher-order effects are attributed to each of the interacting variables. It is clear from inspection that the results given in Fig. 4.6 (a–c) indicate a minor role of higher-order effects. However, for completeness, we provide a detailed breakdown on first- and higher-order indices in the supplementary material presented in Sect. 4.B.

In the absence of interaction, the relevance of the uncertainties is determined by their relative magnitude. In this regard, Fig. 4.6 (d) shows the isolated effect of selected input variables on the standard deviation of damage estimates. The comparison with Figs. 4.6 (b) and (c) shows that the source of uncertainty

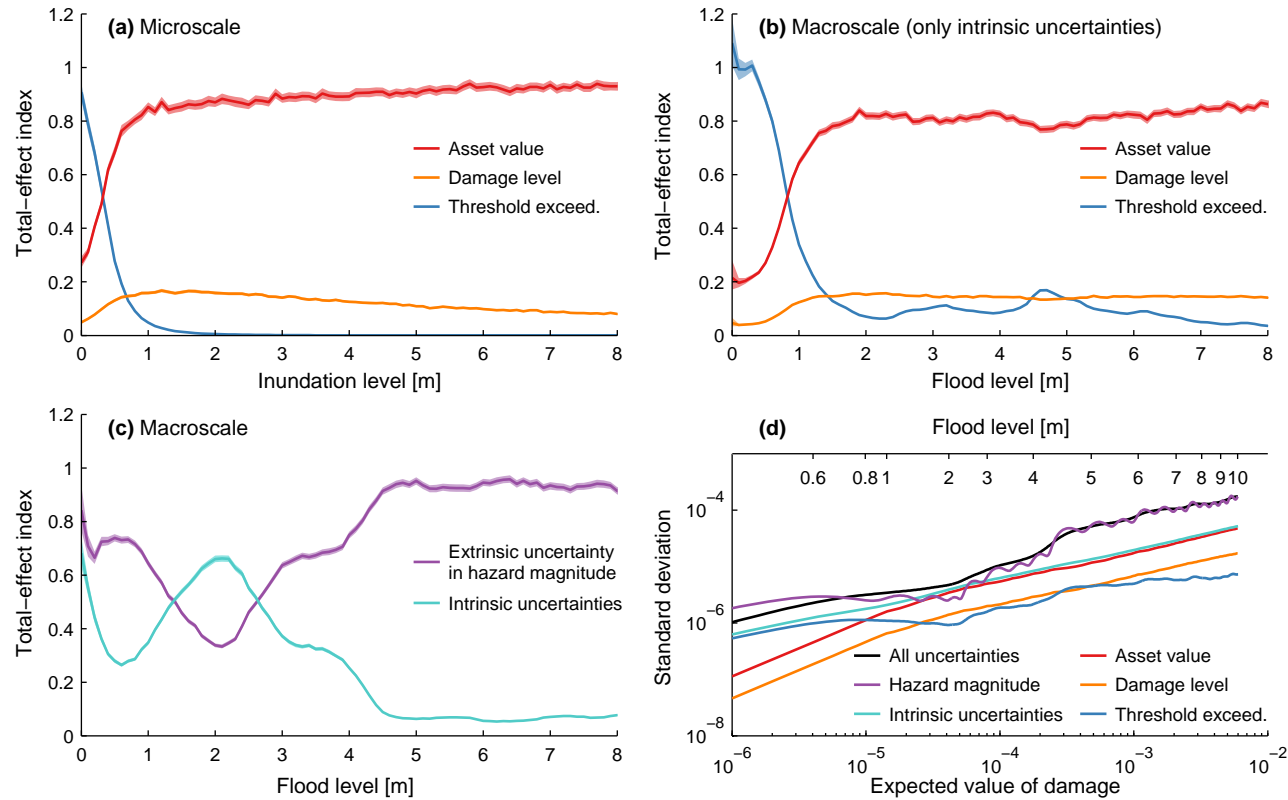


Figure 4.6:

(a–c) show the results of the vBSA (total-effect index) for the Lisbon case study at different scales. Shaded areas indicate boot-strapped confidence bands. For microscale damages, (a) shows the attributable effect of intrinsic uncertainty in asset value, damage, and threshold exceedance on the total variance. Similarly, (b) shows the effect of the intrinsic uncertainties on the variance of the aggregated portfolio. In (c), the portfolio-aggregated microscale uncertainties are weighed against the hazard uncertainty, i.e. error in estimated flood level. (d) shows the standard deviation against the expected value of flood damages on log–log scale. Each curve includes the uncertainty sources indicated by the legend.

exhibiting the largest standard deviation is also the dominating factor in the sensitivity analysis.

The sensitivity results obtained for the second case study – storm damage in a hypothetical German city – are similar to the Lisbon case. Figure 4.7(a) shows the relative contributions of the intrinsic uncertainties to the variance of the microscale damage. Despite the different shapes of the microscale damage function [cf. Figs. 4.5(c) and (f)] there is a strong resemblance to Fig. 4.6(a). A different behaviour is seen at an exceedance wind speed of 70 m s^{-1} , where the microscale damage function reaches saturation. At this point, complete destruction has taken place, leaving only the uncertainty of the original asset value.

On the macroscale level, intrinsic uncertainties show a sensitivity that is similar to the microscale level. The curves shown in Fig. 4.7(b) are considerably smoother than those of the Lisbon case study. This underlines the conjecture that the irregularities in the Lisbon case study are due to the heterogeneous portfolio distribution. This aspect is also reflected in the relation between intrinsic uncertainties and the extrinsic uncertainty in the hazard magnitude in Fig. 4.7(c). Here, the uncertainty in the hazard magnitude dominates for almost the entire range of gust speed. The narrowing at very low gust speeds is a result of the interdependence between the uncertainties in the exceedance and the hazard magnitude when the portfolio is barely affected. Finally, Fig. 4.7(d) complements the sensitivity results, showing the standard deviation of the potential storm damage against the expected value.

4.6 Conclusions

Based on damage assessments for coastal flood and storm hazards, a unified damage function was identified and embedded into a probabilistic framework for the consideration of uncertainty.

While an exchange of information between the various hazard communities could potentially trigger methodological improvement (Merz et al., 2010), the approaches for assessing direct damage are typically hazard specific (Meyer et al., 2013). Hence, this study has investigated the analogies of the approaches for coastal flood, storm damage, and heat-related mortality. The defining property of these approaches is the consideration of granular portfolios of exposed items (e.g. residential buildings) or people. In our view, the applicability of the unified approach extends to any hazard that affects such a granular portfolio. Furthermore, the unified approach represents a synthesis of synthetic bottom-up and empirical top-down damage evaluation. With its broad scope, it is seen as a potential building block towards a theory of damage functions.

Cross-hazard comparison of uncertainties within the unified approach has the potential to provide valuable insight on the nature and relevance of uncertainties along the causal chain. From a practitioner's point of view, determining the most relevant sources of uncertainty is arguably more important than quan-

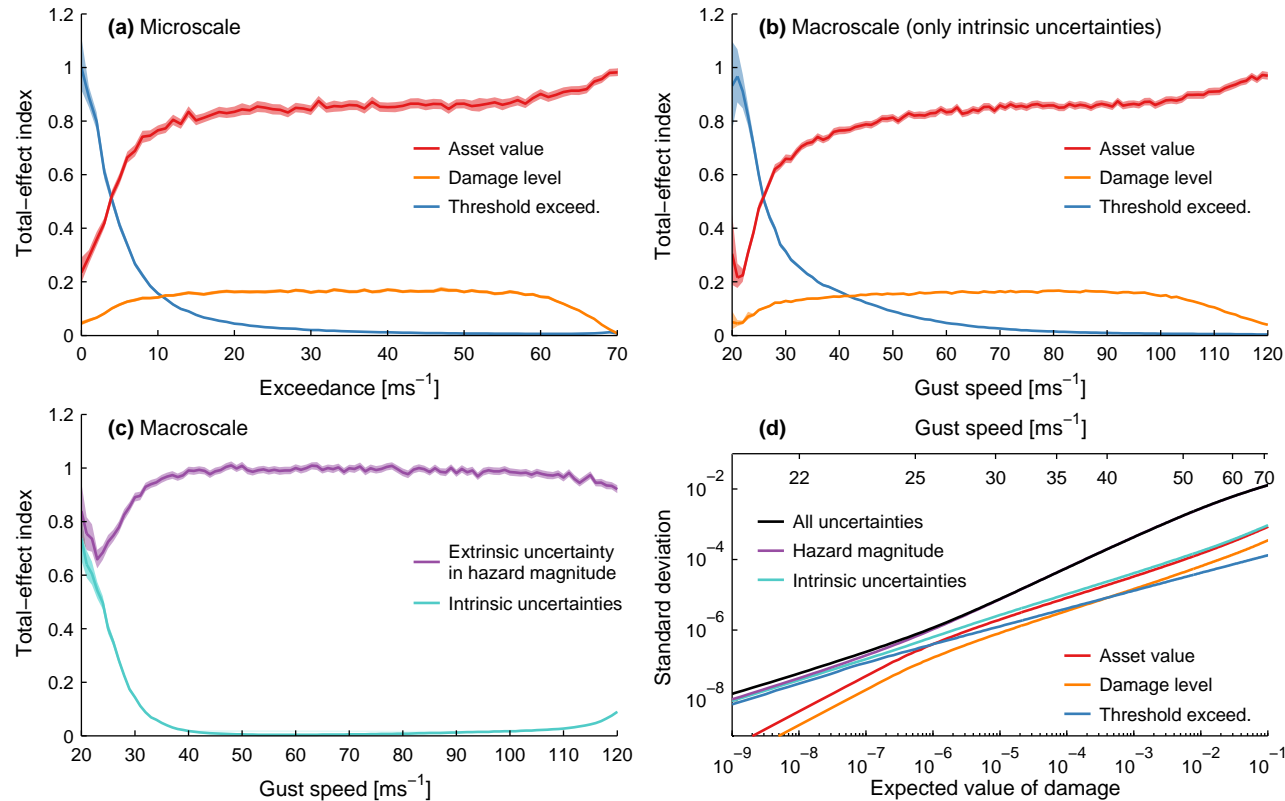


Figure 4.7: (a–c) show the results of the vBSA (total-effect index) for the German storm damage case study at different scales. Shaded areas indicate boot-strapped confidence bands. For microscale damages, (a) shows the attributable effect of intrinsic uncertainty in asset value, damage, and threshold exceedance on the total variance. Similarly, (b) shows the effect of the intrinsic uncertainties on the variance of the aggregated portfolio. In (c), the portfolio-aggregated microscale uncertainties are weighed against the hazard uncertainty, i.e. error in estimated flood level. (d) shows the increasing standard deviation against the expected value of damage estimates on a log–log scale. Each curve includes the uncertainty sources indicated by the legend.

tifying each potential uncertainty source. Serving this purpose, valuable insight could be gained from a variance-based sensitivity analysis of the unified damage function. The analysis goes beyond similar studies (e.g. Egorova et al., 2008; de Moel and Aerts, 2011) by considering uncertainty on both the microscale and macroscale levels, as well as at different hazard magnitude. Investigating both the case of coastal flooding for the city of Lisbon and the case of storm damage in a German town, a set of general conclusions could be drawn.

On a general level, extrinsic and intrinsic sources of uncertainty were distinguished. Extrinsic sources manifest as a random bias for the entire portfolio (e.g. hazard magnitude), while intrinsic uncertainties arise locally and affect individual portfolio items (w.r.t. asset value, damage level, and threshold exceedance).

As demonstrated by both case studies, extrinsic uncertainty can play a crucial role as the dominant source of uncertainty. In contrast to the intrinsic uncertainties, whose aggregated effect (i.e. in terms of the standard deviation of the macroscale damage) increases sub-linearly with portfolio size due to diversification, the effect of extrinsic uncertainty is directly proportional to portfolio size. Hence, given a sufficiently large portfolio and uncertainty in the hazard magnitude, intrinsic uncertainty sources may be negligible for damage assessment. This is of particular importance in climate science, where practitioners often deal with ensemble simulations exhibiting large model spreads. It is also relevant for natural hazard research, where extreme value theory often implies broad confidence intervals for extreme events.

An example where this result allows for additional insight is the work of Heneka and Ruck (2008). In their damage assessment, uncertainty was attributed to a random bias on the threshold distribution for each post-code area. However, the assumed bias is equivalent to an uncertainty in the hazard magnitude, i.e. error from physical modelling. Such uncertainty in gust estimation is not only more intuitive than a threshold bias but also consistent with the validation results of the employed atmospheric model (Hofherr and Kunz, 2010).

Considering the relevance of intrinsic uncertainty sources, our results show that the composition of uncertainty within the microscale damage function largely determines the role of intrinsic uncertainties at the portfolio level.

Amongst the intrinsic uncertainties, the uncertainty due to local threshold exceedance (being a combination of local hazard fluctuations and local variations in hazard threshold) is only significant for low hazard magnitudes. This magnitude range may not be relevant in certain cases, e.g. focussing on high-end scenarios or including protective measures such as sea walls. The case studies also show the extent to which variability in asset values can dominate intrinsic uncertainty. While that uncertainty could be reduced if spatially resolved data were available, this is typically not the case for data-scarce regions within developing countries, which are also more severely affected by natural disasters (IPCC, 2012).

Despite the different microscale damage functions used, both case studies show a similar sensitivity to uncertainties. This indicates that the validity of our conclusions on uncertainty reaches beyond the considered hazards. Moreover, the effect of different microscale damage functions (of the same one-parameter family) could be simulated by a re-scaling. For the sensitivity results, for example, a more shallow microscale damage function would result in a stretch along the hazard axis, while preserving overall behaviour.

The effect of large-scale protection measures, e.g. sea walls, was not considered in this study for two reasons. Firstly, such measures are specific to flood hazards and have no counterpart for other hazards, such as wind storms. Secondly, sea walls modify the incident hazard by interrupting events below the design protection level and are hence not an immediate component of damage estimation. However, it is known that the probability of protection failure, e.g. crevasses, represents a major source of uncertainty for damage assessment (de Moel et al., 2012).

In practice, there are some limitations to the unified damage function that arise from the simplicity of the approach. At increased cost and effort of data acquisition, more specialized approaches could provide superior damage estimates (e.g. Kreibich et al., 2010; Pita et al., 2013). However, the strengths of the discussed approach are in its versatility and the ability to provide valuable insight for applications where detailed data for calibration and validation are missing. The latter aspect is highlighted by our general conclusions on uncertainties. Given the evident lack of reliable information on uncertainty, as encountered for the parameterizations of our case studies, the results may guide further investigation.

Addressing the need for comprehensive approaches for risk analyses and management, we have shown that certain damage functions for coastal floods and windstorms are two facets of a unified damage function. Further, it was indicated how this unified approach could be extended to the estimation of heat-wave fatalities.

With its wide applicability to the assessment of both loss and fatalities, the unified damage function has the potential to facilitate knowledge transfer between climate-related hazards and to narrow the gap for a multi-hazard damage assessment. Moving towards this goal, the interdependence and cascading effects of climate-related hazards become of wider concern. For further research, we hence propose the extension of the unified approach to include non-stationary hazard thresholds.

Acknowledgements. We appreciate valuable discussions with U. Ulbrich and L. Krummenauer. This work was produced using Copernicus data and information funded by the European Union – EU-DEM layers. This work was supported by the European Community’s Seventh Framework Programme under grant agreement no. 308497 (Project RAMSES).

Appendices to Chapter IV

4.A Uncertainty Parameterization

4.A1 Lisbon Case Study for Coastal Flooding

Hazard Magnitude Uncertainty

For our case study region, the Portuguese coast and in particular Cascais, Fortunato et al. (2014) estimate a tidal uncertainty of 5 cm and an uncertainty of approximately 10 cm for extreme water levels calculated by a dedicated circulation model. Based on this result and due to the lack of information on the distribution of uncertainty, we make the assumption of a normally distributed error in overall flood level with a standard deviation of 10 cm. If ensemble predictions of surge levels were available, the ensemble spread (standard deviation) could serve as a indicator for the forecast error (Flowerdew et al., 2009, 2010).

Threshold Exceedance Uncertainty

Modelling flood damages, exceedance uncertainty is mostly driven by errors related to the elevation model used. For Portugal, statistical validation of the EU-DEM against ICESat measurements (EEA, 2014) indicates a mean error > 0.5 m and an average standard deviation of approximately 2 m. However, errors in flood-prone lowlands are expected to be strongly spatially correlated and to exhibit less local fluctuations (Hallegatte et al., 2013). In the lack of a detailed DEM validation for Lisbon, we assume a modest normally distributed pixel error with a standard deviation of 0.2 m.

Damage Level Uncertainty

Actuarial practice suggests that the log-normal distribution may serve as a first approximation to the broadly skewed damage claim distributions (Lawrence, 1988). By applying a constant scale factor, the log-normal distribution represents a multiplicative error term that is proportional to the average damage caused. Defining the microscale damage curve as the mean of the log-normal distribution, we set the scale factor such that the standard deviation $\sigma = 0.1$ at a relative damage $d = 0.5$, implying a standard deviation of approximately 20% for $d \ll 1$. The upper tail of the log-normal damage distribution is truncated at $d = 1$, which represents complete destruction and loss.

Asset Value Variation

Regarding storm or flood damages to individual buildings, the built-up values can be approximated by the distribution in house prices. For the case of Tokyo,

Ohnishi et al. (2011) show that house prices generally follow a log-normal distribution, with price bubbles affecting mainly the tails of the distribution. While comparable studies are not available for the European region, one may assume that relative house prices follow a similar distributional shape and width. On relative terms, the results by Ohnishi et al. (2011) translate to a log-normal distribution normalized to an average value $\mu = 1$ and with a standard deviation $\sigma = 0.5$.

4.A2 Storm Damages in a German Building Portfolio

Hazard Magnitude Uncertainty

For maximum wind gusts, which are required for the assessment of storm damages, Prah1 et al. (2012) report a strong variation between measurements at nearby sites and estimate that 75 % of measurements fall within the range of $\pm 1.5 \text{ m s}^{-1}$. Reports show an even stronger modelling uncertainty when comparing gust estimates from a mesoscale atmospheric model from a mesoscale atmospheric model with measured gusts (e.g. Ágústsson and Ólafsson, 2009; Hofherr and Kunz, 2010). In our calculations, we hence assume wind gust uncertainty to follow normal distribution with a standard deviation $\sigma = 1.5 \text{ m s}^{-1}$.

Threshold Exceedance Uncertainty

Wind gusts exhibit a strong spatial variability at short ranges. This aspect is demonstrated, inter alia, by the fact that the 3 s gust factor (relating extreme wind gust to mean wind speed) drops by more than 20 % if spatial averaging is applied for short distances less than 1 km (Mitsuta and Tsukamoto, 1989). While there is no indication in the scientific literature on the uncertainty in storm hazard threshold, the macroscale uncertainty in storm gust speed poses an upper bound for the local gust variability. In line with macroscale gust speed uncertainty, we assume a normally distributed local variability, albeit with a reduced standard deviation of 1 m s^{-1} .

Damage Level Uncertainty and Variation in Asset Values

In the lack of local empirical studies for the uncertainty in damage levels or the variation in asset values, we employ an identical parameterization for both the coastal flooding and the storm hazard case studies. The parameterization for the damage level uncertainty and the variation in asset values is described in Sect. 4.A1.

4.B Supplementary Material

4.B1 Additional Indices for the Sensitivity Analysis

A vBSA allows to explain output variance by the contributions from explanatory variables (Saltelli et al., 2008). The general method is described in Sect. 4.5.1. For the estimation of the first-order effect we do not employ the estimator recommended by Saltelli et al. (2010), which appears to be robust only for variables with zero mean. Instead, we use the corresponding Jansen estimator (Jansen, 1999; Saltelli et al., 2010) whose results rapidly converge with increasing sample size s . Hence, the first-order effects index FO_i is given by

$$FO_i = 1 - \frac{\frac{1}{2s} \sum_{k=1}^s (\mathcal{F}(\mathbf{B})_k - \mathcal{F}(\mathbf{C}_{(i)})_k)^2}{\sigma^2}, \quad (4.16)$$

with

$$\sigma^2 = \frac{1}{2s} \sum_{k=1}^s (\mathcal{F}(\mathbf{A})_k^2 + \mathcal{F}(\mathbf{B})_k^2) - \left(\frac{1}{s} \sum_{k=1}^s \mathcal{F}(\mathbf{A})_k + \mathcal{F}(\mathbf{B})_k \right)^2. \quad (4.17)$$

The extension to higher-order effects (interactions) is straight-forward. For second-order effects, we construct matrix $\mathbf{C}_{(i,j)}$ such that we take all columns $l \notin \{i, j\}$ from \mathbf{A} and all columns $l \in \{i, j\}$ from \mathbf{B} . To estimate the second-order effect index $SO_{i,j}$, we replace $\mathbf{C}_{(i)}$ with $\mathbf{C}_{(i,j)}$ in Eq. (4.16) and subtract first-order effects of input variables i and j . It follows that

$$SO_{i,j} = 1 - \frac{\frac{1}{2s} \sum_{k=1}^s (\mathcal{F}(\mathbf{B})_k - \mathcal{F}(\mathbf{C}_{(i,j)})_k)^2}{\sigma^2} - FO_i - FO_j; \quad (4.18)$$

for $i \neq j$.

Similarly, we calculate the third-order effect index $TO_{i,j,k}$ by constructing the corresponding matrix $\mathbf{C}_{(i,j,k)}$ and subtracting low-order terms,

$$TO_{i,j,k} = 1 - \frac{\frac{1}{2s} \sum_{k=1}^s (\mathcal{F}(\mathbf{B})_k - \mathcal{F}(\mathbf{C}_{(i,j,k)})_k)^2}{\sigma^2} - FO_i - FO_j - FO_k - SO_{i,j} - SO_{i,k} - SO_{j,k} \quad (4.19)$$

for $i \neq j \neq k \neq i$.

It is clear from inspection, that Eqs. (4.18) and (4.19) simplify considerably for models with only two and three random variables, respectively. For models with only two random variables, the second-order effect index becomes

$$SO_{1,2} = 1 - FO_1 - FO_2. \quad (4.20)$$

Similarly, for models with three random variables the third-order effect index simplifies to

$$TO_{1,2,3} = 1 - FO_1 - FO_2 - FO_3 - SO_{1,2} - SO_{1,3} - SO_{2,3}. \quad (4.21)$$

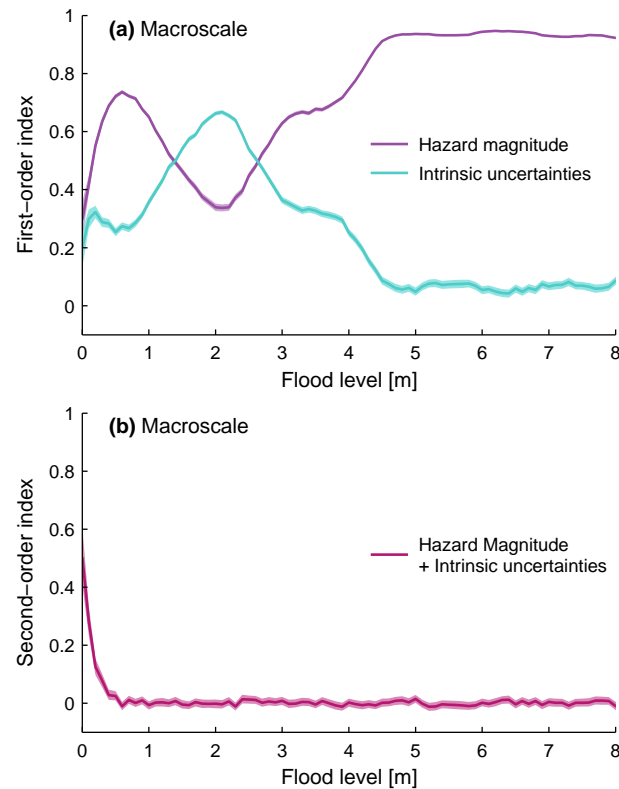


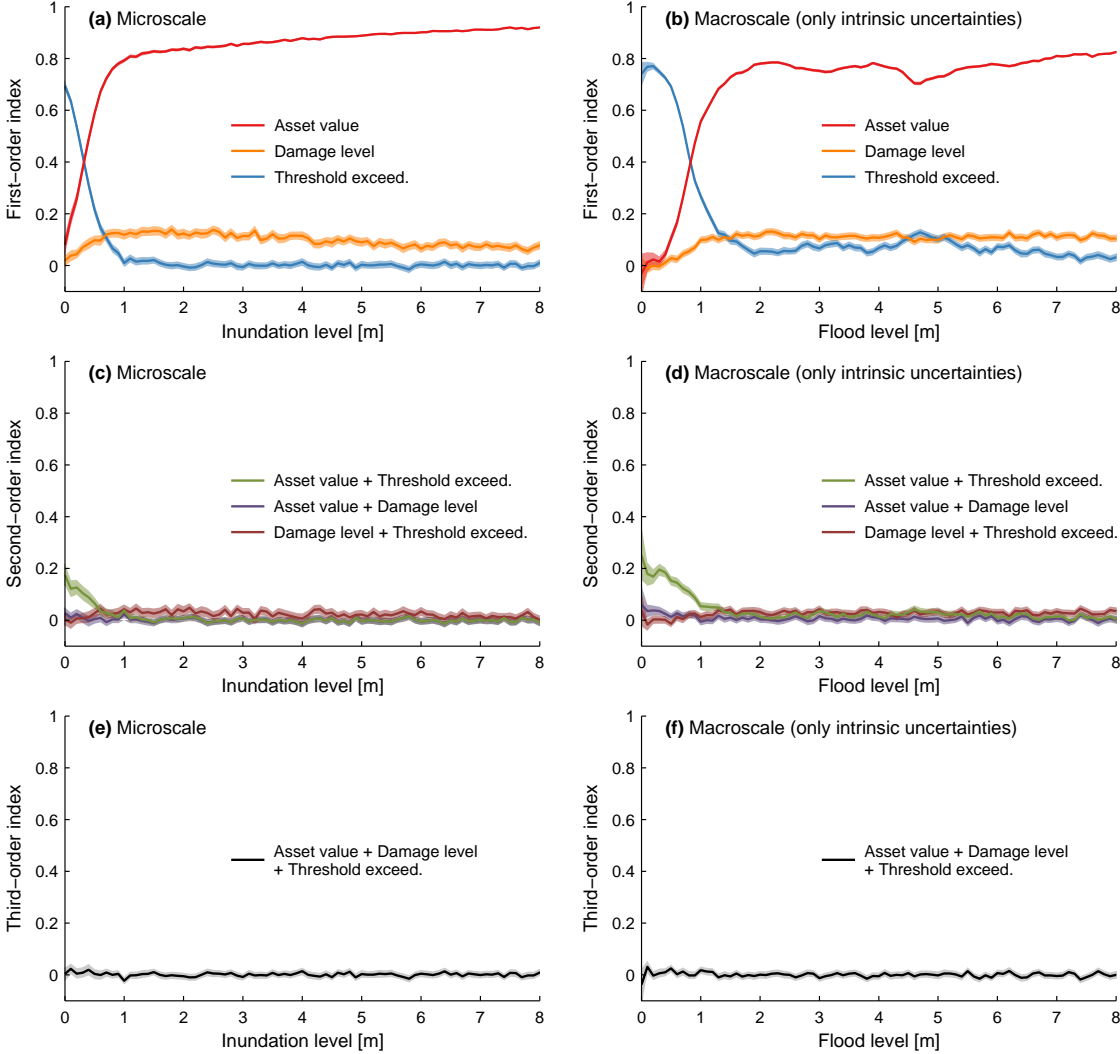
Figure 4.8: Results of the sensitivity analysis of the macroscale damage function for the Lisbon case study, relating the joint effect of intrinsic uncertainties to the effect of uncertainty in the hazard threshold. Panel (a) shows the direct, first-order effect, while panel (b) shows the second-order effect due to interaction between the uncertainty sources.

4.B2 Additional Results for the Lisbon Case Study

Figure 4.8 shows the first- and second-order effect indices of intrinsic and extrinsic (hazard threshold) uncertainties [cf. Fig. 4.6 (c)]. The interaction seen for flood levels below 0.5 m is due to the fact that the uncertainty in the hazard threshold determines the occurrence of a damage at such low flood levels and that, consequently, the intrinsic uncertainties are conditional on the occurrence of a damaging event.

Figure 4.9 shows the first-, second-, and third-order effect indices for the intrinsic uncertainties in both the microscale and the macroscale damage function. If compared with the total-effects index [cf. Fig. 4.6 (a–b)], it is seen that the first-order effects are the dominant contribution to the total effects index. Panels (c) and (d) show that there is some interaction between the variation in asset value and the uncertainty of the threshold exceedance. However, this interaction is limited to inundation levels below 1 m and only contributes lightly to the over-

Figure 4.9: Results of the sensitivity analysis of the microscale (a, c, and e) and the macroscale (b, d, and f) damage function for the Lisbon case study, taking into account only intrinsic uncertainties. Each column comprises the first-, second-, and third-order effects of the respective uncertainty sources on the output variance. First-order effects are directly attributable to a source of uncertainty, while higher-order effects arise from interactions between two or more uncertain variables.



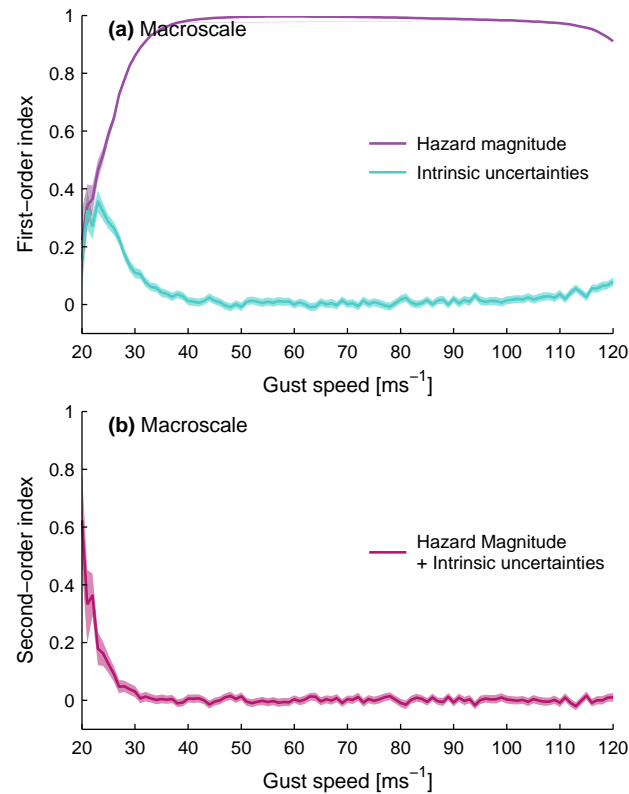


Figure 4.10: Results of the sensitivity analysis of the macroscale damage function for the German storm damage case study, relating the joint effect of intrinsic uncertainties to the effect of uncertainty in the hazard threshold. Panel (a) shows the direct, first-order effect, while panel (b) shows the second-order effect due to interaction between the uncertainty sources.

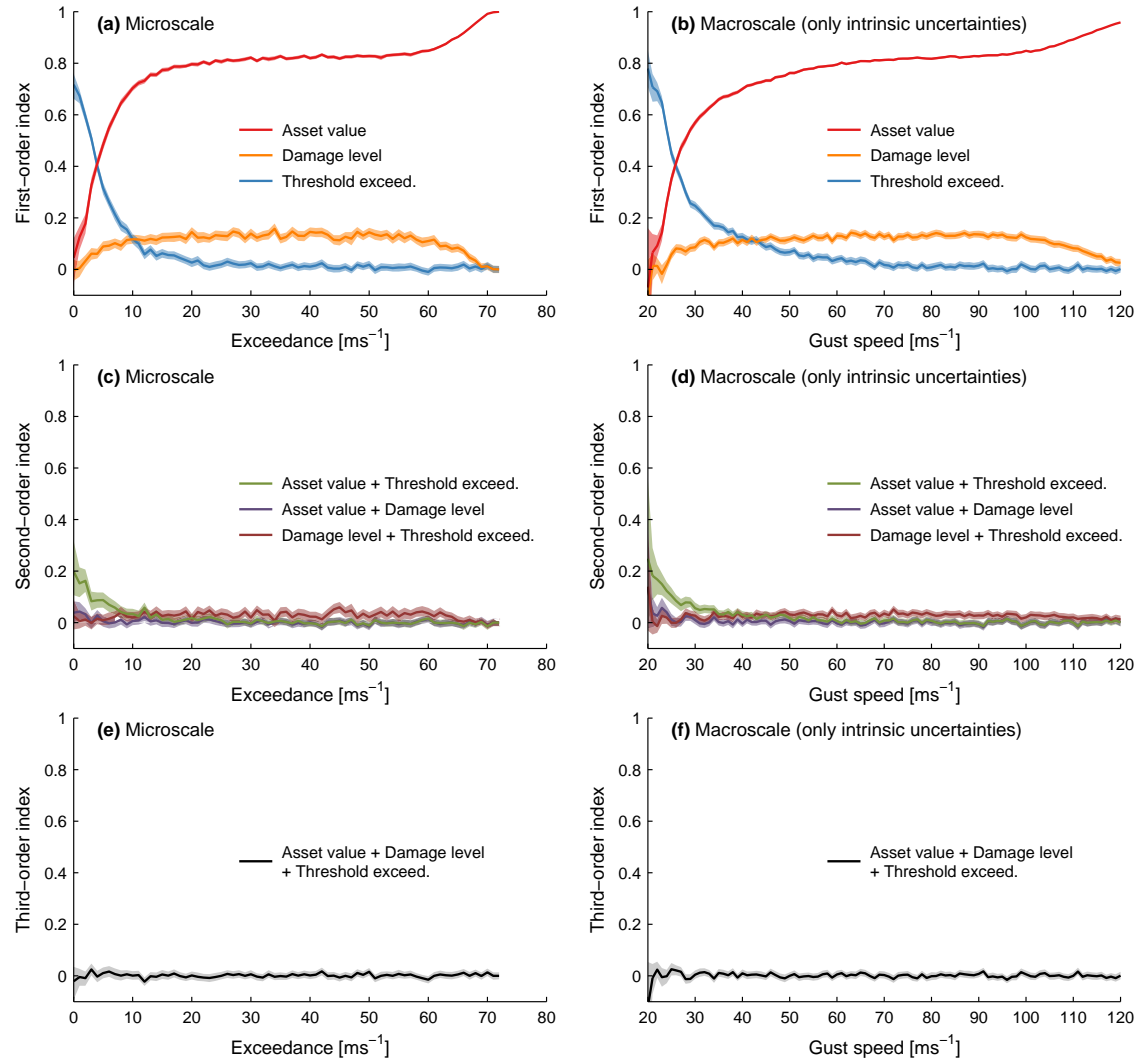
all model variance (less than 0.2 of output variance). Panels (e–f) show that third-order effects are negligible.

4.B3 Additional Results for the Storm Case Study

Figure 4.10 shows the first- and second-order effect indices of intrinsic and extrinsic (hazard threshold) uncertainties within the macroscale damage function [cf. Fig. 4.7(c)]. There is some interaction at low hazard magnitudes, analogous to the Lisbon case study (cf. Fig. 4.9).

Figure 4.11 shows the first-, second-, and third-order effect indices for the intrinsic uncertainties in both the microscale and the macroscale damage function [cf. Fig. 4.7(a–b)]. The same reasoning as for the Lisbon case study applies (cf. Sec. 4.B2 and Fig. 4.8).

Figure 4.11: Results of the sensitivity analysis of the microscale (**a, c, and e**) and the macroscale (**b, d, and f**) damage function for the German storm damage case study, taking into account only intrinsic uncertainties. Each column comprises the first-, second-, and third-order effects of the respective uncertainty sources on the output variance. First-order effects are directly attributable to a source of uncertainty, while higher-order effects arise from interactions between two or more uncertain variables.





Conclusions and Outlook

5.1 General Achievements

The work at hand has been focussed on the analysis and the development of damage functions in order to contribute to their fundamental understanding as well as to the improvement of damage estimation. These damage functions relate the intensity of natural hazards to the direct economic losses caused. As such, damage functions are particularly helpful in assessing the adverse impacts of natural hazards whose characteristics are altered by climate change. Such adverse impacts are the consequence of complex physical processes and the resulting damage signal is typically non-linear. Taking the example of the storm–loss relation, even small increases in wind speed can invoke a drastic increase of expected loss. Accurate high-resolution damage functions, as provided for German winter storms, are essential for the decision support on climate change and the handling of climate change risks. The undertaking of their validation and the incorporation of uncertainty are a necessity for creating reliable estimates of potential damages. Following this route, the obtained results improve the accuracy and validity of damage functions and will be helpful to assess the availability of risk financing, e.g. insurance and other financial instruments.

The overarching goal of this work has been to advance the understanding of climate-related damage functions. This goal has been met by addressing damage functions along three distinct research facets: *depth*, *breadth*, and *scope*.

In *depth* the wind–loss relation was explored for winter storms across Germany, resulting in a novel storm damage function which for the first time covers the entire range of possible losses.

The *breadth* of storm damage functions for Germany has been reviewed and assessed, thereby developing new methodology custom-tailored to the properties of storm loss data.

Finally, the *scope* of the presented research was widened to include further hazards, revealing a common damage function applicable to both windstorm and coastal flooding and possibly others.

Investigating into these three research facets, the work at hand has advanced the understanding of damage functions in multiple ways, beginning with a spot-

light on storm damage functions and concluding with a multi-disciplinary insight into the common grounds and uncertainties of damage functions.

The novel storm damage function has been developed with the aim to reflect the entire range of observed loss. This fundamental approach is in contrast to prior attempts that were tailored to extreme or highly aggregated losses. The comparison with other established models confirmed that the novel damage function performs at par with the current best models for German storm loss. Overall, it provides improved loss estimates over a wider range of gust speed than competing models. Geographically, the power-law shape of the damage function has been found applicable throughout Germany and there is no indication that it would not apply to further European countries.

The comparison of storm damage functions has shown a great amount of residual variability, which highlights the need for a more fundamental understanding of the damaging processes. That said, the findings also indicate a limitation to the merits of increasing model complexity. This is the case, e.g. for storm damage functions, where residual variability could be linked mainly to uncertainty from the gust observation. Unfortunately, most approaches for developing more detailed damage functions are severely hampered by limited data availability and model resolution. In this light, it is concluded that practitioners should focus on simple and accessible damage functions, which are susceptible to further analysis especially in the field of uncertainty.

Beyond windstorms, damage functions can be employed to model damages caused by different climate-related hazards. In this regard, the work at hand has identified a simple mathematical form of a unified damage function applicable both to storm and flood loss. This finding suggests that further formalization towards a universal damage function may be feasible, providing both transparent and comparable methodology for the assessment of diverse climate impacts. While flood damage assessment is a typical example for the application of damage functions, it may also be worthwhile to extend the concept of damage functions to heat-related mortality. In particular, the functional approach could prove beneficial for characterizing the shape of empirical mortality curves.

With its wide regard for climate-related hazards and their associated damages, the work at hand has been placed at the interface of natural hazards research, the atmospheric sciences, and actuarial science. By keeping all considerations as general as possible, fundamental insights into the mechanics of damage functions and into the interplay between the involved uncertainties were gained. The general nature of the employed methodology makes this work truly inter-disciplinary and distinguishes it from many studies in this field.

In the following sections, each of the posed research questions, [RQ1](#) through [RQ3](#), will be revisited. The corresponding contributions from Chapters [II–IV](#) will be reviewed and interlinked. Alongside a discussion of existing limitations, the results are set into a broader context and their scientific relevance is highlighted. Finally, [Sect. 5.6](#) provides an outlook on follow-up research and some concluding remarks.

5.2 The Challenge from Hazard–Loss Data

The properties of damage data related to natural hazards pose a challenge both for the calibration and the evaluation of damage functions. As outlined in Sect. 1.3, these data are characterized by i) high dynamic range, ii) skewed distribution, iii) heteroscedasticity, and iv) ambiguity.

Dealing with storm damages, the work in Chapters II and III has addressed the challenging properties of storm loss data. It was seen that conventional least-squares fitting causes the damage curve to align to the highest loss. This could be observed, for example, when fitting the damage function proposed by Klawns and Ulbrich (2003) to loss data in Fig. 3.2(c). In general, least-squares fitting may cause an unknown bias due to the scarcity of extreme events and the heteroscedastic uncertainty that grows with expected loss. Even with aggregated (e.g. annual) loss figures such bias may not be avoidable. For example, losses for extreme storm events typically exceed the other losses by orders of magnitude, such that the single most damaging storm frequently dominates annual aggregates.

One solution to the problem is to employ maximum likelihood estimation (MLE) and to model heteroscedasticity explicitly. Following this approach, a novel storm damage function was derived in Chapter II, where loss uncertainty was modelled via a log-normal distribution with constant scale factor. The choice of distribution was guided by the observation that a logarithmic transformation of losses [e.g. as depicted in Fig. 2.1(a)] would produce approximately Gaussian residuals. While the assumption of log-normal uncertainty captivates by its simplicity, it is not expected to hold in general, since the underlying premise of a multiplicative error term cannot be justified on theoretical grounds. Instead, a more general description of uncertainty is presented on the basis of a unified damage function (Chapter IV). In this model, the overall uncertainty is obtained as a convolution of nested uncertainty distributions (see also discussion in Sect. 5.4). While being heteroscedastic, the resulting uncertainty bands [cf. Fig. 4.2(g)] are not of constant shape as was assumed in the log-normal approximation.

In this work it has become clear that the calibration of damage functions must rely on adequate assumptions on the shape and extent of uncertainty. The employed MLE is not only superior to least-squares estimation but also allows for the consideration of arbitrary uncertainty distributions. Hence, going beyond the work at hand, there is an opportunity to incorporate the theoretical insights from the uncertainty analysis into the MLE scheme. Such would increase the robustness of the calibration and have a fertilizing effect for further improvement of damage functions.

Beyond the development of damage functions, loss-data characteristics also play an important role when performing a comparison of different damage models. In the present case, four non-nested damage functions were compared, each predicting an expected value of loss. Any simple comparison based on ab-

solute deviations, such as R^2 , would be biased for the same reason that impairs least-squares fitting: high dynamic range with very few singular extremes that exhibit heteroscedastic error. Furthermore, damage functions may show different performance depending on the magnitude of storm events. In this regard, the few extreme losses are of particular (monetary) relevance.

The work at hand has followed common practice by comparing the non-nested models by their prediction skill, using separate validation data that were not included in the training sample (cross-validation). However, the strong positive skew of the loss distribution and the resulting scarcity of extreme losses impose a dilemma for the determination of skill. On the one hand, absolute metrics are dominated by singular events, since the most severe loss may outweigh the second most severe loss by as much as an order of magnitude. As a consequence, the validation statistics are not reliable. Relative metrics, on the other hand, reduce the weight of extreme loss events. This comes at the risk of giving preference to a model that performs well for the abundance of mid-range losses, while performing worse for the highly relevant extreme losses. Moreover, relative metrics cannot be employed for data that exhibit ambiguity (i.e. the stochastic occurrence or non-appearance of loss at the same hazard intensity) since the treatment of zeroes is inherently problematic.

In order to overcome the dilemma, the range of substantial loss was stratified into three loss classes and all models were evaluated for each class separately. Furthermore, minor losses that are subject to ambiguity but bear no relevance for total loss figures were discarded. A first comparison was based on relative metrics, giving approximately equal weight to each of the data points within a loss class. Secondly, a novel statistical test based on binomial statistics was employed to test the null hypothesis that two models have equal skill.

In response to the specific characteristics of the loss data, the employed two-stage comparison of damage functions has reached beyond conventional approaches to measure the performance of damage functions. Most importantly, the comparison has addressed the fact that damage models may show varying performance at different loss ranges. This is highly relevant for damage assessment given that the empirical losses range over several orders of magnitude. Furthermore, the identification of the best-matching curve may support the search for a fundamental hazard–loss relation.

In summary, the work at hand has addressed the difficulties that arise from the particular properties of hazard–loss data. Since these difficulties are not simply mitigated by increased data availability, the use of adequate methodology is of high relevance. The results indicate that practitioners should refrain from using conventional least-squares methods and employ MLE together with a thorough uncertainty model similar to the one derived in Chapter IV. Stratification has been employed effectively to analyse performance at different scales. At the lack of a more fundamental statistical approach – taking into account scale, skew, and heteroscedasticity – stratification balances the weight of different loss regimes.

5.3 The Wind–Loss Relationship (RQ1)

The relation between insured storm loss and storm intensity is a matter of ongoing research. Storm damages are clearly dependent on the construction practices and building regulations, which in turn originate, at least partly, from the local storm climate. The regional dependence complicates the transferability of damage functions and together with a general lack of loss information impedes the revelation of the wind–loss relationship. This issue has been addressed by the First Research Question:

What is the statistical wind–loss relationship for German residential buildings, and how does it compare to existing damage functions?

In Chapter II the wind–loss relationship was analysed based on high-resolution loss data for the sector of German residential buildings. In contrast to other studies, the data was best described by power-law curves with high exponents. With an average of approximately 10 the exponents were considerably higher than the cubic or quartic behaviour suggested by Munich Re (2001).

The power-law model represents a simplification of a more general sigmoid curve, namely the cumulative distribution function of the log-logistic distribution. It has a simple and intuitive parameterization, where the exponent defines the steepness of the curve and the offset parameter represents the point at which half of the portfolio value is lost.

The power-law relationship was observed individually for 439 regions at NUTS 3 level. The wind–loss relationship as given by this curve deviates from prior expectation on both ends – for small losses occurring beneath the 98th wind percentile and for the extrapolation to extreme losses in the tail of the loss distribution.

The empirical loss data shows substantial losses beneath the 98th wind percentile for every region throughout Germany. In general these losses bear additional information and were found to support the power-law shape of the damage function. While the presented results give no indication that the 98th percentile constitutes a threshold for the occurrence of loss, it has been argued that the percentile does reflect regional vulnerability (Klawns and Ulbrich, 2003; Leckebusch et al., 2007; Donat et al., 2011b). This premise could not be confirmed in this work, finding no correlation between exponent or offset and the 98th percentile of maximum daily gust. However, weak correlation between offset and altitude of the employed DWD station [Fig. 2.3(d)] indicated that the offset parameter also acts as a scaling factor, if the wind station is located at an altitude different to that of the average settlement.

Although not supported by the results, the suitability of the 98th wind percentile to incorporate regional vulnerability into the damage function cannot be ruled out in general. Within the novel damage function, the power-law exponent – defining the steepness of the curve – is the prime indicator for local vulnerability. While its spatial distribution across Germany (Fig. 2.2) shows a clear

prevalence of relatively low exponents for the North-Western parts of Germany, no significant correlations with wind percentiles or basic socio-economic data¹ were found.

Steep power-laws with large exponents are often hard to distinguish from a similar exponential relationship. Amongst other empirical models, the exponential hypothesis was tested as part of the model comparison in Chapter III. The results in Figs. 3.4 and 3.5 clearly that an exponential relationship fares well for relatively low losses, while extreme losses that contribute most significantly to the total accumulated loss² can be strongly overestimated.

Whereas the exponential function marks the upper limit of potential damage functions in terms of steepness, cubic (power-law) models constitute the lower limit, i.e. less steep approaches. On theoretical grounds, a purely cubic wind-loss relation had been proposed (e.g. Lamb, 1991, or recently Kantha, 2008) and was initially backed by empirical findings of Munich Re (1993). Later, considering a different set of storms Munich Re (2001) have reported higher exponents in the range of 4 to 5. Based on the available loss data the presumption of power-laws with exponents less than 5 must be generally rejected, as only significantly larger exponents with an average of 9.8 were found. However, it is not possible to rule out potential bias coming from the employed loss data. In fact, the results show that a cubic relationship could be transformed to a steeper curve similar to the novel power-law model. This has been demonstrated in Fig. 3.6, where small losses were truncated from the distribution of building losses, an effect comparable to a deductible. This finding suggests that there are mechanisms by which the steep damage curves found here could be reconciled with considerations based on the available kinetic energy of the wind.

In the regime of extreme losses, the employed power-law approach is also supported by the threshold model proposed by Klawns and Ulbrich (2003) and refined in Donat et al. (2011b). As derived analytically in Sect. 3.A3, the threshold leads to a local gradient of the curve that is much steeper than its asymptotically cubic behaviour. When applied to the typical wind speeds of extreme losses, the local gradient corresponds to a power law with an exponent of approximately 10, matching nicely with the observed average exponent of 9.8. The congruence is also reflected by the model comparison, where both the novel power-law damage function and the threshold model excel at the prediction of extreme losses (see summary in Tab. 3.6). But despite the similarity for historical extremes, it should be noted that the curves will strongly diverge for unprecedented extremes beyond the data support.

Available data on insured storm loss have typically been spatially aggregated. Since this is also the case for the data at hand, the novel damage function considers losses that were accumulated for a large set of individual buildings. However, the model comparison includes a model which combines a stylized portfolio representation with a mean damage function for individual buildings

¹ Socio-economic data comprised figures for population, buildings, income per capita, as well as their respective densities.

² See loss distribution in Fig. 3.1 (a).

(Heneka and Ruck, 2008). While the approach showed good overall performance, it is reliant on ad hoc assumptions about the portfolio and the damage curve for individual buildings. In the absence of more detailed loss data, these assumptions cannot be validated and their geographic dependence remains unclear.

In summary, this work has demonstrated that storm loss from German homeowners insurance follows a steep power law over a wide range of loss, improving upon previous approaches to damage estimation. Furthermore, the performance of the novel damage function was positively assessed against competing models. For extreme loss, partial congruence with competing approaches was found, strengthening the fundamental power-law premise made in this work.

The steepness of the damage function is of importance especially in the light of a changing climate, which may entail storms of unprecedented intensity. Clarity is much needed, as gradients of various damage functions can differ drastically with strong implication on the extrapolation of damage estimates. This work has contributed to this goal not only by developing a novel damage function, but also by identifying interrelations between different approaches.

5.4 The Role of Uncertainties in Damage Functions (RQ2)

The story of damage functions is also a story of uncertainty. Uncertainties arise on all stages along the causal chain, beginning with the hazard exposure, through the damaging processes, and terminating with the value at risk. Common approaches to evaluate uncertainties comprise scenario analysis and sensitivity analysis, but have fallen short of providing a deeper understanding of the propagation of uncertainty within the damage function, from the individual structure to the macroscale portfolio. In order to close this gap, the issue was placed at the core of the Second Research Question:

How are the sources of statistical uncertainty in damage functions interrelated, and what is their importance on different scales?

The answer to this research question was approached from two different angles. From an empirical perspective, the uncertainty associated with the loss estimates from the novel storm damage function was quantified in Chapter II. From a more general point of view, the relevance of different sources of uncertainty was investigated based on a unified approach to damage functions. The corresponding results from a global sensitivity analysis have been presented in Chapter IV and show how the sources of uncertainty affect both the microscale and the macroscale level of the unified damage function.

Beginning the discussion with the latter approach, the presented research has for the first time addressed the sensitivity of both the microscale damage func-

tion (single structure) and the aggregated macroscale damage function (portfolio). The overall loss variance could be attributed to the individual sources of uncertainty by means of a variance-based sensitivity analysis. In prior studies, similar uncertainty analysis has been limited to the attribution of overall variance³. Further level of detail was gained from considering the attribution of variance as a function of hazard intensity, i.e. gust speed or flood height. A key finding from this approach is that the sensitivity pattern of intrinsic uncertainties at the microscale level (i.e. local variations of the hazard intensity or building properties within the portfolio) persists also on the macroscale portfolio level. Fortunately, the relative magnitude of intrinsic uncertainties can be reduced by diversification, which leads to convergence to the expected value as formulated by the law of large numbers. In contrast, the effect of extrinsic uncertainty (i.e. variations of variables that describe the overall hazard intensity for the entire portfolio) scales proportionally to the portfolio size. With increasing portfolio size, and hence increasing diversification, it may be feasible to limit the treatment of uncertainty to extrinsic sources (e.g. the overall flood height or gust speed).

The importance of extrinsic uncertainty was also supported by the empirically derived storm damage function, as presented in Chapter II. A multiplicative error model was used to describe the variance of loss observations, and model residuals were found to follow an approximate log-normal distribution. An analysis of the spatial variation of wind gust measurements indicated strong uncertainty of gust estimates. As a matter of fact, a Gaussian uncertainty of gust speed would cause a log-normal loss uncertainty, if transformed by an exponential damage function. Since exponential curves are hardly discernible from power laws at sufficiently high exponents, an approximate log-normal distribution should indeed be expected. Hence, the results indicate that loss uncertainty was caused primarily by the extrinsic gust uncertainty. This finding is in line with the expectation that intrinsic uncertainties play a minor role for large building portfolios.

While the analysis of the wind–loss relation and of the associated uncertainty was supported by an abundance of empirical loss data, this is generally not the case for other hazards, where losses are monitored either insufficiently or less frequently. Nevertheless, since the sensitivity analysis has been based on the unified damage function⁴, the findings are expected to hold also for other hazards.

The sensitivity analysis has shown that interactions between different uncertainties are negligible (Figs. 4.9 and 4.10) and, hence, that their significance is defined by their direct contribution to the loss variance. This finding has practical relevance for the consideration of uncertainty in damage modelling, as it indicates an approximately additive accumulation of output variance. In practice, a simple comparison of output variance from different uncertainty sources

³ Examples for the attribution of overall variance are the case studies by Apel et al. (2004); de Moel and Aerts (2011); de Moel et al. (2012).

⁴ The applicability of the unified damage function is addressed in the discussion of RQ3.

could suffice to determine the dominating source of uncertainty [demonstrated in Fig. 4.5 (d)]. Conversely, such a comparison would also allow the identification of uncertainty sources that could be neglected.

The sensitivity analysis has been focussed on statistical uncertainties and their propagation within the unified damage function. Additional (epistemic) model uncertainty arises from the choice of model and its parameterization. The intercomparison of storm damage functions in Chapter III provides an indication of these epistemic uncertainties by considering four different damage functions. Since all damage functions were applied to the same set of data, they have been subject to the same amount of statistical uncertainty. Hence, changes in the magnitude of overall uncertainty can be attributed to the model choice or the parameterization. In this regard, the percentage errors given in Tab. 3.4 and 3.9 indicate strong levels of residual error for all damage functions and thus suggest that model differences are less significant than statistical uncertainty from wind or loss data.

The presented findings are of a general nature and are applicable also to more complicated damage models. As the results show, the analysis of uncertainties on the microscale level can be employed to draw conclusions also for macroscale loss estimation. It is believed that this finding also holds for more complex models, since the existence of a microscale damage relation is an implicit assumption of every macroscale damage function.

5.5 The Unification of Damage Functions for Climate-Related Hazards (RQ3)

Damage functions are widely used to quantify the adverse effects from diverse natural hazards such as windstorms and coastal flooding. Despite the broad scope, modellers generally limit their assessment to a specific hazard and often focus on selected case studies only. While the quality of the assessment merits such a narrow approach, increasing complicity may block the view on the fundamental characteristics of damage functions. The Third Research Question has hence been formulated with the intention to bring together the separate approaches for different climate-related hazards and to deepen the theoretical understanding of a unified approach:

What are the commonalities between damage functions for the different climate-related hazards windstorm and coastal flooding, and how could these damage functions be unified?

The answer to the Third Research Question has been guided by three boundary conditions: applicability, transparency, and transferability. A general approach should be applicable to a wide set of climate-related natural hazards, and thereby provide transparent methodology for an appraisal of the adverse effects of climate change. Transfer of methodology is of particular concern for regions with limited data availability.

Subject to the aforementioned boundary conditions, existing approaches in the fields of storm damage and coastal flood damage assessment were considered. As elaborated in Chapter IV, analogous approaches were found in the works of Heneka and Ruck (2008) and Hinkel et al. (2014). While both damage functions had been developed independently with a view on their particular hazards, the treatment of the hazard threshold was identified as their main difference. Bringing both approaches together, the hazard threshold can either be described implicitly by a distribution function or explicitly based on direct observation. The implicit representation has particular relevance, as it reduces data requirements by choice of a suitable parametric distribution function. The parameters of this distribution are more readily estimated than individual thresholds and can be linked to socio-economic conditions, thus allowing a parameterization also for data scarce regions.

The unified damage function, parameterized according to Heneka and Ruck (2008), was also included in the comparison of storm damage functions (c.f. Chapter III). The results have shown that the constraints imposed by the choice of portfolio distribution have a positive effect on the robustness of the parameterization. Quantitatively, the unified approach showed a performance similar to the competing models, with slightly worse predictions for extreme losses. In favour of the unified damage function, it should be noted that the differences between the various models were generally less significant than the uncertainty of loss due to gust speed observation.

Broadening the scope of the unified damage function, it was proposed to apply the unified damage function to the relation between temperature and heat-related mortality. While there is much research on the empirical relationship between temperature and excess mortality, there is no common description of the resulting curves.⁵ The added value of introducing the damage-function approach is in the understanding that the mortality curve follows from the underlying distribution of heat tolerance. This relation opens the opportunity to infer the shape of the distribution of heat-tolerance from mortality data. Furthermore, the reliability of extrapolating excess mortality for extreme temperatures may be improved, since the shape of the distribution imposes constraints on the behaviour of the damage curve beyond its support.

From a general point of view, the segmentation of the macroscale damage function into a microscale damage function and a distribution of hazard thresholds represents an assumption that may not necessarily be fulfilled. The assumption clearly holds for flood damages, where water levels are required to exceed the elevation level of the building. For the case of storm damage, the situation is less clear cut. Storm damage levels are a result of (cascading) component failures and thus depend on the quality and sturdiness of construction.

From a statistical perspective the segmentation constitutes just one of many possible representations, even if these may not be grounded on physical consid-

⁵ It is common practice to infer curves of excess mortality by non-parametric smoothing methods. Examples of this approach can be found in Gasparri et al. (2015) and Martinez et al. (2016).

erations. However, the question arises, which representation holds true for the actual underlying hazard–loss relation. This aspect links the present discussion with the results from the First and Second Research Questions, especially the model comparison in the light of strong uncertainty. Having compared the unified damage function⁶ against competing statistical models for storm damage, it was found that the uncertainty from the model choice falls below the data uncertainty emanating from the hazard magnitude. Hence, while the decision on the best possible representation of the hazard–loss relation remains outstanding, the benefit from employing the unified damage function – the systematic and transparent approach – outweighs potential modelling uncertainty.

When regarding hazards beyond those explored, the main criterion should be whether a statistical damage function can provide sufficient information on the considered risk. For example, despite the vast amount of loss caused by European windstorms, individual damages are typically relatively small and do not pose a critical threat to human life. Accordingly, regional losses can be well captured by statistical approaches and the low average damage does not warrant the development of more elaborate engineering-based approaches. Quite the opposite, torrential river flow as a consequence of fluvial flooding may affect only few built-up structures but may cause critical damage due to fluvial erosion, undercutting, or floating debris. Nonetheless, in regions where flow velocity plays a lesser role, damage from fluvial flooding may be largely determined by inundation height. In this case, the unified damage function could be applied in a similar fashion to the Lisbon case study in Sect. 4.4.

Beyond climate-related hazards, the application to seismic risk would in principle be feasible, but in contrast to other hazards seismic shocks have an immediate effect on the integrity of built-up structures and thus directly endanger human lives. Since statistical models could provide only a rough loss estimate, the nature of the hazard clearly warrants the development of more sophisticated engineering-based models.

While emphasising the applicability of the unified damage function to different natural hazards, there are also limitations to the approach. The founding assumptions are granularity with regard to the considered portfolio and independence of the damaging processes. These assumptions do not permit damage cascading from one structure to another and in principle determine the focus of the damage function on direct damages.

Across the different hazard domains, there is generally little information available on the shape of macroscale damage functions. This shortfall entails the importance of the unified approach, as it is capable of linking microscale with macroscale damage. It is concluded that, due to its wide applicability, the approach provides a step forward towards a common theory of damage functions. As such, the model has already formed the basis for the analysis of uncertainty propagation in RQ2 and is likely to enable further insight on the determinants of the shape of macroscale damage functions.

⁶ Represented in the comparison by the model of Heneka and Ruck (2008).

5.6 Outlook and Concluding Remarks

Following the discussion of the scientific advances contributed by the work at hand, these will now be set into a broader context with an outlook into prospective research.

The handling of complex loss data has been shown to constitute a key challenge for the development of damage functions. Common fitting methods are flawed due to their failure to incorporate the non-standard properties of loss data. The employed MLE was found to be the tool of choice, being capable to incorporate flexible models of uncertainty. However, uncertainty of loss estimates is a result of a complex interplay between various sources of uncertainty. The modelling of loss uncertainty, as demonstrated for the unified damage function, could improve the fitting of damage functions by replacing simplifying assumptions such as the employed log-normal loss uncertainty. In combination with MLE this could further increase the quality of loss estimates and enable new insight into the nature of the hazard–loss relation. The proposed methodology would be general in nature and should be applicable to any kind of (natural) hazard data.

The defining properties of macroscale damage functions are poorly understood. Typically these functions are either represented by a statistically inferred damage curve or result from the aggregation of microscale damages. However, an *a priori* understanding of what determines the shape of the macroscale damage functions is still missing. Clearly, a deeper and more general understanding of damage functions is needed. Contributing to this task, the work at hand has improved the understanding of macroscale storm damage functions as well as elaborated on a unification of damage function for multiple hazards. On these grounds it is seen as a step towards the grand goal of a theory of damage functions.

By their very nature, statistical damage function are heavily reliant on the availability of data. In order to transfer these damage functions to data-scarce regions, it is important to infer the determinants that define the shape of the damage function. For windstorm damage it has been argued that local vulnerability is governed by continual adaptation to the local storm climate in the form of building codes and practices. Establishing a link between the storm climate and the vulnerability could foster the transfer of damage functions into regions where loss data are missing and only the storm climate is observed. While a correlation between the parameters of the damage function and commonly employed proxies for the storm climate (e.g. wind percentiles) could not be confirmed in this work, strong regional patterns in vulnerability were observed. This suggests that the observed vulnerability patterns are due to building properties which may not be directly related to storm climate, e.g. traditional construction practices. Prospective work should illuminate the benefit of obtaining detailed data on the exposure. The work at hand has shown that current knowledge on storm damage functions remains insufficient to explain

local vulnerability patterns and further research is needed to enable accurate loss estimation for data-scarce regions.

It is believed that the thesis at hand will be of value to practitioners in the related fields of natural hazards research and the atmospheric sciences. It should encourage researchers to breach the frontiers of their discipline to fertilize the development of universal, transparent, and applicable methodology for the assessment of climate-related hazards.

Bibliography

- Ágústsson, H. and Ólafsson, H. (2009). Forecasting wind gusts in complex terrain. *Meteor. Atmos. Phys.*, 103(1-4):173–185.
- Apel, H., Thielen, A. H., Merz, B., and Blöschl, G. (2004). Flood risk assessment and associated uncertainty. *Nat. Hazards Earth Syst. Sci.*, 4(2):295–308.
- Bedford, T. and Cooke, R. (2001). *Probabilistic Risk Analysis – Foundations and Methods*. Cambridge University Press, Cambridge, UK.
- Bernaola-Galván, P., Oliver, J., Hackenberg, M., Coronado, A., Ivanov, P., and Carpena, P. (2012). Segmentation of time series with long-range fractal correlations. *Eur. Phys. J. B*, 85(6):1–12.
- Blackburn, S., Marques, C., de Sherbinin, A., Modesto, F., Ojima, R., Oliveau, S., and Bolde, C. C. P. (2013). Mega-urbanisation on the coast. In Pelling, M. and Blackburn, S., editors, *Megacities and the Coast – Risk, Resilience and Transformation*, pages 1–21. Routledge, New York, USA.
- Boettle, M., Kropp, J. P., Reiber, L., Roithmeier, O., Rybski, D., and Walther, C. (2011). About the influence of elevation model quality and small-scale damage functions on flood damage estimation. *Nat. Hazards Earth Syst. Sci.*, 11(12):3327–3334.
- Boettle, M., Rybski, D., and Kropp, J. P. (2013). How changing sea level extremes and protection measures alter coastal flood damages. *Water Resour. Res.*, 49(3):1199–1210.
- Boettle, M., Rybski, D., and Kropp, J. P. (2016). Quantifying the effect of sea level rise and flood defence – a point process perspective on coastal flood damage. *Nat. Hazards Earth Syst. Sci.*, 16(2):559–576.
- Bouwer, L. M. and Wouter Botzen, W. J. (2011). How sensitive are US hurricane damages to climate? Comment on a paper by W. D. Nordhaus. *Clim. Change Econ.*, 02(01):1–7.
- Box, G. E. and Cox, D. R. (1964). An analysis of transformations. *J. Roy. Stat. Soc. B*, 26(2):211–252.
- Büttner, G., Soukup, T., and Sousa, A. (2007). CLC2006 technical guidelines. Technical Report 17, European Environmental Agency, Copenhagen, Denmark.
- Cammerer, H., Thielen, A. H., and Lammel, J. (2013). Adaptability and transferability of flood loss functions in residential areas. *Nat. Hazards Earth Syst. Sci.*, 13(11):3063–3081.
- Cardona, O., van Aalst, M., Birkmann, J., Fordham, M., McGregor, G., Perez, R., Pulwarty, R., Schipper, E., and Sinh, B. (2012). Determinants of risk: exposure and vulnerability. In IPCC (2012), pages 65–108.
- Coles, S. and Tawn, J. (2005). Bayesian modelling of extreme surges on the UK east coast. *Phil. Trans. R. Soc. A*, 363(1831):1387–1406.

- Costa, L. and Kropp, J. P. (2013). Linking components of vulnerability in theoretic frameworks and case studies. *Sustain. Sci.*, 8(1):1–9.
- CRED (2015). *The Human Cost of Natural Disasters*. The Centre for Research on the Epidemiology of Disasters (CRED), Brussels, Belgium.
- Cusack, S. (2013). A 101 year record of windstorms in the Netherlands. *Clim. Change*, 116(3-4):693–704.
- de Moel, H. and Aerts, J. C. J. H. (2011). Effect of uncertainty in land use, damage models and inundation depth on flood damage estimates. *Nat. Hazards*, 58(1):407–425.
- de Moel, H., Asselman, N. E. M., and Aerts, J. C. J. H. (2012). Uncertainty and sensitivity analysis of coastal flood damage estimates in the west of the Netherlands. *Nat. Hazards Earth Syst. Sci.*, 12(4):1045–1058.
- de Moel, H., Jongman, B., Kreibich, H., Merz, B., Penning-Rowsell, E., and Ward, P. J. (2015). Flood risk assessments at different spatial scales. *Mitig. Adapt. Strategies Glob. Chang.*, 20(6):865–890.
- Deck, O. and Verdel, T. (2012). Uncertainties and risk analysis related to geohazards: From practical applications to research trends. In Emblemavag, J., editor, *Risk Management for the Future - Theory and Cases*. InTech, Rijeka, Croatia.
- Dee, D. P., Uppala, S. M., Simmons, A. J., Berrisford, P., Poli, P., Kobayashi, S., Andrae, U., Balmaseda, M. A., Balsamo, G., Bauer, P., Bechtold, P., Beljaars, A. C. M., van de Berg, L., Bidlot, J., Bormann, N., Delsol, C., Dragani, R., Fuentes, M., Geer, A. J., Haimberger, L., Healy, S. B., Hersbach, H., Hólm, E. V., Isaksen, I., Kållberg, P., Köhler, M., Matricardi, M., McNally, A. P., Monge-Sanz, B. M., Morcrette, J.-J., Park, B.-K., Peubey, C., de Rosnay, P., Tavolato, C., Thépaut, J.-N., and Vitart, F. (2011). The ERA-Interim reanalysis: configuration and performance of the data assimilation system. *Q. J. R. Meteorolog. Soc.*, 137(656):553–597.
- Deroche, M.-S., Choux, M., Codron, F., and Yiou, P. (2014). Three variables are better than one: detection of European winter windstorms causing important damages. *Nat. Hazards Earth Syst. Sci.*, 14(4):981–993.
- Divoky, D., Battalio, R., Dean, B., Collins, I., Hatheway, D., and Scheffner, N. (2005). Stillwater. FEMA coastal flood hazard analysis and mapping guidelines – focused study report, Federal Emergency Agency (FEMA), Washington, D.C., USA.
- Donat, M. G., Leckebusch, G. C., Wild, S., and Ulbrich, U. (2011a). Future changes in European winter storm losses and extreme wind speeds inferred from GCM and RCM multi-model simulations. *Nat. Hazards Earth Syst. Sci.*, 11(5):1351–1370.
- Donat, M. G., Pardowitz, T., Leckebusch, G. C., Ulbrich, U., and Burghoff, O. (2011b). High-resolution refinement of a storm loss model and estimation of return periods of loss-intensive storms over Germany. *Nat. Haz. Earth Sys. Sci.*, 11(10):2821–2833.
- Dorland, C., Tol, R. S. J., and Palutikof, J. P. (1999). Vulnerability of the Netherlands and Northwest Europe to storm damage under climate change. *Clim. Change*, 43:513–535.

- EEA (2014). *EU-DEM Statistical Validation, prepared for the European Environmental Agency (EEA) by DHI GRAS*. European Environmental Agency, Copenhagen, Denmark. <http://ec.europa.eu/eurostat/documents/4311134/4350046/Report-EU-DEM-statistical-validation-August2014.pdf>, accessed 15-05-2015.
- Egorova, R., van Noortwijk, J. M., and Holterman, S. R. (2008). Uncertainty in flood damage estimation. *Int. J. Riv. Bas. Manage.*, 6(2):139–148.
- Emanuel, K. (2005). Increasing destructiveness of tropical cyclones over the past 30 years. *Nature*, 436(7051):686–688.
- Etienne, C. and Beniston, M. (2012). Wind storm loss estimations in the Canton of Vaud (Western Switzerland). *Nat. Hazards Earth Syst. Sci.*, 12(12):3789–3798.
- Feser, F., Barcikowska, M., Krueger, O., Schenk, F., Weisse, R., and Xia, L. (2015). Storminess over the North Atlantic and northwestern Europe – a review. *Q. J. R. Meteorolog. Soc.*, 141(687):350–382.
- Flowerdew, J., Horsburgh, K., and Mylne, K. (2009). Ensemble forecasting of storm surges. *Mar. Geod.*, 32(2):91–99.
- Flowerdew, J., Horsburgh, K., Wilson, C., and Mylne, K. (2010). Development and evaluation of an ensemble forecasting system for coastal storm surges. *Q. J. R. Meteorolog. Soc.*, 136(651):1444–1456.
- Fortunato, A., Li, K., Bertin, X., and Rodrigues, M. (2014). Determination of extreme sea levels along the Portuguese coast. In *Actas das 3.as Jornadas de Engenharia Hidrográfica*, pages 151–154, Lisbon, Portugal. Instituto Hidrográfico.
- Fuchs, S., Heiss, K., and Hübl, J. (2007). Towards an empirical vulnerability function for use in debris flow risk assessment. *Nat. Hazards Earth Syst. Sci.*, 7(5):495–506.
- Gasparrini, A., Guo, Y., Hashizume, M., Lavigne, E., Zanobetti, A., Schwartz, J., Tobias, A., Tong, S., Rocklöv, J., Forsberg, B., Leone, M., De Sario, M., Bell, M. L., Guo, Y.-L. L., Wu, C.-f., Kan, H., Yi, S.-M., de Sousa Zanotti Stagliorio Coelho, M., Saldiva, P. H. N., Honda, Y., Kim, H., and Armstrong, B. (2015). Mortality risk attributable to high and low ambient temperature: a multicountry observational study. *Lancet*, 386(9991):369–375.
- GDV (2013). *Naturgefahrenreport 2013*. Gesamtverband der Deutschen Versicherungswirtschaft e.V., Berlin, Germany.
- Gerstengarbe, F.-W., Werner, P. C., Österle, H., and Burghoff, O. (2013). Winter storm- and summer thunderstorm-related loss events with regard to climate change in Germany. *Theor. Appl. Climatol.*, 114(3–4):715–724.
- Golnaraghi, M., Etienne, C., Sapir, D. G., and Below, R. (2014). *Atlas of Mortality and Economic Losses from Weather, Climate and Water Extremes (1970–2012)* [Williams, M. and Castonguay, S., editors]. WMO-No. 1123. World Meteorological Organization, Geneva, Switzerland.
- Hacking, I. (1984). *The Emergence of Probability: A Philosophical Study of Early Ideas about Probability, Induction and Statistical Inference*. Cambridge University Press, Cambridge, UK.

- Hallegatte, S. (2008). An adaptive regional input-output model and its application to the assessment of the economic cost of Katrina. *Risk Anal.*, 28(3):779–799.
- Hallegatte, S., Green, C., Nicholls, R. J., and Corfee-Morlot, J. (2013). Future flood losses in major coastal cities. *Nature Clim. Change*, 3(9):802–806.
- Hallegatte, S., Hourcade, J.-C., and Dumas, P. (2007). Why economic dynamics matter in assessing climate change damages: Illustration on extreme events. *Ecol. Econom.*, 62(2):330–340.
- Hamid, S., Kibria, B. G., Gulati, S., Powell, M., Annane, B., Cocke, S., Pinelli, J.-P., Gurvey, K., and Chen, S.-C. (2010). Predicting losses of residential structures in the state of Florida by the public hurricane loss evaluation model. *Stat. Methodol.*, 7(5):552–573.
- Hammond, M., Chen, A., Djordjević, S., Butler, D., and Mark, O. (2015). Urban flood impact assessment: A state-of-the-art review. *Urban Water J.*, 12(1):14–29.
- Held, H., Gerstengarbe, F.-W., Pardowitz, T., Pinto, J. G., Ulbrich, U., Born, K., Donat, M. G., Karremann, M., Leckebusch, G. C., Ludwig, P., Nissen, K. M., Österle, H., Prah, B. F., Werner, P. C., Befort, D. J., and Burghoff, O. (2013). Projections of global warming-induced impacts on winter storm losses in the German private household sector. *Clim. Change*, 121(2):195–207.
- Heneka, P. and Hofherr, T. (2011). Probabilistic winter storm risk assessment for residential buildings in Germany. *Nat. Hazards*, 56:815–831.
- Heneka, P., Hofherr, T., Ruck, B., and Kottmeier, C. (2006). Winter storm risk of residential structures – model development and application to the German state of Baden-Württemberg. *Nat. Hazards Earth Syst. Sci.*, 6(5):721–733.
- Heneka, P. and Ruck, B. (2004). Development of a storm damage risk map of Germany – a review of storm damage functions. In *Proceedings of the International Conference “Disasters and Society – From Hazard Assessment to Risk Reduction”*, Karlsruhe, Germany.
- Heneka, P. and Ruck, B. (2008). A damage model for the assessment of storm damage to buildings. *Eng. Struct.*, 30(12):3603–3609.
- Higham, N. J. (2002). Computing the nearest correlation matrix – a problem from finance. *IMA J. Numer. Anal.*, 22(3):329–343.
- Hinkel, J., Lincke, D., Vafeidis, A. T., Perrette, M., Nicholls, R. J., Tol, R. S. J., Marzeion, B., Fettweis, X., Ionescu, C., and Levermann, A. (2014). Coastal flood damage and adaptation costs under 21st century sea-level rise. *Proc. Natl. Acad. Sci. USA*, 111(9):3292–3297.
- Hofherr, T. and Kunz, M. (2010). Extreme wind climatology of winter storms in Germany. *Clim. Res.*, 41(2):105–123.
- Holmes, J. D. (2015). *Wind Loading of Structures*. CRC Press, Taylor and Francis Group, Boca Raton, USA, 3rd edition.
- Huang, Z., Rosowsky, D. V., and Sparks, P. R. (2001). Long-term hurricane risk assessment and expected damage to residential structures. *Rel. Eng. Sys. Saf.*, 74(3):239–249.

- Huttenlau, M. and Stötter, J. (2011). The structural vulnerability in the framework of natural hazard risk analyses and the exemplary application for storm loss modelling in Tyrol (Austria). *Nat. Hazards*, 58(2):705–729.
- Hyndman, R. J. and Koehler, A. B. (2006). Another look at measures of forecast accuracy. *Int. J. Forecasting*, 22(4):679–688.
- Iman, R. L. and Conover, W. J. (1982). A distribution-free approach to inducing rank correlation among input variables. *Commun. Stat. Simulat.*, 11(3):311–334.
- IPCC (2012). *Managing the Risks of Extreme Events and Disasters to Advance Climate Change Adaptation: A Special Report of Working Groups I and II of the Intergovernmental Panel on Climate Change* [Field, C., Barros, V., Stocker, T., Qin, D., Dokken, D., Ebi, K., Mastrandrea, M., Mach, K., Plattner, G.-K., Allen, S., Tignor, M., and Midgle, P., editors]. Cambridge University Press, Cambridge, UK, and New York, NY, USA.
- IPCC (2014). Summary for policymakers. In Field, C. B., Barros, V. R., Dokken, D. J., Mach, K. J., Mastrandrea, M. D., Bilir, T. E., Chatterjee, M., Ebi, K. L., Estrada, Y. O., Genova, R. C., Girma, B., Kissel, E. S., Levy, A. N., MacCracken, S., Mastrandrea, P. R., and White, L. L., editors, *Climate Change 2014: Impacts, Adaptation, and Vulnerability. Part A: Global and Sectoral Aspects. Contribution of Working Group II to the Fifth Assessment Report of the Intergovernmental Panel on Climate Change*. Cambridge University Press, Cambridge, UK, and New York, NY, USA.
- Jansen, M. J. (1999). Analysis of variance designs for model output. *Comput. Phys. Commun.*, 117(1–2):35–43.
- Jongman, B., Kreibich, H., Apel, H., Barredo, J. I., Bates, P. D., Feyen, L., Gericke, A., Neal, J., Aerts, J. C. J. H., and Ward, P. J. (2012). Comparative flood damage model assessment: towards a European approach. *Nat. Hazards Earth Syst. Sci.*, 12(12):3733–3752.
- Kantha, L. (2008). Tropical cyclone destructive potential by integrated kinetic energy. *Bull. Amer. Meteor. Soc.*, 89(2):219–221.
- Khanduri, A. and Morrow, G. (2003). Vulnerability of buildings to windstorms and insurance loss estimation. *J. Wind Eng. Ind. Aerodyn.*, 91(4):455–467.
- Klawa, M. and Ulbrich, U. (2003). A model for the estimation of storm losses and the identification of severe winter storms in Germany. *Nat. Haz. Earth Sys. Sci.*, 3(6):725–732.
- Klugman, S. A., Panjer, H. H., and Willmot, G. E. (2008). *Loss Models: From Data to Decisions*. Wiley Series in Probability and Statistics. John Wiley & Sons, Hoboken, New Jersey, 3rd edition.
- Kohavi, R. (1995). A study of cross-validation and bootstrap for accuracy estimation and model selection. In *Proceedings of the International Joint Conference on Artificial Intelligence (IJCAI)*, volume 14(2), pages 1137–1145, Montreal, Canada. IJCAI, California, USA.
- Koks, E. E., Bočkarjova, M., de Moel, H., and Aerts, J. C. J. H. (2015). Integrated direct and indirect flood risk modeling: Development and sensitivity analysis. *Risk Anal.*, 35(5):882–900.

- Kreibich, H., Bubeck, P., Kunz, M., Mahlke, H., Parolai, S., Khazai, B., Daniell, J., Lakes, T., and Schröter, K. (2014). A review of multiple natural hazards and risks in Germany. *Nat. Hazards*, 74(3):2279–2304.
- Kreibich, H., Seifert, I., Merz, B., and Thielen, A. H. (2010). Development of FLEMOcs – a new model for the estimation of flood losses in the commercial sector. *Hydrolog. Sci. J.*, 55(8):1302–1314.
- Lamb, H. H. (1991). *Historic storms of the North Sea, British Isles and Northwest Europe*. Cambridge University Press, Cambridge, UK.
- Lawrence, R. J. (1988). Applications in economics and business. In Crow, E. L. and Shimizu, K., editors, *Lognormal Distributions: Theory and Applications*, pages 229–266. Marcel Dekker, New York, USA.
- Leckebusch, G. C., Ulbrich, U., Fröhlich, L., and Pinto, J. G. (2007). Property loss potentials for European midlatitude storms in a changing climate. *Geophys. Res. Lett.*, 34(5):L05703.
- Leone, M., D'Ippoliti, D., De Sario, M., Analitis, A., Menne, B., Katsouyanni, K., de' Donato, F., Basagana, X., Salah, A., Casimiro, E., Dortbudak, Z., Iniguez, C., Peretz, C., Wolf, T., and Michelozzi, P. (2013). A time series study on the effects of heat on mortality and evaluation of heterogeneity into European and Eastern-Southern Mediterranean cities: results of EU CIRCE project. *Environ. Health*, 12(1):55.
- Martinez, G. S., Baccini, M., De Ridder, K., Hooyberghs, H., Lefebvre, W., Kendrovski, V., Scott, K., and Spasenovska, M. (2016). Projected heat-related mortality under climate change in the metropolitan area of Skopje. *BMC Public Health*, 16(1):1–12.
- McGranahan, G., Balk, D., and Anderson, B. (2007). The rising tide: assessing the risks of climate change and human settlements in low elevation coastal zones. *Environ. Urban.*, 19(1):17–37.
- Merz, B., Kreibich, H., Schwarze, R., and Thielen, A. (2010). Review article "Assessment of economic flood damage". *Nat. Hazards Earth Syst. Sci.*, 10(8):1697–1724.
- Merz, B., Kreibich, H., Thielen, A., and Schmidtke, R. (2004). Estimation uncertainty of direct monetary flood damage to buildings. *Nat. Hazards Earth Syst. Sci.*, 4(1):153–163.
- Merz, B. and Thielen, A. (2009). Flood risk curves and uncertainty bounds. *Nat. Hazards*, 51(3):437–458.
- Mestre, O., Gruber, C., Prieur, C., Caussinus, H., and Jourdain, S. (2011). SPLIDHOM: A method for homogenization of daily temperature observations. *J. Appl. Meteorol. Climatol.*, 50(11):2343–2358.
- Meyer, V., Becker, N., Markantonis, V., Schwarze, R., van den Bergh, J. C. J. M., Bouwer, L. M., Bubeck, P., Ciavola, P., Genovese, E., Green, C., Hallegatte, S., Kreibich, H., Lequeux, Q., Logar, I., Papyrakis, E., Pfurtscheller, C., Poussin, J., Przyluski, V., Thielen, A. H., and Viavattene, C. (2013). Review article: Assessing the costs of natural hazards – state of the art and knowledge gaps. *Nat. Hazards Earth Syst. Sci.*, 13(5):1351–1373.
- Miller, R. G. (1974). The jackknife – a review. *Biometrika*, 61(1):1–15.

- Mitsuta, Y. and Tsukamoto, O. (1989). Studies on spatial structure of wind gust. *J. Appl. Meteor.*, 28(11):1155–1160.
- Mölter, T., Schindler, D., Albrecht, A. T., and Kohnle, U. (2016). Review on the projections of future storminess over the North Atlantic European region. *Atmos.*, 7(4):60.
- Munich Re (1993). *Winterstürme in Europa – Schadenanalyse 1990 - Schadenspotentiale*. Münchener Rückversicherungs-Gesellschaft, Munich, Germany.
- Munich Re (2001). *Winterstürme in Europa (II) – Schadenanalyse 1999 - Schadenspotentiale*. Münchener Rückversicherungs-Gesellschaft, Munich, Germany.
- Munich Re (2013). *Topics Geo – Natural Catastrophes 2012 – Analyses, Assessments, Positions*. Münchener Rückversicherungs-Gesellschaft, Munich, Germany.
- Munich Re (2015). *Topics Geo – Natural Catastrophes 2014 – Analyses, Assessments, Positions*. Münchener Rückversicherungs-Gesellschaft, Munich, Germany.
- Murnane, R. J. and Elsner, J. B. (2012). Maximum wind speeds and US hurricane losses. *Geophys. Res. Lett.*, 39(16):L16707.
- Nordhaus, W. D. (2010). The economics of hurricanes and implications of global warming. *Clim. Change Econ.*, 01(01):1–20.
- Ohnishi, T., Mizuno, T., Shimizu, C., and Watanabe, T. (2011). *The Evolution of House Price Distribution*. RIETI Discussion Paper Series 11-E-019. Research Institute of Economy, Trade and Industry, Tokyo, Japan.
- Olsen, A. H. and Porter, K. A. (2011). What we know about demand surge: Brief summary. *Nat. Hazards Rev.*, 12(2):62–71.
- Pinelli, J.-P., Gurley, K., Subramanian, C., Hamid, S., and Pita, G. (2008). Validation of a probabilistic model for hurricane insurance loss projections in florida. *Reliab. Eng. Syst. Saf.*, 93(12):1896–1905.
- Pinto, J. G., Fröhlich, E. L., Leckebusch, G. C., and Ulbrich, U. (2007). Changing European storm loss potentials under modified climate conditions according to ensemble simulations of the ECHAM5/MPI-OM1 GCM. *Nat. Hazards Earth Syst. Sci.*, 7(1):165–175.
- Pita, G. L., Pinelli, J.-P., Gurley, K. R., and Hamid, S. (2013). Hurricane vulnerability modeling: Development and future trends. *J. Wind Eng. Ind. Aerodyn.*, 114:96–105.
- Poulter, B. and Halpin, P. N. (2008). Raster modelling of coastal flooding from sea-level rise. *Int. J. Geogr. Inf. Sci.*, 22(2):167–182.
- Powell, M. D. and Reinhold, T. A. (2007). Tropical cyclone destructive potential by integrated kinetic energy. *Bull. Amer. Meteor. Soc.*, 88(4):513–526.
- Prahl, B. F., Rybski, D., Burghoff, O., and Kropp, J. P. (2015). Comparison of storm damage functions and their performance. *Nat. Hazards Earth Syst. Sci.*, 15(4):769–788.
- Prahl, B. F., Rybski, D., Boettle, M., and Kropp, J. P. (2016). Damage functions for climate-related hazards: Unification and uncertainty analysis. *Nat. Hazards Earth Syst. Sci.*, 16(5):1189–1203.

- Prahl, B. F., Rybski, D., Kropp, J. P., Burghoff, O., and Held, H. (2012). Applying stochastic small-scale damage functions to German winter storms. *Geophys. Res. Lett.*, 39(6):L06806.
- Prettenthaler, F., Albrecher, H., Koberl, J., and Kortschak, D. (2012). Risk and insurability of storm damages to residential buildings in Austria. *Geneva Pap. R. I. – Iss. P.*, 37(2):340–364.
- Roberts, J. F., Champion, A. J., Dawkins, L. C., Hodges, K. I., Shaffrey, L. C., Stephenson, D. B., Stringer, M. A., Thornton, H. E., and Youngman, B. D. (2014). The XWS open access catalogue of extreme European windstorms from 1979 to 2012. *Nat. Hazards Earth Syst. Sci.*, 14(9):2487–2501.
- Ruppert, D., Wand, M. P., and Carroll, R. J. (2003). *Semiparametric Regression*. Cambridge Series in Statistical and Probabilistic Mathematics. Cambridge University Press, Cambridge, UK.
- Rybski, D. and Neumann, J. (2011). A review on the Pettitt test. In Kropp, J. and Schellnhuber, H.-J., editors, *In Extremis*, pages 202–213. Springer, Berlin/Heidelberg, Germany.
- Saltelli, A., Annoni, P., Azzini, I., Campolongo, F., Ratto, M., and Tarantola, S. (2010). Variance based sensitivity analysis of model output. Design and estimator for the total sensitivity index. *Comput. Phys. Commun.*, 181(2):259–270.
- Saltelli, A., Ratto, M., Andres, T., Campolongo, F., Cariboni, J., Gatelli, D., Saisana, M., and Tarantola, S. (2008). *Global Sensitivity Analysis. The Primer*. John Wiley & Sons, Chichester, UK.
- Schwierz, C., Köllner-Heck, P., Zenklusen Mutter, E., Bresch, D., Vidale, P.-L., Wild, M., and Schär, C. (2010). Modelling European winter wind storm losses in current and future climate. *Clim. Change*, 101:485–514.
- Simiu, E. and Scanlan, R. H. (1996). *Wind Effects on Structures: Fundamentals and Applications to Design*. John Wiley, New York, USA, 3rd edition.
- Smith, D. I. (1994). Flood damage estimation – a review of urban stage-damage curves and loss functions. *Water SA*, 20(33):231–238.
- Sparks, P. R. and Bhinderwala, S. A. (1994). Relationship between residential insurance losses and wind conditions in Hurricane Andrew. In *Hurricanes of 1992: Lessons Learned and Implications for the Future*, pages 111–124. ASCE, Reston, Virginia, USA.
- Stafoggia, M., Forastiere, F., Agostini, D., Biggeri, A., Bisanti, L., Cadum, E., Caranci, N., de’Donato, F., De Lisio, S., De Maria, M., Michelozzi, P., Miglio, R., Pandolfi, P., Picciotto, S., Rognoni, M., Russo, A., Scarnato, C., and Perucci, C. A. (2006). Vulnerability to heat-related mortality: A multicity, population-based, case-crossover analysis. *Epidemiol.*, 17(3):315–323.
- Swiss Re (1993). *Stürme Über Europa: Schäden und Szenarien*. Swiss Re Ltd, Zurich, Switzerland.
- Swiss Re (2014). *Sigma – Natural Catastrophes and Man-made Disasters in 2013*. Swiss Re Ltd, Zurich, Switzerland.

- Thunnissen, D. P. (2003). Uncertainty classification for the design and development of complex systems. In *PMC2003 - 3rd Annual Predictive Methods Conference*, Newport Beach, USA. June 16-17.
- Thywissen, K. (2006). Core terminology of disaster risk reduction: A comparative glossary. In Birkmann, J., editor, *Measuring Vulnerability to Natural Hazards*, pages 448–496. UN University Press, Tokyo, Japan.
- UN-Habitat (2008). *State of the World's Cities 2008/2009 – Harmonious Cities*. United Nations Human Settlements Programme, Nairobi, Kenya.
- UN-Habitat (2011). *Cities and Climate Change: Global Report on Human Settlements 2011*. United Nations Human Settlements Programme, Nairobi, Kenya.
- Unanwa, C., McDonald, J., Mehta, K., and Smith, D. (2000). The development of wind damage bands for buildings. *J. Wind Eng. Ind. Aerodyn.*, 84(1):119–149.
- Venema, V. K. C., Mestre, O., Aguilar, E., Auer, I., Guijarro, J. A., Domonkos, P., Vertacnik, G., Szentimrey, T., Stepanek, P., Zahradnicek, P., Viarre, J., Müller-Westermeier, G., Lakatos, M., Williams, C. N., Menne, M. J., Lindau, R., Rasol, D., Rustemeier, E., Kolokythas, K., Marinova, T., Andresen, L., Acquafredda, F., Fratianni, S., Cheval, S., Klancar, M., Brunetti, M., Gruber, C., Prohom Duran, M., Likso, T., Esteban, P., and Brandsma, T. (2012). Benchmarking homogenization algorithms for monthly data. *Clim. Past*, 8(1):89–115.
- Vickery, P., Skerlj, P., Lin, J., Twisdale, L., Young, M., and Lavelle, F. (2006). HAZUS-MH hurricane model methodology. II: damage and loss estimation. *Nat. Hazards Rev.*, 7(2):94–103.
- Walker, G. R. (2011). Modelling the vulnerability of buildings to wind – a review. *Can. J. Civ. Eng.*, 38(9):1031–1039.
- Wan, H., Wang, X. L., and Swail, V. R. (2010). Homogenization and trend analysis of Canadian near-surface wind speeds. *J. Clim.*, 23(5):1209–1225.
- Wang, X. L. (2008). Accounting for autocorrelation in detecting mean shifts in climate data series using the penalized maximal t or F test. *J. Appl. Meteorol. Climatol.*, 47(9):2423–2444.
- Wang, X. L., Chen, H., Wu, Y., Feng, Y., and Pu, Q. (2010). New techniques for the detection and adjustment of shifts in daily precipitation data series. *J. Appl. Meteorol. Climatol.*, 49(12):2416–2436.
- Watson, C. C. and Johnson, M. E. (2004). Hurricane loss estimation models: opportunities for improving the state of the art. *Bull. Amer. Meteor. Soc.*, 85:1713–1726.
- World Bank (2015). *Gross Domestic Product 2014*. World Development Indicators database, World Bank, 18 September 2015. <http://data.worldbank.org/data-catalog/GDP-ranking-table>, accessed 22-10-2015.
- World Bank and United Nations (2010). *Natural Hazards, Unnatural Disasters: The Economics of Effective Prevention*. TheWorld Bank and The United Nations, Washington D.C., USA.
- Zhou, B., Rybski, D., and Kropp, J. P. (2013). On the statistics of urban heat island intensity. *Geophys. Res. Lett.*, 40(20):5486–5491.

Declaration

I hereby declare that this dissertation is a product of my own research endeavours and has been prepared without illegitimate assistance. The work is original except where indicated by reference in the text and no part of the dissertation has been submitted for any other degree. This dissertation has not been presented to any other university for examination.

Berlin, 10 July 2016

Boris Frederic Prah

I hope I didn't brain my damage!

— Homer J. Simpson, *El Viaje Misterioso de Nuestro Jomer*

Colophon

This document was typeset using a customised version of the typographical look-and-feel `classicthesis` developed by André Miede. The style was inspired by Robert Bringhurst's seminal book on typography "*The Elements of Typographic Style*". `classicthesis` is available for both \LaTeX and \LyX :

<http://code.google.com/p/classicthesis/>